TECHNICAL REPORT STANDARD TITLE PAGE

1. Report No.	2. Government Accession No.	3. Recipient's Catalog No.
CFHR 3-8-75-177-7		

4. Title and Subtitle	5. Report Date
CONTINUOUSLY REINFORCED CONCRETE PAVEMENT: STRUCTURAL PERFORMANCE AND DESIGN/CONSTRUCTION VARIABLES	May 1977
	6. Performing Organization Code

7. Author(s)	8. Performing Organization Report No.
Pieter J. Strauss, B. Frank McCullough, and W. Ronald Hudson	Research Report 177-7

9. Performing Organization Name and Address	10. Work Unit No.
Center for Highway Research The University of Texas at Austin Austin, Texas 78712	11. Contract or Grant No. Research Study 3-8-75-177
	13. Type of Report and Period Covered
12. Sponsoring Agency Name and Address Texas State Department of Highways and Public Transportation; Transportation Planning Division P. O. Box 5051 Austin, Texas 78763	Interim
	14. Sponsoring Agency Code

15. Supplementary Notes

Work done in cooperation with the Department of Transportation, Federal Highway Administration. Research Study Title: "Development and Implementation of the Design, Construction and Rehabilitation of Rigid Pavements"

16. Abstract

The structural performance of continuously reinforced concrete pavements (CRCP) on two sections of the interstate highway system in Texas is analyzed by employment of regression techniques. A probabilistic model is used in relating the distressed area of the pavement to theoretical models of fatigue and thus stress in the pavement system. Additional models for load transfer by means of dowel action of the longitudinal steel reinforcement and aggregate interlock are developed to explain the distinction in performance of different types of CRCP in Texas. Utilization of theoretical models allows the extrapolation of the results to other conditions, but discrepancies still exist between the theoretically explainable and the actual occurrence of distress. This difference is explained in terms of other construction, environmental and design variables. It is found that variation in pavement properties is a big contributor to distress. Important variables in this respect include pavement roughness and the subsequent variation in dynamic wheel loading, deflections and surface curvature which relate to layer stiffnesses and the variance of crack spacing which can be interpreted as a nonuniformity in slab properties. Final equations are derived which can be used in the design of new pavements or in the prediction of future distress on existing pavements.

17. Key Words	18. Distribution Statement
continuously reinforced concrete pavement, regression, pavement distress, prediction of distress, load transfer, stress, dynamic loading	No restrictions. This document is available to the public through the National Technical Information Service, Springfield, Virginia 22161.

19. Security Classif. (of this report)	20. Security Classif. (of this page)	21. No. of Pages	22. Price
Unclassified	Unclassified	184	

Form DOT F 1700.7 (8-69)

CONTINUOUSLY REINFORCED CONCRETE PAVEMENT: STRUCTURAL PERFORMANCE AND DESIGN/CONSTRUCTION VARIABLES

by

Pieter J. Strauss
B. Frank McCullough
W. Ronald Hudson

Research Report Number 177-7

Development and Implementation of the Design, Construction and Rehabilitation of Rigid Pavements

Research Project 3-8-75-177

conducted for

Texas
State Department of Highways and Public Transportation

in cooperation with the
U. S. Department of Transportation
Federal Highway Administration
Bureau of Public Roads

by the

CENTER FOR HIGHWAY RESEARCH
THE UNIVERSITY OF TEXAS AT AUSTIN

May 1977

The contents of this report reflect the views of the authors, who are responsible for the facts and the accuracy of the data presented herein. The contents do not necessarily reflect the official views or policies of the Federal Highway Administration. This report does not constitute a standard, specification, or regulation.

PREFACE

This report presents a detailed analysis of the results of a condition survey of continuously reinforced concrete pavements (CRCP) that was surveyed under Research Project 3-8-74-21. Sections of the Interstate Highways 45 and 10 through Districts 17 and 13 respectively, were analyzed using theoretical models which were combined through regression techniques.

The purpose of this report is to present the results of the study in the form of two equations, the one to be used for design of new CRCP and the second for the prediction of future distress in terms of the present structural condition and certain design/construction variables. It is also the intent to enhance an understanding of the structural performance of CRCP whereby sound rehabilitation techniques can be employed in pavement maintenance.

The cooperation of the staff of the Center for Highway Research of The University of Texas at Austin as well as the assistance of the personnel of the State Department of Highways and Public Transportation is greatly appreciated.

Pieter J. Strauss
B. Frank McCullough
W. Ronald Hudson

LIST OF REPORTS

Report No. 177-1, "Drying Shrinkage and Temperature Drop Stresses in Jointed Reinforced Concrete Pavement," by Felipe R. Vallejo, B. Frank McCullough, and W. Ronald Hudson, describes the development of a computerized system capable of analysis and design of a concrete pavement slab for drying shrinkage and temperature drop.

Report No. 177-2, "A Sensitivity Analysis of Continuously Reinforced Concrete Pavement Model CRCP-1 for Highways," by Chypin Chiang, B. Frank McCullough, and W. Ronald Hudson, describes the overall importance of this model, the relative importance of the input variables of the model and recommendations for efficient use of the computer program.

Report No. 177-3, "A Study of the Performance of the Mays Ride Meter," by Yi Chin Hu, Hugh J. Williamson, B. Frank McCullough, and W. Ronald Hudson, discusses the accuracy of measurements made by the Mays Ride Meter and their relationaship to roughness measurements made with the Surface Dynamics Profilometer.

Report No. 177-4, "Laboratory Study of the Effect of Non-Uniform Foundation Support on CRC Pavements," by Enrique Jimenez, W. Ronald Hudson, and B. Frank McCullough, describes the laboratory tests of CRC slab models with voids beneath them. Deflection, crack width, load transfer, spalling, and cracking are considered. Also used is the SLAB 49 computer program that models the CRC laboratory slab as a theoretical approach. The physical laboratory results and the theoretical solutions are compared and analyzed and the accuracy is determined (being prepared for submission).

Report No. 177-5, "A Comparison of Two Inertial Reference Profilometers Used to Evaluate Airfield and Highway Pavements," by Chris Edward Doepke, B. Frank McCullough, and W. Ronald Hudson, describes a United States Air Force owned profilometer developed for measuring airfield runway roughness and compares it with the Surface Dynamics Profilometer using plotted profiles and mean roughness amplitude data from each profilometer.

Report No. 177-6, "Sixteenth Year Progress Report on Experimental Continuously Reinforced Concrete Pavement in Walker County," by Thomas P. Chesney and B. Frank McCullough, is a summary of data collection and analysis over a 16-year period. During that period, numerous findings resulted in changes in specifications and design standards. These data will be valuable for shaping guidelines for future construction.

Report No. 177-7, "Continuously Reinforced Concrete Pavement: Structural Performance and Design/Construction Variables," by Pieter J. Strauss, B. Frank McCullough, and W. Ronald Hudson, presents a detailed analysis of design, construction, and environmental variables that may have an effect on the structural performance of a CRCP.

ABSTRACT

The structural performance of continuously reinforced concrete pavements (CRCP) on two sections of the interstate highway system in Texas is analyzed by employment of regression techniques. A probabilistic model is used in relating the distressed area of the pavement to theoretical models of fatigue and thus stress in the pavement system. Additional models for load transfer by means of dowel action of the longitudinal steel reinforcement and aggregate interlock are developed to explain the distinction in performance of different types of CRCP in Texas. Utilization of theoretical models allows the extrapolation of the results to other conditions, but discrepancies still exist between the theoretically explainable and the actual occurrence of distress. This difference is explained in terms of other construction, environmental and design variables. It is found that variation in pavement properties is a big contributor to distress. Important variables in this respect include pavement roughness and the subsequent variation in dynamic wheel loading, deflections and surface curvature which relate to layer stiffnesses and the variance of crack spacing which can be interpreted as a nonuniformity in slab properties. Final equations are derived which can be used in the design of new pavements or in the prediction of future distress on existing pavements.

KEY WORDS: continuously reinforced concrete pavement, regression, pavement distress, prediction of distress, load transfer, stress, dynamic loading

SUMMARY

A detailed analysis of design, construction and environmental variables that may have an effect on the structural performance of a CRCP is presented in this report. The variables are tied together by theoretical models where possible to allow for extrapolation outside conditions prevailing at the sites investigated. Stress is calculated in the pavement whereupon the number of load applications till failure can be determined. A stochastic model provides the link between number of load applications and measurable distress. Since several coefficients are unknown for the structural performance of a CRCP, a regression analysis is used to derive the values of these equations. The final equations that can be put together are employed in designing new CRCP and in predicting future distress on existing pavements.

This study is part of an evaluation study of CRCP structural performance of highways in the rural districts of Texas and is based on information from two districts in Texas. A gross analysis concentrates on all the highways surveyed but excludes some of the design and construction variables that can only be obtained from construction records. Both studies will be useful in the pavement management system presently employed in Texas.

IMPLEMENTATION STATEMENT

The analysis of the structural performance of continuously reinforced concrete pavements on the basis of theoretical models provides for the extrapolation of results to conditions other than those prevailing at the test sites. The resulting equations for design and maintenance purposes can therefore be used to predict structural failure both on new and existing pavements. Assessment of the variables involved provides a groundwork for the evaluation of maintenance techniques and enhances an understanding of the manifestation of different distress types.

Several recommendations are included in the report which will be beneficial in CRCP design, maintenance and rehabilitation.

TABLE OF CONTENTS

CHAPTER 5. THE REGRESSION ANALYSIS

CHAPTER 6. DISCUSSION AND APPLICATION OF RESULTS

APPENDICIES

CHAPTER 1. INTRODUCTION

The structural performance of a pavement is of concern to both maintenance and design engineers since premature structural failure reflects undesirable design and construction methods and means the incurrence of untimely maintenance cost. In order to quantify the structural condition of continuously reinforced concrete pavements (CRCP) from which an assessment of the structural condition of the pavement is possible, a condition survey of all CRCP in the rural areas of Texas was initiated in 1974 (Ref 1).

The results of the condition survey provide a means of comparing the structural performance of different highways on the basis of a quantitative comparison of the similar types of distress. The significance of the manifestation of different types of distress and their relative effect on the overall structural performance of CRCP, however, still have to be analyzed. An analysis which considers the different design, construction and environmental variables and their contribution to an eventual structural failure in the form of a punch-out can be beneficial both from a design point of view and for the prediction of future structural failure for maintenance or rehabilitation planning.

BACKGROUND

The design and construction of continuously reinforced concrete pavements does not incorporate transverse joints for contraction or expansion; instead, a random pattern of transverse cracks is allowed to develop as a result of shrinkage and temperature changes. Longitudinal steel reinforcement is placed in the slab to ensure a narrow crack width, thus preventing the intrusion of surface water and foreign matter. Hence, good load transfer at cracks is retained for a great part of pavement life and better structural performance is provided. Since transverse joints are nonexistent, a major source of rigid pavement maintenance is excluded from CRCP. Thus, theoretically, CRCP can be considered as maintenance free over a good part of the design life.

The use of continuously reinforced concrete as a pavement has become very popular in Texas since 1960. This particular type of pavement structure seemed especially desirable on the heavily travelled Interstate Highway System, where an extended maintenance-free pavement life was essential for successful pavement management. However, in practice, it was found that maintenance was required on certain pavement sections much sooner than expected. Furthermore, there was a considerable variation in structural performance of the pavements, not only from district to district, but also from section to section. In order to quantify this variation objectively, a project was initiated to measure the condition of the pavement in a relatively rapid and inexpensive way. This work was completed in 1974. It provided the basis for a study into the relative importance of design, environmental and construction variables on the structural performance of a continuously reinforced concrete pavement (CRCP) which will be described in this report.

OBJECTIVE

Two thousand miles (3219 km) of 24-foot (7.32 m) wide CRCP pavement that has been built in the rural areas of Texas since 1958 was surveyed for cracking, spalling, pumping, punch-outs, and repair-patches. In order to research the relative importance of all possible variables on the structural performance of a CRCP, 56 sections were selected on the Interstate Highway System for a detailed study. Design and construction information were retrieved from construction plans and files which together with field measurements of deflection, road roughness, cracking pattern and crack width, could be used in an analysis of structural performance.

The objective of this report is to relate the known design, construction and other variables to the structural performance of a CRCP. Since all the CRCP in Texas will have to be analyzed at some point in time it will be a great advantage to develop analysis and measuring techniques which will assist in the rapid evaluation of pavement condition. Instead of employing an elaborate program of sampling and laboratory testing of specimens, it is intended to engage the Surface Dynamics Road Profilometer for road roughness measurements and the Dynaflect for deflection and surface curvature measurements from which slab and subgrade stiffness values can be derived.

The study is based on information from two highways only and it is the aim to use theoretical models whenever possible which will enable the user to extrapolate the final equations to other conditions. Unfortunately, no single theoretical model exists which can be applied in this respect so that a regression technique is used to tie together as many theoretical models as possible.

SCOPE

The report discusses the variables that potentially can effect structural performance. Although these variables can be evaluated individually by an elaborate field and laboratory study, it will be too extravagant for application in the analysis of several thousand miles (kilometers) of existing highway. Variables that fall in this category include the exact quantification and prediction of settlement and swell of subgrade layers, the fatigue behavior of the concrete in the slab and the quantification of climatic and environmental effects. Instead it is intended to measure the effect of the above mentioned variables in terms of subgrade and slab stiffness and road roughness by using the Dynaflect and Profilometer.

The components that may be of concern in the structural analysis of a CRCP are discussed in Chapter 2. The different models that are discussed include the calculation of stress in a pavement, the importance of settlement, swell and erosion in the change in subgrade support and the properties of the concrete that may have a bearing on structural performance. In an effort to include as many variables as possible, a proposed method of analysis is summarized in the last part of Chapter 2 with special reference to the calculation of stress in the pavement, a fatigue model that relates stress to number of load applications and a stochastic model that bridges the gap between the amount of measurable distress in the pavement and the number of loads applied.

Chapter 3 is devoted to the development of the proposed analysis model which includes the fatigue coefficients that will be derived by regression techniques. The regression technique is discussed in Chapter 4 and the regression analysis itself in Chapter 5. The resulting equations and their significance in maintenance, rehabilitation and design are discussed in Chapter 6 and Chapter 7 concludes the report with a summary of the findings.

CHAPTER 2. DEVELOPMENT OF AN ANALYSIS APPROACH

The structural performance of any pavement for highways or airports built with portland cement or asphaltic concrete depends on the ultimate support from the underlying subgrade, the paving materials, and their behavior under loads, as well as the influence of climatic conditions. A host of publications have discussed possible effects of all these variables on pavement performance and some of the more important aspects need to be discussed and evaluated for this study. It is important, however, to realize initially that the economic quantification of variables is a major restriction on any engineering venture, and this study is no exception.

An attempt will be made in this chapter to describe the different theoretical considerations in the evaluation of structural performance. It will be shown that the wide range of requirements make it almost impossible to tie together all relevant theoretical models into one useful model unless a regression technique is used.

Factors that theoretically influence structural performance and which will be discussed here, can be classified in several categories:

(1) stress in the pavement due to the magnitude of subgrade support, wheel loading, and slab properties;

(2) variation in subgrade support as influenced by moisture, settlement, swell, and other factors;

(3) environmental effects, specifically the variation in moisture, temperature, and their influence on crack spacing and crack width;

(4) the properties of the concrete slab itself with special reference to stiffness and fatigue characteristics.

The first part of the chapter will be devoted to a discussion of the variables that may influence structural performance. In order to combine as many of these variables into one useful model, a proposed method of analysis will be outlined in the second part of the chapter. The relation between stress in the pavement slab and number of load applications will be discussed as well as the proposed method of relating distressed pavement area to an anticipated number of load applications.

FACTORS THAT POTENTIALLY CAN AFFECT STRUCTURAL PERFORMANCE

The structural performance of a pavement is influenced by many factors of which stress is probably the most important. Stress is related to the load on the pavement, the geometry of the layers in the pavement structure and the materials properties. This section will discuss the calculation of stress in a CRCP using different equations and techniques. Subsequently the variables that affect a variation in subgrade support will be touched on with a special reference to environmental influences. Finally the properties of portland cement concrete and their relation to strength and fatigue characteristics will be discussed.

Stress in the Slab under a Wheel Load

The stress in a pavement slab can be calculated if the slab stiffness, subgrade stiffness and the magnitude of the load on the slab is known. Certain basic assumptions simplify the calculation of stress but does not necessarily reflect the true value of stress in a CRCP. These assumptions include:

(1) The slab material is assumed to be isotropic and homogeneous in in all directions which is not always the case because of difficulties in compacting a reinforced slab uniformly in the field. A certain variation in the quality of the mix can also be expected.

(2) A medium thick slab is assumed in which only flexure and torsion need to be considered, thus a two dimensional problem (Ref 2). This is not always the case in a CRCP where diaphram action and stretching due to horizontal shrinkage and thermal movements can be of importance.

(3) Some stress equations assume uniform contact between slab and subgrade which again is not always true because of swell, settlement and erosion of the subgrade which may result in voids under the slab due to membrane action of the slab as mentioned under (2) above.

Some useful methods need to be discussed which will be of value in the development of the structural performance equation.

Timoshenko (Ref 3) developed equations for bending moments, and therefore stress, in a slab which is simply supported around the edge. Westergaard (Ref 4) extended this theory and applied it to a slab on an elastic foundation where the stiffness of the subgrade is measured in terms of a coefficient k which is called the modulus of subgrade reaction. This formulation of subgrade reaction is sometimes referred to as a Winkler foundation.

Westergaard derived stress equations of the same format for edge and and interior loading conditions. This will be discussed in more detail in Chapter 3 where the similarity between the equations will be shown to be a function of slab geometry and load configuration.

The Westergaard solution has been widely used for portland cement concrete pavements, but several researchers (Refs 5, 6, and 7) have questioned the validity of the approach for continuously reinforced concrete pavements (CRCP) which have closely spaced transverse cracking. Zuk (Ref 7) suggested an alternate approach by substituting k with an aggregate interlock modulus k_3, a restraint for the action of steel reinforcement k_2, and a subgrade modulus k_1. The Zuk equation recognizes the basic concept in a CRCP, namely the need to distinguish between the load transfer characteristics of the aggregate interlock and the steel reinforcement but difficulty in evaluating k_2 and k_3 complicates the use of the equation.

Several computer programs were developed to solve the differential equation for an elastic slab on an elastic subgrade. A discrete element method was employed by Hudson and Matlock (Ref 8) using a physical model consisting of a system of elements whose behavior could properly be described by algebraic equations. This is similar to models for articulated beams and plates pioneered by Newmark in 1949 (Ref 5). The physical model consists of a system of rigid bars connected by deformable elastic joints, with torsion bars connecting adjacent parallel bars.

Experience with the model indicated that reasonable results were obtained. The accuracy increases with a decrease in bar-element lengths, although the lengths will most certainly depend on the dimensions of the problem as well as the accuracy required (Ref 8).

This method of stress evaluation has several advantages, especially with reference to a CRCP analysis:

(1) the load can be varied in magnitude and position;

(2) the materials and slab properties can be varied from point to point,

(3) discontinuities such as cracks and edges at any location in the slab itself can be treated, and

(4) the slab support can be varied from point to point to account for nonuniform as well as "zero support" conditions.

Distrete-element methods were also developed to solve for stress in a slab (Ref 9). One of these methods was suggested by Huang and Wang (Ref 10) and is based on the theory of minimum potential energy. The slab is divided into small elements interconnected at a finite number of nodal points, which yields a stiffness matrix, the equations of which are solved by high-speed computer. The subgrade is assumed to be of the Winkler type.

One other method of stress analysis that deserves attention is the simulation of a CRCP by a beam on an elastic (Winkler) foundation. Derivation of equations to be used in this respect are included in Appendix 1 of this report. Simulation of a CRCP as a beam on an elastic foundation seems to be justified if it is kept in mind that the longitudinal reinforcement ensures a maximum amount of load transfer at the cracks so that the CRCP can be considered almost uniform, especially in the early part of its life. The load is assumed to be a strip load on a beam of unit width. The implication of the assumption that a CRCP can be simulated by a beam, will be discussed in more detail in Chapter 6.

The role that load transfer at the crack plays in a CRCP is of increasing importance. Thus the possibility of moment transfer is compared to shear load transfer through aggregate interlock and dowel action of the steel reinforcement in Appendix 2. It is pointed out that dowel action is probably of prime importance with aggregate interlock playing a significant role. Load transfer is an important consideration in the successful structural performance of a CRCP and will be included in the performance model that will be discussed later on in this report.

Several methods of stress calculation were introduced in this section, some of which cannot be used without resorting to a computer. The Westergaard solution has been applied widely and is accepted as a reliable equation for jointed pavements as well as for CRCP in good condtion; i.e., without deterioration in the cracks. The use of the beam simulation in the structural analysis of CRCP also seem to be worth considering. However, all the methods discussed above will play a role in the development of a structural performance model in the next chapter of this report.

Subgrade Support

The dependence of bending stresses in a portland cement concrete slab on the magnitude and position of the load, the stiffness of the slab, and the stiffness of the subgrade have been discussed in the previous section. Of these factors, the subgrade support or stiffness can probably be considered to be the least predictable over the design life of the pavement because of the probablility of settlement, swell, pumping, and erosion, which may result in a loss of support or even create voids under the slab. An understanding of factors that may contribute to a change in subgrade support is necessary for the proper prediction of structural performance of the pavement; therefore they need to be discussed in more detail. The first concept that will be dealth with is the modelling of subgrade through theory. This will be followed by a discussion on the influence of environmental and time effects on subgrade support.

Mathematical Models. The subgrade support has been modelled as a dense liquid, that is the subgrade reaction is a linear function of the deformation. This approach was first introduced into rigid pavement design by Westergaard and, although the concept is open to criticism, it is still in wide use. The biggest concern stems from the fact that a subgrade soil supporting a pavement is not uniform and is not an idealized elastic mass, as represented by the k value.

Alternatives that have been proposed include the suggestion by Vesic and Saxena to modify k by the ratio of Young's Modulus for the concrete pavement to that of the subgrade, and the elastic solid concept introduced by Hogg and Holl (Ref 5). The first proposal is not significantly different from the Westergaard approach, but it attempts to refine the Winkler approach by a more scientific characterization of subgrade materials properties. The elastic solid subgrade theory considers the subgrade foundation to be a semi-infinite elastic half space, and was used by Holl (Ref 11) to solve for stress in a thin plate on an elastic foundation. Thus, the subgrade support is a function of the elastic properties, and was originally used by Boussinesq to solve the problem of a perpendicular load on a semi-infinite solid (Ref 12).

All the criteria mentioned above, which are used for subgrade characterization, somehow involve the elastic behavior of subgrade materials in rigid pavements. Experience has shown that deformation of the subgrade is actually of much more consequence to rigid pavement performance. Deformation usually manifests itself in the form of loss in subgrade support and can be defined in terms of subgrade settlement, or subsidence; swell of clay subgrades, which causes voids in adjacent sections; and hydraulic erosion, most commonly defined as pumping.

Soil Moisture. The moisture content in soils plays an important role in the settlement, swell and erosion of subgrade layers. Important sources of moisture are through percolation, seepage, osmotic and suction movements. Percolation and seepage are only possible through gravitational potential, whereas migration of moisture due to a different in ion concentration in the soil water, is called osmotic movement. The latter is generally ignored, since ion concentrations are generally low in soil water.

Water found in the pavement structure originates from a wide variety of sources, but the most abundant source undoubtedly is precipitation or supply from surface water. Other important contributors are ground water and seepage as a result of roadside landscaping and irrigation. Surface water from rain enters cracks and openings in portland cement concrete pavements, and estimates from research at the University of Maryland (Ref 13) indicated a range of from 70 percent of runoff entering cracks 0.035-in.(0.89- mm) wide to 97 percent entrance of 0.125-in. (3.18-mm) cracks. Studies by McCullough et al (Ref 14) indicated "dramatic increases in the permeability of cracks with widths greater than 0.023 in. (0.58 mm), with almost instantaneous flooding of the transverse cracks at a width of 0.03 in. (0.76 mm)." The entrance of water through the adjacent unpaved shoulder area also may be considerable if the slope of the shoulder is not greater than twice the slope of the pavement (Ref 13). This condition often occurs when the longitudinal slope of a drainage ditch is less then mentioned above or when vegetation in the ditch itself impairs its drainage capability.

Suction can be defined as a negative pressure in the pores of the soil structure, because of the capillary movement of moisture from a lower to a higher (in elevation) source. Thus, suction is basically an interaction of fluid and solids. The migration of water in this way is considered to be the

most import factor in stabilizing pavement moisture content. Suction is not a constant for a soil, but changes with a change in moisture content and density. Other factors that influence suction are soil structure, temperature, relative humidity, and whether the soil is in a setting or drying cycle (Ref 15).

The water content of a subgrade soil has been shown to depend on many factors. One of the most important aspects that has not been discussed is the availability of water and the change in the source with a change in environment.

The moisture content in a soil depends on the climate of the region. Actual moisture in the soil can be calculated if the capacity of the soil to store water, evapotranspiration and rainfall are known. Thornthwaite (Ref 16) suggested a simple way to calcualte moisture in the soil by using a moisture index which combines evapotranspiration, drainage and capacity. This will not be investigated in more detail here since the effect of moisture will actually be measured in terms of actual subgrade support.

The permeability of the soil has been mentioned, but the factors that influence permeability need more attention. The factor that influences permeability the most is probably the non-capillary pores content (Ref 17). The non-capillary pores can be associated with the soil structure, which changes with density in a cohesionless soil and with moisture content in a clay. The degree of saturation changes the capillary and suction forces in a soil, and therefore also affects permeability. Permeability in saturated flow is significant in rigid pavement performance in that it affects the seepage of water from the pavement itself in the event of the occurrence of pumping, as is discussed in Appendix 3.

Soil moisture variation has a profound influence on the strength of a subgrade, and therefore on the behavior of a pavement. Thom (Ref 18), for example in reporting on a ten year study at 100 stations, suggested that moisture changes in the top 1 to 2 feet (0.3 to 0.6 meter) of soil, can be related to surface temperature as well as the amount of hours of rain more than 0.01 inches/hour (.25 mm/hour). This in turn results in variations in deflections with a seasonal change (Refs 19 and 20) which affects pavement behavior and thus structural performance.

The most important effect of free water, or even a high moisture content in the base layer, is the hydraulic erosion in the form of pumping, where pumping can be defined as the ejection of soil and water from beneath a

pavement due to the deflection of the slab at a joint, edge, or crack (Ref 21). This phenomenon has been a major concern to highway engineers since World War II, and it was investigated to a great extent in 1948 by a committee of the Highway Research Board (Ref 22). Pumping also contributed significantly to the failures of rigid pavements at the AASHO Road Test (Ref 23). Since hydraulic erosion is considered to be of such great importance, a more detailed study is included under Appendix 3 of this report.

Temperature Effects

Variations in temperature cause thermal stresses in a concrete slab. A temperature gradient through the thickness of a concrete slab results in warping stresses which can be calculated if the thermal coefficient, modulus of elasticity, temperature differential and the actual dimensions of the slab are known (Ref 6). Longitudinal thermal stresses in the slab of a continuously reinforced concrete pavement is a result of a change in average slab temperature and is a function of crack spacing, creep, the amount of steel, friction between the slab and the base, as well as slab properties as mentioned above. Associated with the problem of horizontal slab movement is the change in load transfer at the crack as the crack width changes. Nowlen (Ref 24) investigated the change in load transfer with a change in aggregate size and crack width, but without steel reinforcement. This will be discussed in more detail in a later paragraph, where it will be related to the structural performance of a CRCP.

Temperature also affects the engineering behavior of soils and specifically the properties of clay (Ref 25) but the effect is so small that it is not worth considering in this study.

Properties of Concrete

Concrete is a composite material which consists essentially of a binding medium within which are embedded particles or fragments of a relatively inert mineral filler. The cement paste has been defined as the active part of concrete. The strength performance of concrete, either in a structure or on a road, is largely influenced by the properties of the paste, assuming a high quality aggregate is used. This is particularly true for the fatigue characteristics of a concrete which is discussed in the next paragraph.

Fatigue of Concrete. Fatigue in concrete has been under investigation since about 1900 with the majority of work being done in the past 25 years. Fatigue can be defined as the process of progressive, permanent structural change occurring in a material which is subjected to conditions which produce time fluctuating stresses and strains. The need to understand the mechanics of fatigue has been emphasized lately by the greater demand for more economical structures which could carry an increasing number of different dynamic and static loads.

The main problem in researching fatigue is the different failure modes, i.e., failure in compression, diagonal tension failure in shear, failure in tension and fracture of reinforcing steel bond with concrete. Three different loading conditions exist for the concrete in a CRCP. The first is flexural loading of the concrete in the slab between two transverse cracks. This condition is generally designed for when stress in the slab is calculated. The second condition occurs at the crack itself where the failure of aggregate interlock and thus load transfer by this means, is a function of shear loading of the aggregate or the concrete at the crack. Direct loading of the concrete below the steel, as a result of dowel action of the steel reinforcement at the crack, as well as tensile loading of the concrete on either side of the steel constitutes the third type of loading experienced in a CRCP. The latter two loading conditions are discussed more extensively in Appendix 2 of this report.

There is no doubt that cracks are present between aggregate and mortar, even before any external loading has been applied. These flaws act as stress raisers and minute volumes of the matrix are stressed to the ultimate strength of the paste when stresses resulting from shrinkage, temperature differentials, or applied loads occur. The critical regions are tips of flaws or faults which act as high stress concentrators. Stress relief is only possible by a formation of micro-cracks which leads to fracture or failure.

Murdock and Kesler (Ref 26) found that the higher the stress, the shorter the fatigue life and the smaller the range from minimum to maximum loading, the longer the fatigue life.

Hilsdorf and Kesler (Ref 27) were the first to investigate the influence of the rest period on the behavior of concrete. Rest periods of more than five minutes had no effect on fatigue strength. With rest periods of zero to five minutes, the fatigue strength increases substantially from 62 percent,

at no rest period, to 68 percent of static ultimate flexural strength, at a 5 minute rest period.

Although little research has been done on the influence of concrete properties in fatigue life, the general conclusion is that concrete properties have no effect on fatigue life if fatigue strength is defined in terms of static ultimate strength. It has been shown, however, that the presence of early flaws have a significant influence on crack propogration and thus strength. It can therefore, be assumed that severe shrinkage, curing problems, bleeding, and cement properties that influence the above mentioned characteristics, may influence fatigue strength of a pavement slab to a certain degree. Much more research is required to confirm this however. An interesting finding is that the failure strain for concrete under repeated loading is significantly greater than that under static loading.

Strength of Concrete. The strength of the portland cement concrete affects the fatigue life and thus the structural performance of the pavement. Several other desirable properties such as stiffness, watertightness, resistance to abrasion and weathering, are associated with a higher strength concrete. However, stronger concrete usually exhibits more shrinkage, therefore, it is more crack susceptible, which is an undesirable property for pavements.

The quantity of water relative to that of cement, can be considered as the important factor that determines the strength of concrete. The exact change depends on the materials, the age of the specimen, the magnitude of water/cement ratio and the testing procedure. A decrease in the water-cement ratio, reduces the workability of the mix, whereby the density is impaired due to poor compaction, which leads to a reduction in strength in the field. Orchard (Ref 28) reports that concrete strength decreases by 30 percent with 5 percent void content and 50 percent with 10 percent void content if the voids are due to poor compaction. Compaction voids are generally interconnected and large as opposed to the dispersed, isolated and micro-voids, caused by air entrainment chemicals, which is used for improved workability and increased durability.

The performance of vibration equipment is important in compacting concrete, but depends on the workability of the concrete. For maximum compaction the workability requirements may vary extensively for different vibrators.

A research study in Britain (Ref 29) suggested that the best compaction down to the bottom of a 9-inch (22.86-cm) slab, with a screed vibrator, was achieved at an optimum water/cement ratio of 6.4 U. S. gals/sack (0.57 W/C). A 5.8 U.S. gals/sack (0.52 W/C) and 7.0 U.S. gals/sack (0.62 W/C) water content resulted in about the same depth-density distribution. Other important considerations are the speed of compaction, the amplitude and frequency of vibration, as well as the weight of the vibrator. The density of the concrete not only affects strength but is also related to the stiffness of the concrete. The American Concrete Institute, Building Code (Ref 30), suggests a relationship for the static modulus of elasticity in pounds per square inch:

$$E = \gamma_c^{1.5}\ 33\ \sqrt{f'_c} \tag{2.1}$$

where:

γ_c = density of the concrete in lb/ft^3

f'_c = compressive strength of the concrete (psi),

if the modulus cannot be measured. This relationship is valid for concrete densitities between 90 and 155 lb/ft^3 (1442 Kg/m^3 and 2483 Kg/m^3) and can be considered only an approximation for use in pavement design and performance since the secant modulus depends not only on materials properties, as suggested by the equation, but also on the magnitude, speed, and method of loading. Materials properties, which can be implied from the relationship, that have a significant influence on the modulus of elasticity are the richness of the mix, water-cement ratio, curing conditions, moisture content of the concrete, and the kind and gradation of the aggregate (Ref 31).

The type and gradation of aggregate used in the manufacturing of concrete play a dominant role in its ultimate strength and thermal behavior. Generally, a continuous well-graded aggregate is preferred for maximum density and strength which can be attained with the minimum amount of cement. This reduces the shrinkage and improves the durability of concrete, both desirable properties in a portland cement concrete pavement. The importance of a proper grading in the smaller size cannot be overlooked in this respect since a lack of

fines, less than 0.0116-inch (0.300-mm) material, contributes to a high void ratio, permeability, and bleeding. An increase in fines increases the water requirement and shrinkage and thus reduces durability and strength. The properties of the coarse fraction, however, exert the biggest influence on the thermal properties of a concrete. Although the richness of a mix has an influence on the thermal expansion (a 10 percent increase in thermal expansion with a doubling of cement content), a change in coarse aggregate fraction from limestone to siliceous river gravel may increase thermal movement three times to about 5 X 10^{-6} in/in per ^{0}F (9 X 10^{-6} mm/mm per ^{0}C) (Refs 28 and 31).

Load transfer at a crack is a function of concrete properties and, specifically, of the coarse aggregate shape and size. Nowlen (Ref 24), in a laboratory and field study of load transfer characteristics of different aggregates, found that larger maximum sizes of aggregates contributed more to the preservation of load transfer at a crack in a slab, with an increase in loading. The study indicated that natural gravel aggregates could be simulated by a sphere in a matrix (Fig 2.1), whereby a vertical movement f is possible before contact is made. This concept is discussed in more detail in Appendix 2 of this report. This simulation did compare very well with field measurements of relative movement at a crack before load is transferred from one to the other side of the crack. Nowlen measured a vertical movement of 0.0035 inch (0.09 mm) for 3/4-inch (19-mm) aggregate at a 0.035-inch (0.9-mm) crack width, and 0.001 inch (0.025 mm) for 1-1/2-inch (38-mm) stone at the same crack width. The abrasion of the coarse aggregate was important in the sustenance of load transfer with an increase in loading. Aggregate of a Los Angeles Abrasion Loss Value (LA) of 17, performed just as well after 100,000 load cycles as at the start of the test, whereas aggregate with a value of 28 had lost about 50 percent of its load transfer capabilities after the same number of cycles. The same was true for a crushed stone, although a crushed stone with a LA of 28 had lost 20 percent of its capabilities after 100,000 load cycles (Ref 24).

One other aspect of concrete strength that is of concern, especially in the design and structural performance of a CRCP, is its relationship to crack spacing and crack width. Several studies were made to quantify the relationship between concrete strength, steel stress, friction between slab and base, and crack spacing/crack width. As a result of one of these studies (Ref 14), a program was developed which enables the designer to predict crack

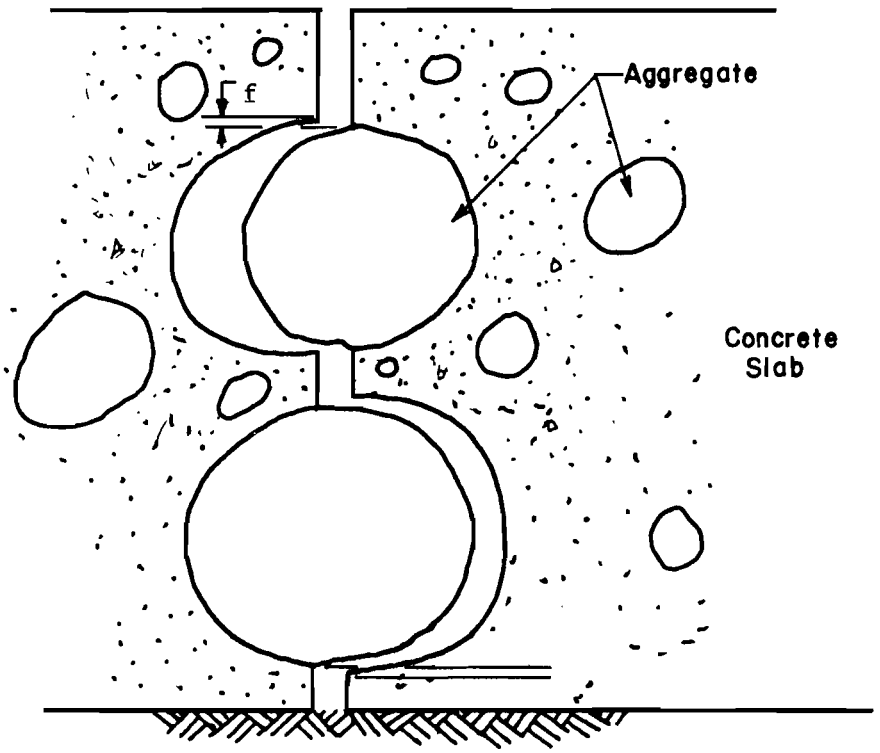

Fig 2.1. Simulation of coarse aggregate in concrete by spheres (Ref 24).

spacing, crack width, and steel stress. The importance of the steel reinforcement in withstanding the stress developing from thermal activity and drying shrinkage was investigated by Shelby and McCullough (Ref 32). Both these studies indicate the importance of restraining concrete strength within narrow limits since concrete of too great strength causes high steel stress, wide crack widths, and large crack spacing. On the other hand, if the concrete strength is too low, slab stiffness is sacrificed, because of the decrease in flexural strength and through a reduction in crack spacing.

STUDY HYPOTHESIS

Several potential contributors to poor structural performance of rigid pavements have been discussed under different headings. The traditional approach to pavement design has been to address the problem from a stress analysis point of view, which still is a sound attack. Since structural failure is a time dependent phenomenon, the fatigue behavior of materials cannot be severed from stress analysis, which brings about a requirement to know the loading conditions and materials properties. Add to this the significance of subgrade support and, thus, the relative importance of swell, settlement, and erosion behavior, and it becomes evident that structural performance involves more than just stress analysis.

An appraisal of existing theories on different aspects on rigid pavement design, that may affect its structural performance, has shown that many variables need to be evaluated. Most of the information is only attainable through a program of extensive measurements and evaluation which involves the incurrence of considerable costs. As a first step, construction files containing information on the initial conditions, quality of materials and workmanship can be surveyed. Since a limited amount of data is available from these files, techniques for the reasonable assessment of in-situ pavement characteristics, need to be considered. Therefore the evaluation of a great variety of variables is necessary before the accurate prediction of settlement, swell, erosion, fatigue behavior and structural failure will be possible from a purely theoretical point of view. The extensive field and laboratory program that will be necessary to accomplish this goal is contrary to the aim of the study namely the development of a viable but economical evaluation technique of the structural performance of existing CRCP which

can also be used to predict the extent of future structural failures. However it is necessary to base the evaluation technique on theory in order to ensure sensitivity of the final structural performance model to as many variables as possible.

A flow diagram of the concepts that were discussed and their relation to each other is shown in Fig 2.2. In order to calculate stress, values for the magnitude of loading, slab stiffness and subgrade support is required. Subsequently the number of load applications to failure relates to the stress in the pavement and can be calculated from the following equation:

$$\text{Number of loads } N = C\left(\frac{\sigma}{f}\right)^{d_o} \tag{2.2}$$

if

σ = stress under one load application,

f = strength of the CRCP slab, and

C and d_o = fatigue coefficients

are known. The stress σ can be calculated as indicated previously and the strength f can be measured from laboratory testing. The values for C and d_o are known for different laboratory and field conditions but vary greatly and still have to be established for a CRCP.

The extent of structural failure can physically be measured in the field and can be expressed in units of area. The ratio of area failed to area surveyed can be related to number of load applications through a stochastic model as developed by Darter and Hudson (Ref 33):

$$Z = \frac{\log n - \log N}{S} \tag{2.3}$$

where

N = the theoretical maximum number of load applications possible as determined from 2.2,

n = the actual number of load applications applied so far,

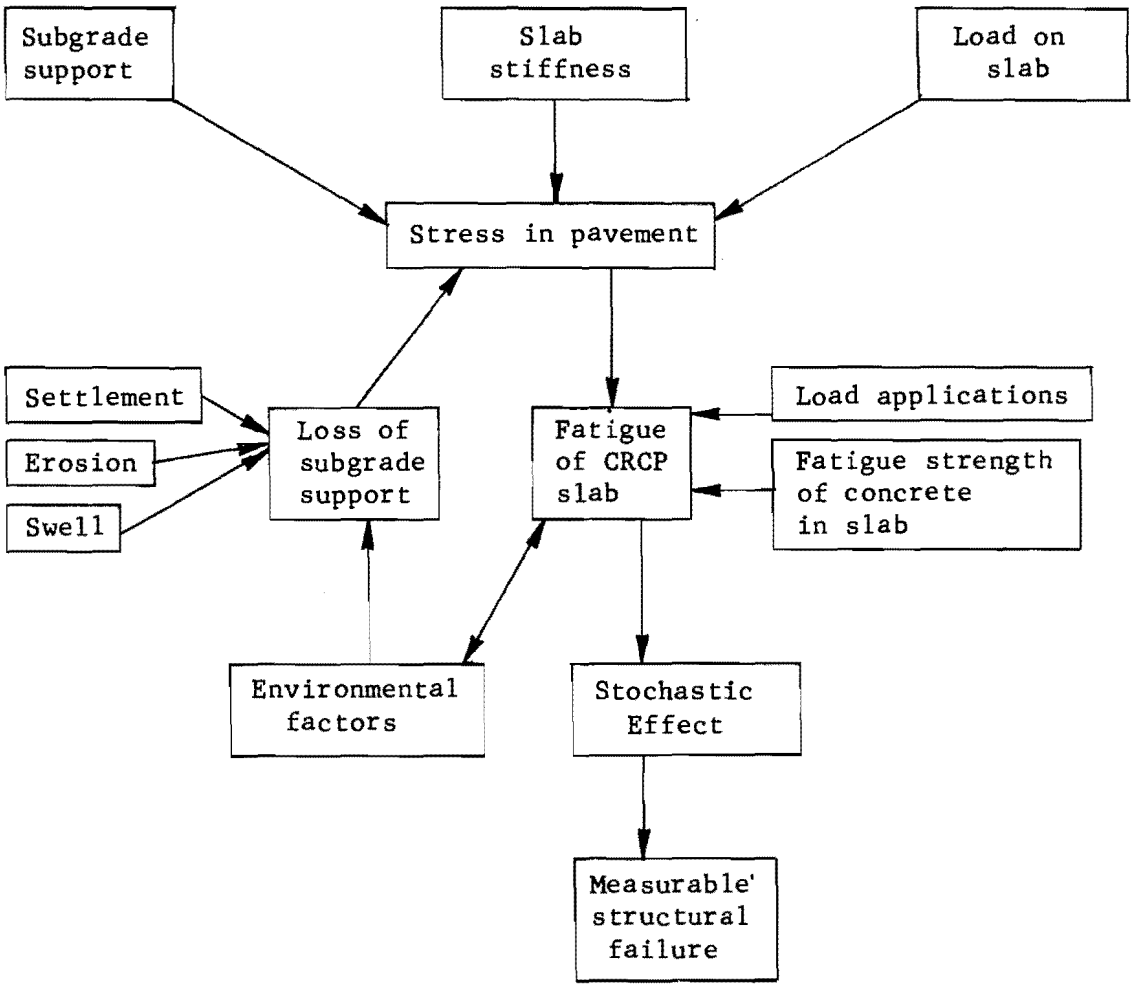

Fig 2.2. Flow diagram indicating theoretical models involved in structural performance analysis of a CRCP.

S = the standard deviation of log N and log n combined, and

Z = the standard normal variable.

The standard normal variable Z can be determined from a table of values of the standard normal distribution function if the ratio area failed to area surveyed is known. The relationship between Z and failed area is summarized in Fig 2.3.

The prediction or the measurement of a loss in subgrade support and the actual values of the fatigue coefficients C and d_o in Eq. 2.2 still need to be determined. It is proposed in the next chapter that the fatigue coefficients be determined through regression analysis and that the loss of subgrade support be quantified by a field measurement of actual subgrade stiffness. Both subgrade and slab stiffness can be measured on existing pavements whereby stress in the slab can be calculated. Thus the flow diagram in Fig 2.2 can be completed with little regard to the relative contribution of settlement, swell, erosion and environmental factors to a variation in subgrade support. The development of the flow diagram as shown in Fig 2.2 is discussed in detail in Chapter 3 where all the relevant theoretical models are tied together using regression techniques.

Several useful theoretical models exist and were discussed previously. These can be incorporated into the regression model whereby extrapolation to conditions other than those prevailing at the test sites will be possible. This will also contribute to the validity of equations derived from the analysis. Hence, the structural performance of a pavement can be associated with variability in the pavement, or the stochastical nature of pavement characteristics, and stress in the pavement due to external loads and environmental factors. The analysis of stress in the pavement includes the materials properties of layers in the pavement structure, different loading conditions as well as geometric characteristics, whereas variation in these factors due to design construction or other factors are associated with the stochastical nature of the analysis. The possibility of including theoretical models and stochastics in a regression analysis, poses no constraint, which makes the analysis of the structural performance of CRCP in this way more attractive. The remainder of the report will, therefore, be devoted to the

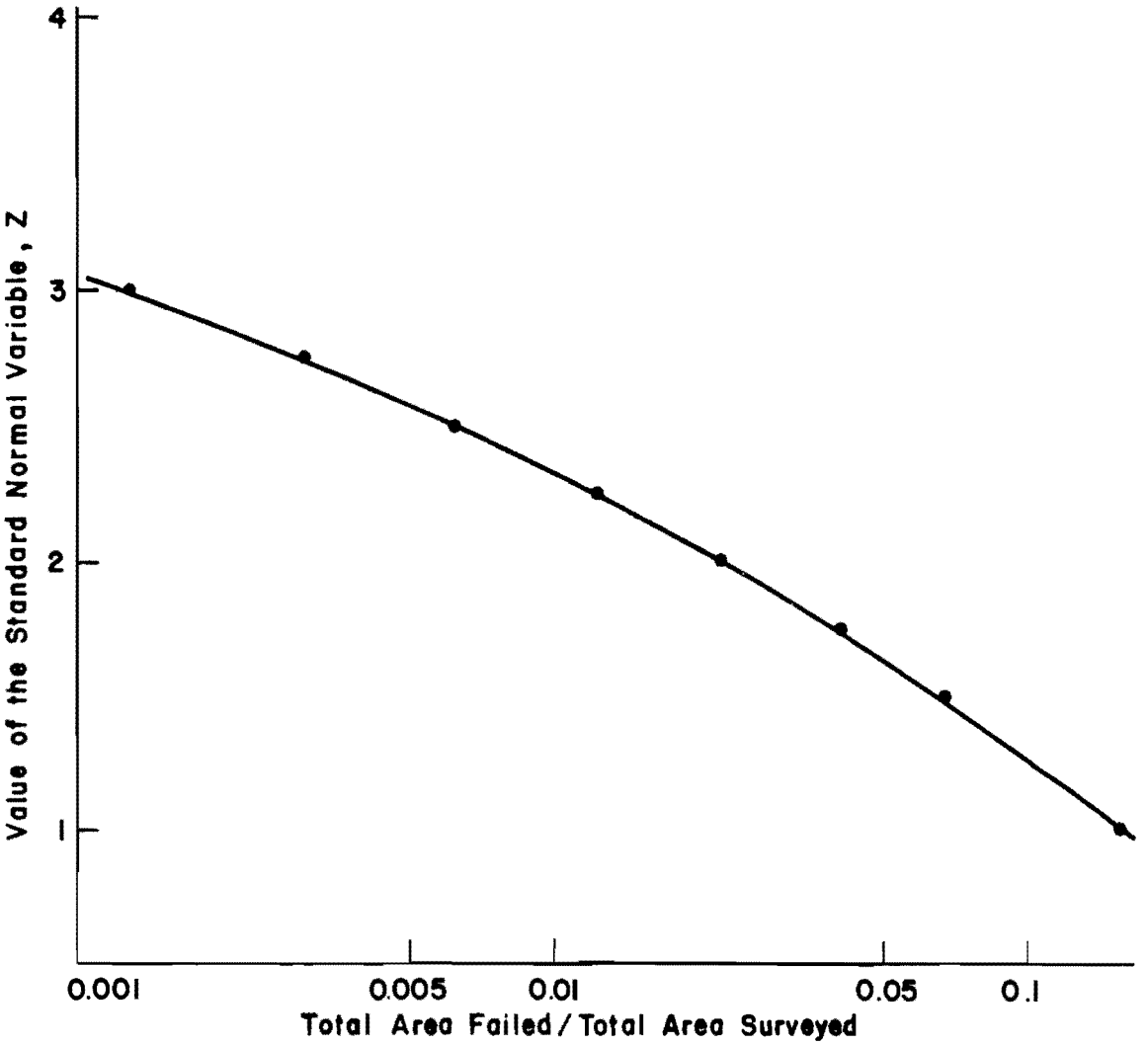

Fig 2.3. The standard normal variable Z as a function of area failed/area surveyed.

development of a regression model. The usage of existing theoretical models, the derivation of required models, the measurement of unavailable data and the arrangement of sections to be analyzed to incorporate as many relevant conditions as possible, are discussed in the next section.

CHAPTER 3. DEVELOPMENT OF ANALYSIS MODELS

Structural failure in a pavement, which can be considered as a progressive phenomenon occurring with time or an increase in loading, is a stochastic concept. Thus, it is associated with the probability of failure at a specific point in the pavement, due to a variation in pavement characteristics. Incorporated in this concept is the fatigue or wear-out function, which is associated with failure due to repeated loading. Since loading and fatigue are stress and strength associated, it is necessary to include a stress function as well as materials properties and the geometric characteristics of the pavement. The variables that relate to stress in a pavement as well as materials properties have been discussed in a previous chapter. This chapter will attempt to pull together all relevant theory which is involved in a stochastic anlaysis of structural performance, including fatigue behavior, that can be used in the proposed regression analysis.

The stochastical approach to distress, which includes the derivation of relationship between the area of distress as measured on the pavement and some theoretical models that were discussed in the previous chapter, will be investigated first. The fatiguing of the CRCP slab and its relationship to stress in the pavement, which includes a field evaluation of the ratio of slab stiffness and subgrade support, is handled next. The last part of the chapter is devoted to the construction of a regression model, which includes a discussion on the load transfer properties of the aggregates and the steel reinforcement.

STOCHASTIC APPROACH TO PERFORMANCE

Reliability in the structural performance of a pavement can be defined as the probability that the structural condition of the pavement will be adequate throughout its design life. Hence, the reliability of a pavement in regard to pumping can be defined as 95 percent, for example, if it is anticipated that 5 percent of the pavement length will experience pumping at some stage of its design life. The length of pavement can be selected

to represent any section and reliability can then be calculated as a ratio of the structurally unfailed area to the total area.

Structural failure is possible through many mechanisms, as discussed in the previous chapter. However, a stress of some sort is necessary for failure to occur in a pavement. Of all possible stresses, stress induced by traffic loading can be considered the most important. Failures as a result of traffic load induced stresses can be caused through either a fatigue mechanism or simply a one-time overload at a weak spot. The latter cannot be considered as time related and, as such, cannot be included in a fatigue analysis.

Darter and Hudson (Ref 33) combined the fatigue concept and reliability to derive an equation that related reliability R to the probability D that the actual number of loads applied n may fall short of the designed number of load applications N :

$$R = P(N > n)$$

Applying the conclusion of Darter and Hudson that both log N and log n can be considered normal distributions, reliability can be written as

$$R = P\left[(\log N - \log n) > 0\right] = P\left[D > 0\right]$$

where

$$D = \log N - \log n \ .$$

Since both log N and log n are normally distributed and have a standard deviation associated with each, D can also be considered as normally distributed. The standard normal variable Z can then be written

$$Z = \frac{D - \overline{D}}{S_D}$$

where

$\bar{D}$ = mean of D , and

S_D = standard deviation of D .

The difference density function f(D) and the concept of failure probability are illustrated in Fig 3.1. For

$$D = 0 ,$$

$$Z = Z_0 = -\frac{\bar{D}}{S_D} = -\frac{\log N - \log n}{\sqrt{S^2_{\log N} + S^2_{\log n}}}$$

where

$S_{\log N}$ = standard deviation of log N, and

$S_{\log n}$ = standard deviation of log n.

Thus, the probability of failure constitutes the area under the curve between

$$Z = -\infty$$

and

$$Z = Z_0$$

or Z can be written

$$Z = \frac{\log n - \log N}{\sqrt{S^2_{\log n} + S^2_{\log N}}} = \frac{\log n - \log N}{\sqrt{S^2}} \qquad (3.1)$$

Practically, it means the failed area needs to be measured and expressed as a percentage of the total area. The Z value can then be determined from any normal distribution table and log N can be determined if log n and S are known.

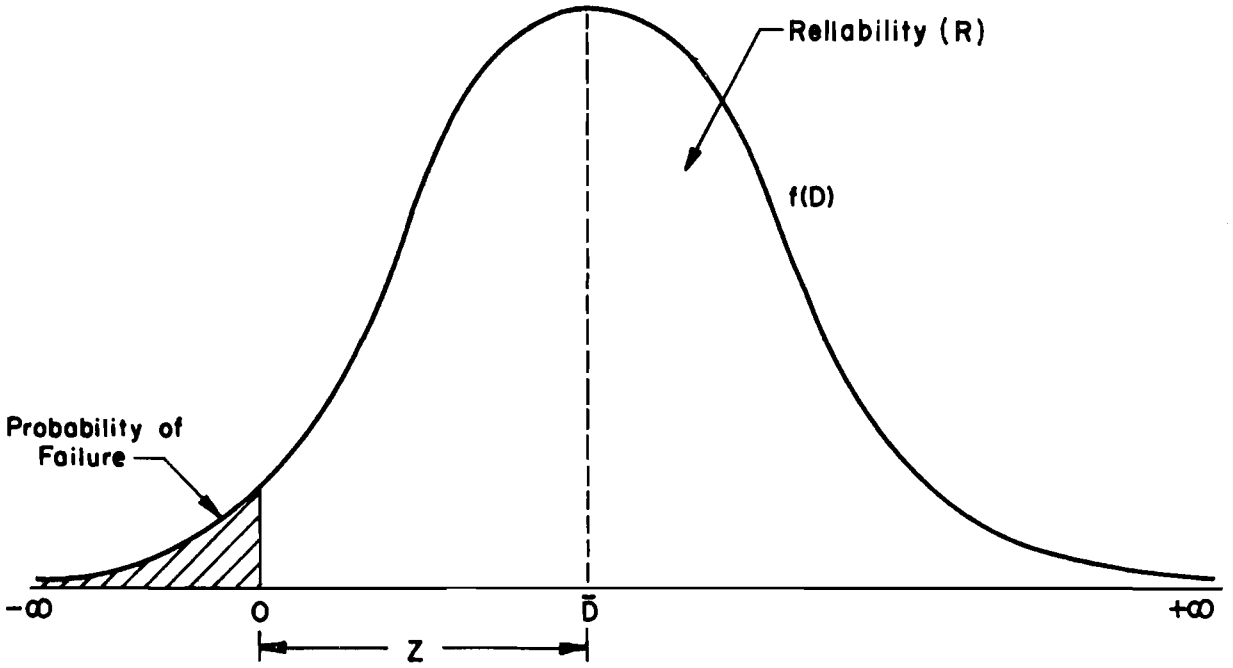

Fig 3.1. Distribution of the difference density function showing probability of failure (Ref 33).

THE FATIGUE CONCEPT IN STRUCTURAL PERFORMANCE

The area that has structurally failed can be related to the actual loads carried, the design number of loads and the variance of measured and design loads. This implies that structural failure does occur not as a result of a single load but because of fatigue of the material under many loads. The fatigue characteristics of concrete have been discussed previously and it was pointed out that, except for the strength of concrete, the only real variation between fatigue curves seems to be the method of load application. Figure 3.2 depicts four different curves, two from field studies, one from a lab study, and one recommended design curve based on several studies. The two field studies (Ref 34) are reported in a form

$$N = C(f_c/\sigma_c)^d \tag{3.2}$$

where

N = number of load applications,
f_c = strength of concrete,
σ_c = stress in the pavement due to one load application,
C = a constant associated with the intercept, and
d = a constant associated with the slope of the curve.

Simulating both the other curves in terms of the same constants, a table can be compiled for different d and C values, as shown in Table 3.1. It is evident from the table that the value of d is lower for actual pavements than for concrete specimens tested in the laboratory. Thus d decreases with a field study and probably depends on the loading conditions.

Since no fixed theoretical values for C and d exist they have to be derived, probably by regression analysis. Different values of C and d can be expected for flexural loading of the slab, the wear-out or fatigue of the aggregate interlock and the bearing of the steel reinforcement on the concrete in load transfer through dowel action. The calculation of stress in the concrete in the action of load transfer has been discussed extensively in Appendices 1 and 2 and the proposed method of calculating flexural stress in the slab due to wheel loads will be discussed in the next paragraph.

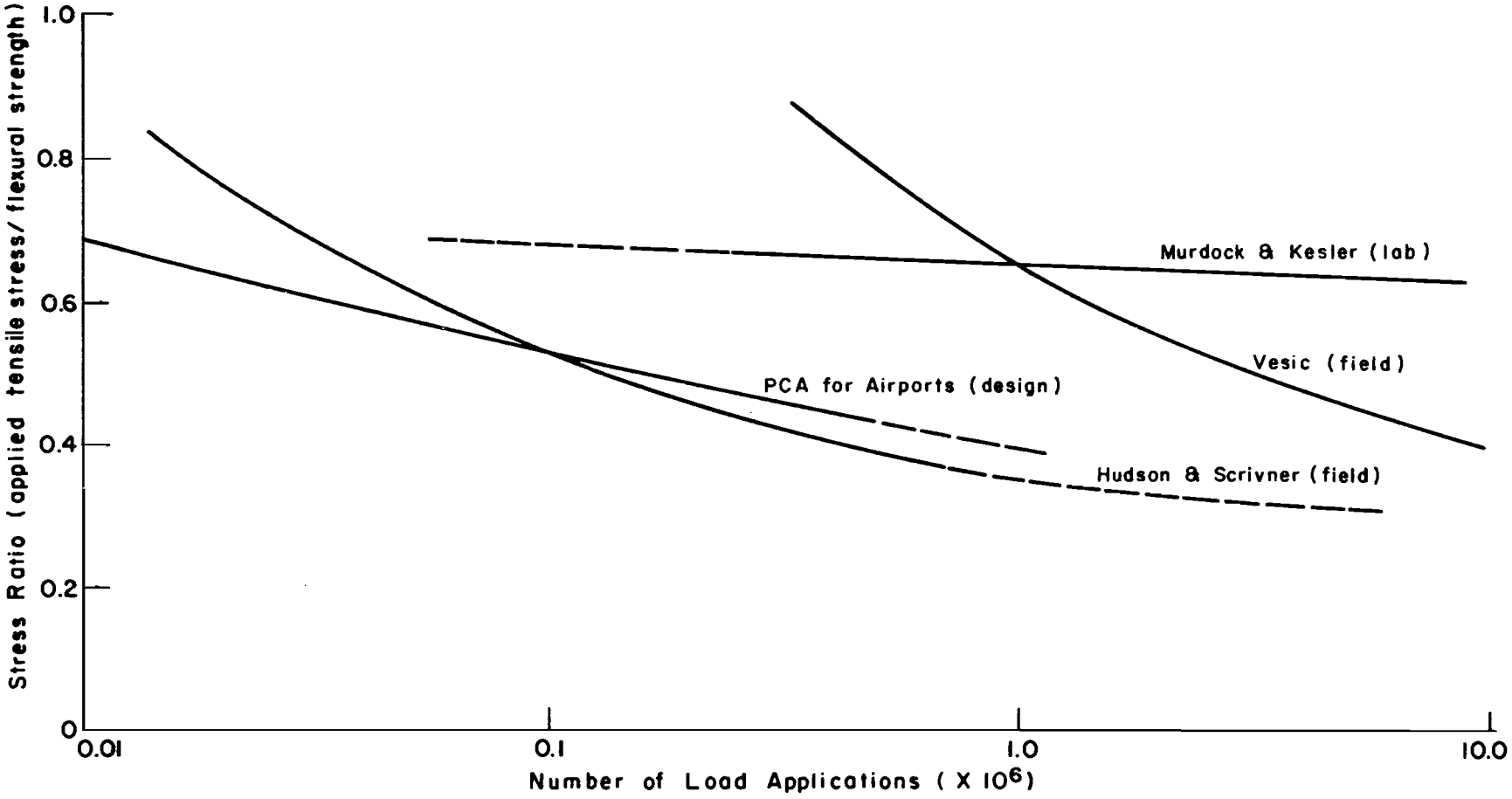

Fig 3.2. Fatigue of concrete: A comparison of various curves derived from design, field and laboratory. (After Ref 34).

TABLE 3.1. VARIATION OF CONSTANTS IN THE CONVENTIONAL FATIGUE EQUATION BY PREVIOUS INVESTIGATORS

Prior Investigations	Values of Constants d	C
Hudson and Scrivner[1]	4.34	8750
Murdock and Kesler[2]	27	0
PCA for airports[3]	8.3	250
Vesic and Saxena[4]	4.0	225,000
FHWA values[5]	3.21	23440

1. Values from the AASHO Road Test (Ref 34)
2. Laboratory compression testing (Ref 26)
3. Recommended for design by PCA (Ref 35)
4. Values from the AASHO Road Test (Ref 36)
5. Field testing of concrete overlays (Ref 37)

However, the strength of the concrete in load transfer through aggregate interlock and dowel action of the steel need to be evaluated for use in Eq. 3.2 since it will be included in the structural performance model.

The frictional strength or the wear resistance of concrete is generally expressed in terms of materials loss and is tested by using rotating discs or wheels, and grinding wheel cutters, with the introduction of grit or sand to act as an abrasive (Ref 29). Unfortunately, these test methods relate to skid resistance testing, but wearing strength in this report refers to the ability of the concrete and aggregate to maintain aggregate interlock and thus load transfer. A correlation exists between concrete strength, abrasion resistance of the coarse aggregate used and the wear resistance of concrete but the importance of the aggregate decreases with an increase in concrete strength, especially for crushing strengths above 6000 psi (41.4 kPa) (Ref 29). It is therefore important to distinguish between concrete and aggregate in their ability to withstand wear. Wearing resistance of the concrete can with confidence be expressed in terms of its paste strength and thus, compressive strength (Ref 29). The most commonly used method to test the wearing resistance of aggregates is the Los Angeles Abrasion Test (LA). The test involves the determination of the percentage of weight loss of the aggregate by rotation of a drum containing the aggregate as well as spherical steel balls (Ref 28). Thus, the wearing resistance of cracks in the slab, as related to the laod transfer through granular interlock, can be expressed in terms of concrete crushing strength and the Los Angeles Abrasion value.

Stress in the concrete that surrounds the longitudinal steel reinforcement at a crack can be considered to consist of a combination of compressive and tensile stresses. This is shown in Fig 3.3, where the stress pattern follows a wave pattern in the longitudinal direction. Bond strength between steel and concrete is assumed to be too small to result in any tensile stress at the steel concrete interface. Considering a cross section through the steel as shown in the second figure of Fig 3.3, it is clear that tensile stress exists in the plane AA of the steel, as a result of compression under the steel. This combination of forces is expressed as a bearing value K_c in Appendix 2. Since K_c is a function of concrete flexural strength, concrete bearing strength in dowel action can be written as $F(f_c)$.

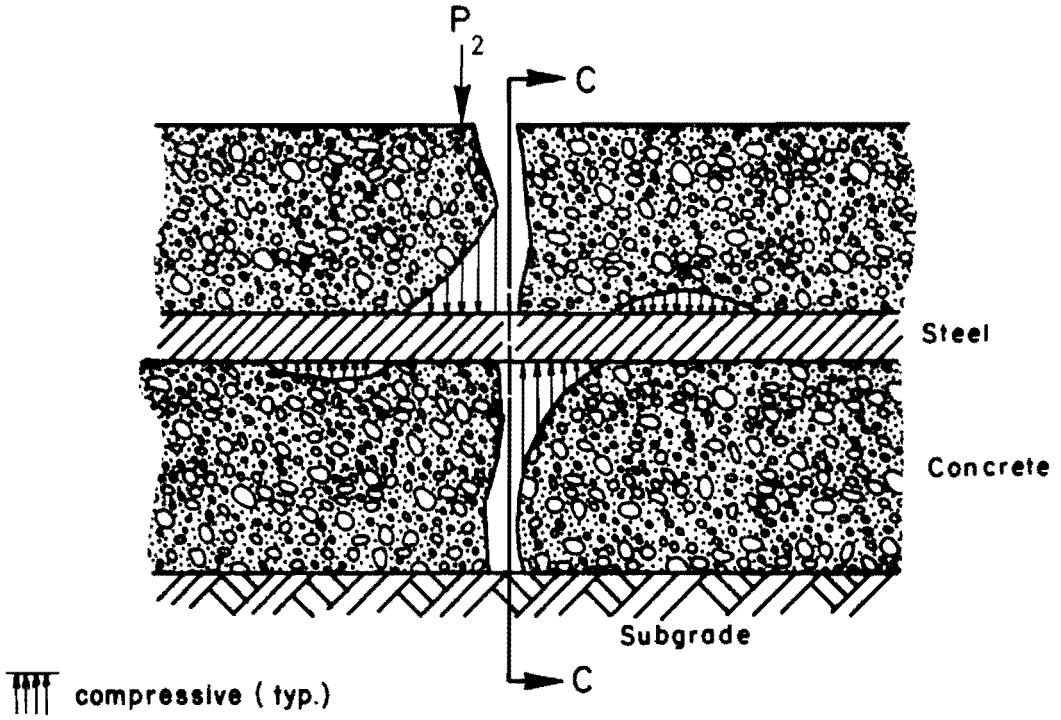

Side View

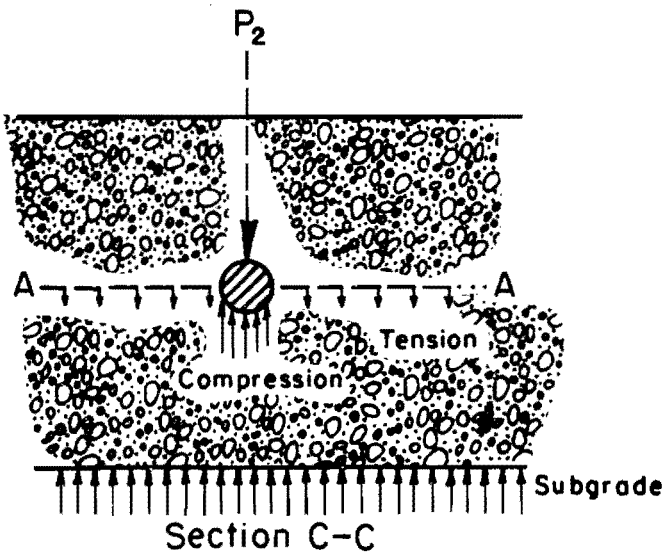

Cross Section

Fig 3.3. Forces in dowel mechanism.

To summarize the fatigue concept in CRCP, the expected number of loads N can be written in terms of a stress ratio,

$$N = C\left(\frac{f_c}{\sigma_c}\right)^d$$

where f_c is the flexural strength if σ_c is taken as flexural stress, f_c is the wearing strength if σ_c is in terms of stress on the aggregate due to aggregate interlock, or f_c is the concrete bearing strength if concrete bearing stress is considered in dowel action by the longitudinal steel reinforcement.

STRESS DUE TO TRAFFIC LOADS

Several formulations of stress analysis were discussed in Chapter 2. The most accurate assessment of stress in the slab undoubtedly is by way of computer analysis if the exact amount of load transferred both by aggregate interlock and dowel action is known for a deteriorated pavement. Since the measurement of load transfer is difficult without an elaborate field study, the use of a regression analysis in determining the coefficients of load transfer in conjunction with a stress calculation can be attempted.

Two approaches can be followed in the calculation of stress in this type of approach. The first is to use the Westergaard equations (Ref 4) with a superpositioning of the Timoshenko solution for edge supported slabs (Ref 3). Superpositioning will mean a square slab supported by the subgrade as well as at the ends. Since a CRCP can be characterized by a finite slab, between cracks, with supports at the cracks and construction joint, a superpositioning of Westergaard and Timoshenko for the purpose of a regression analysis is appropriate. Figure 3.4 shows the position of a finite slab and the simulation as discussed above. Thus the general equation selected for stress is

$$\sigma_{max} = C_1 \frac{(1 + \mu)P}{h^2} \log \frac{\ell}{b} + C_2 \bar{x} \frac{P}{h^2} \qquad (3.3)$$

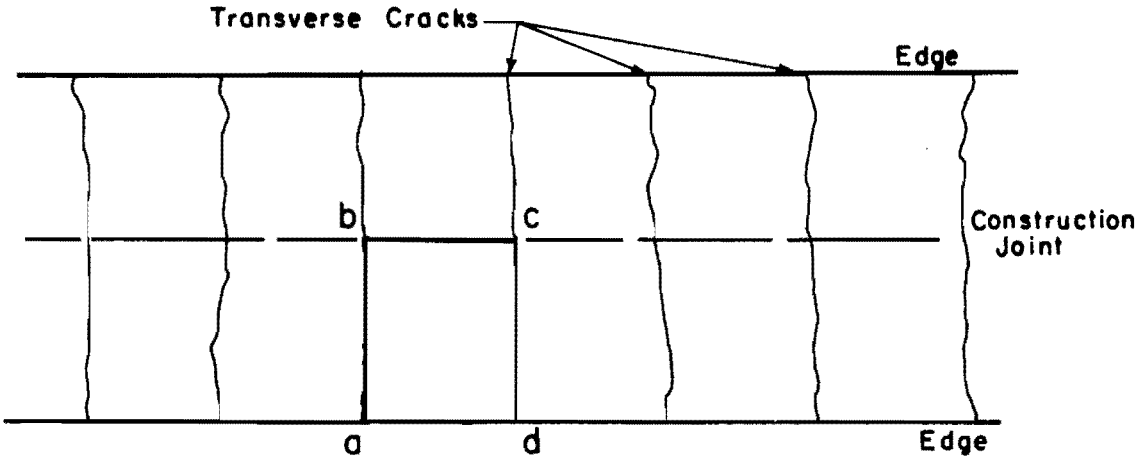

Plan view of CRCP

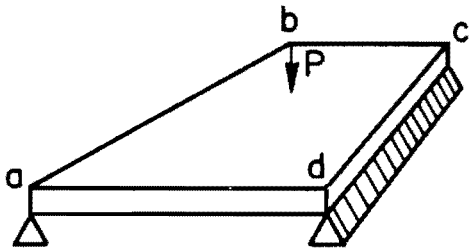

Timoshenko simulation

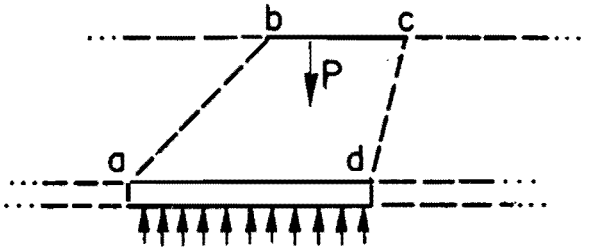

Westergaard simulation

Fig 3.4. Super positioning of Timoshenko and Westergaard approaches for CRCP.

where the maximum stress σ_{max} is now of interest, and

μ = Poisson's ratio,

h = slab thickness,

$\bar{x}$ = transverse crack spacing,

P = load on slab,

$b = \sqrt{1.6a^2 + h^2} - 0.675h$, an equivalent radius,

a = radius of loaded area on slab, and

$\ell^4 = \frac{EI}{k}$, E = modulus of elasticity of the slab,
I = moment of inertia, and
k = modulus of subgrade reaction.

C_1 and C_2 are constants that depend on the positioning of the load in regard to the geometry of the slab and cracks. This can be shown to be true by studying Fig 3.5, which shows the change in stress with a change in load magnitude for different positioning of the load on the slab (The Westergaard equations are used for the plots). The stress due to interior loading can, for all practical purposes, be considered a constant 0.69 times the stress for edge loading and 0.83 times the stress for corner loading. Furthermore, the only differences between the equations for edge and interior loadings are the values of the two coefficients C_1 and C_2 ; compare Fig 3.5 and Eq 3.3. In addition, C_1 and C_2 can also be considered as functions of slab geometry itself, and hence, of load transfer at the cracks.

Secondly, the same concept can be applied to a finite beam on an elastic foundation. This is illustrated in Appendix 1 and in Fig 3.6, where the value of the stress in the middle of the beam, the positioning is shown in Fig 3.6(a), is 0.78 of the beam stress if the load is applied at the end of the infinite beam. In the event of a crack in this infinite beam, the change in load transfer at the crack will have a significant effect on stress, as shown in Fig 3.6(b). Thus, the only difference between a beam loaded at the end, in the middle, or at a crack in the beam with load transfer at the crack is the value of C_3 in

$$\sigma_{max} = C_3 \frac{P}{h^2} \sqrt[4]{\frac{E\,I}{k}} \qquad (3.4)$$

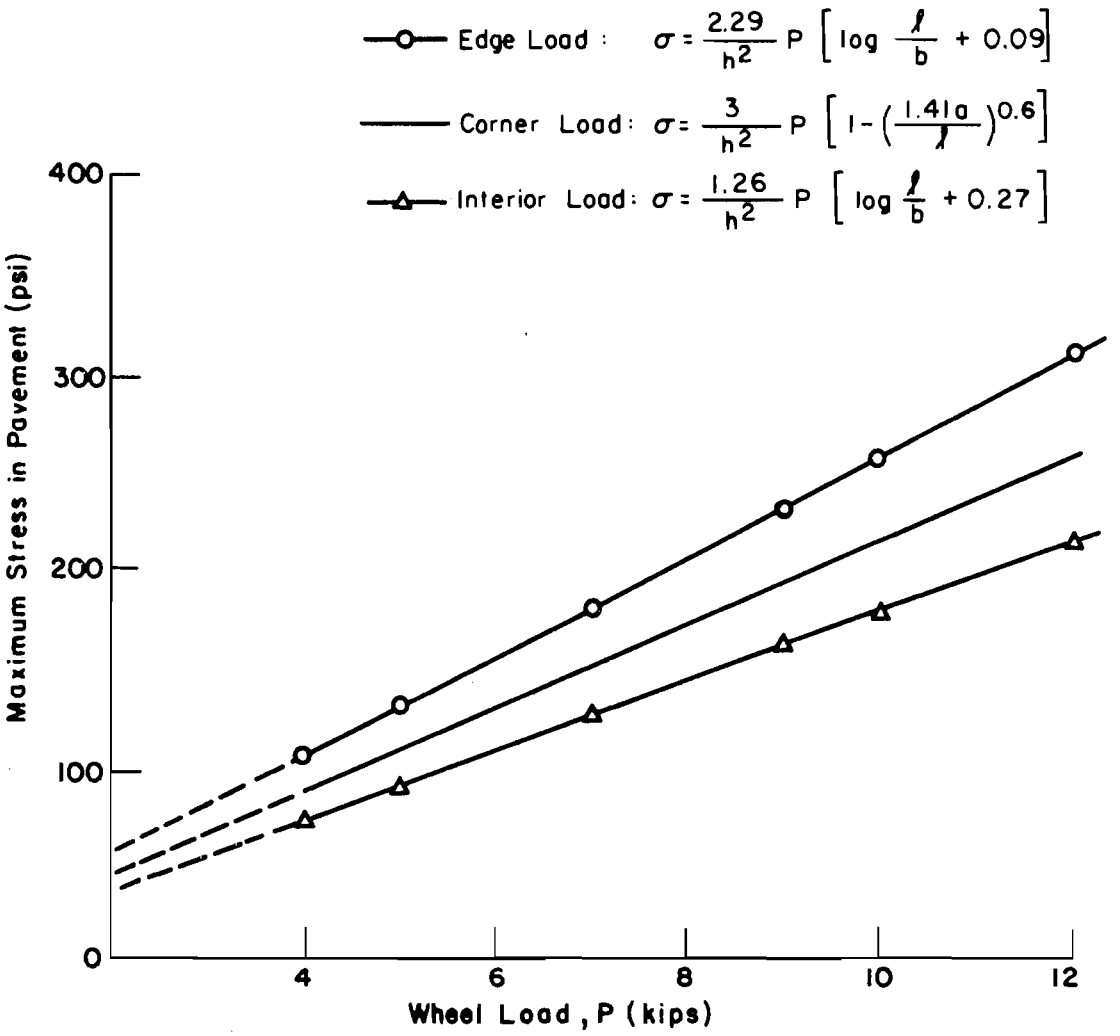

Fig 3.5. The relative change in stress due to changes in load for different positioning of load P on the slab.

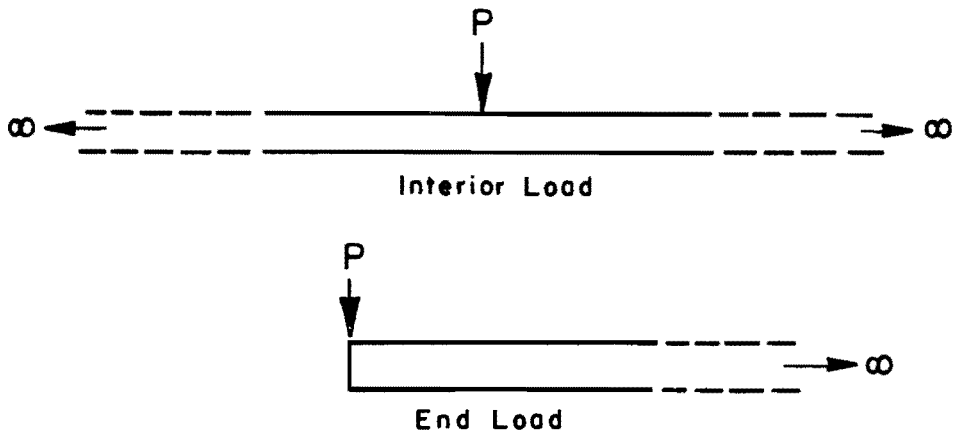

(a) Simulation by infinite beam.

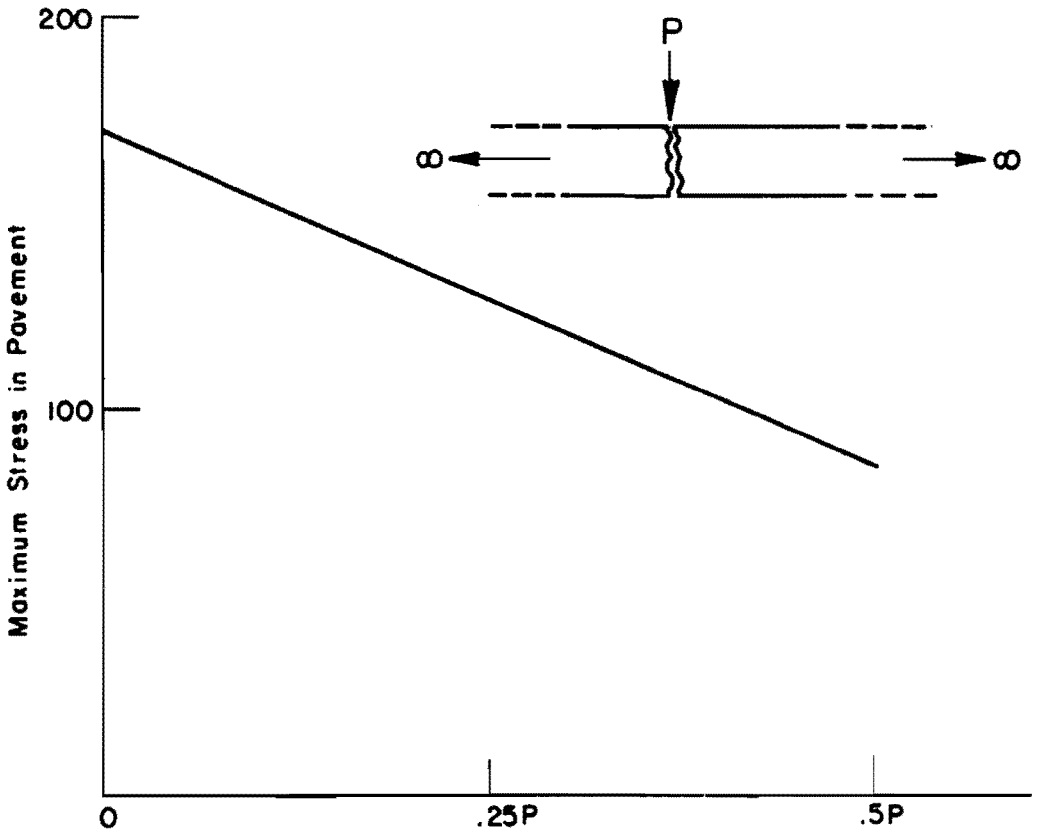

(b) Load transferred at crack.

Fig 3.6. Simulation of stress in CRCP using a beam considering load transfer changes at a crack.

which comes from Eqs A1.7 and A1.8. The inclusion of load transfer models in the stress model will be covered in a later paragraph.

DETERMINATION OF THE SLAB/SUBGRADE STIFFNESS RATIO

The stress in a concrete slab depends on the ratio EI/k as shown in previous paragraphs. The modulus of subgrade reaction is determined by plate load tests for design purposes, but its magnitude in an in-service rigid pavement has to be derived since excavation of the slab to test for k is relatively impossible.

The quantification of the modulus of elasticity E_c of concrete is possible through an elaborate field/laboratory exercise. This is done by the extraction of cores from in-situ pavements and the determination of E_c with triaxial testing equipment, which renders the resilient, dynamic complex or modulus of deformation, depending on the test method and the interpretation of the results. Since the loaded concrete slab is under tension at the bottom, modulus determination by indirect tensile or flexural testing is advantageous, the latter involving the extraction of beams from the concrete slab. However, several studies (Refs 38, 39, 40, and 41) have indicated the advantages of field studies by means of deflection or vibration techniques. An added advantage is the determination of modulus ratio, E/k, the actual information required, which has been proposed and used by several investigators (Refs 5, 6, 39, and 40) with success. Thus, deflections can be measured on a pavement and E/k can be inferred by theory.

Scrivner et al (Ref 40) use the Dynaflect, which induces a steady-state sinusoidal vibration in the pavement with a dynamic force generator to measure deflection at five different distances from the load application. By application of the Burmister multi-layer theory, the stiffness ratio the top layer to that of the infinite bottom layer, E_1/E_2, can be calculated. This theory, however, assumes layers of horizontally infinite extent, which cannot be said of a CRCP. Furthermore, the slab is not always in contact with the subgrade, which requires a different approach in calculating E/k. A finite element approach, which allows for the variation, or the total exclusion of subgrade support in places to simulate voids, is advisable in this respect. Stresses in the x and y directions in the slab can be written as (Ref 12):

$$\sigma_x = \frac{E}{1 - \mu^2}\left[\frac{\partial u}{\partial x} + \mu\frac{\partial v}{\partial y} - Z\left(\frac{\partial^2 w}{\partial x^2} + \mu\frac{\partial^2 w}{\partial y^2}\right)\right]$$

$$\sigma_y = \frac{E}{1 - \mu^2}\left[\frac{\partial v}{\partial y} + \mu\frac{\partial u}{\partial x} - Z\left(\frac{\partial^2 w}{\partial y^2} + \mu\frac{\partial^2 w}{\partial x^2}\right)\right]$$

where

E = modulus of elasticity,
μ = deformation in the x direction,
v = deformation in the y direction, and
w = deformation in the Z direction,

if a homogeneous isotropic material obeying Hooke's law is assumed. If it is assumed that the changes in deformation in the x and y directions are small relative to the element lengths ∂x and ∂y, and since

$$\frac{\partial^2 w}{\partial y^2}$$

and

$$\frac{\partial^2 w}{\partial x^2}$$

depict curvatures of the slab in the y and x directions respectively, stress can be written as

$$\sigma_{ij} = -\left(\frac{EZ}{1 - \mu^2}\right)\left(Q_i + \mu Q_j\right)$$

where

Q = curvature

Thus,

$$E = - \frac{\sigma_{iu}(1 - \mu^2)}{Z(Q_i + \mu Q_j)}$$

with σ_{ij}/Z being a function of the load on the slab and the slab thickness:

$$\frac{\sigma}{Z} = \frac{M}{I}$$

where M, the moment, is purely a function of load P and slab geometry. Thus, the modulus of elasticity of the concrete slab can be written as

$$E = \text{function}\left[\frac{P(1 - \mu^2)}{h^3(Q_i + \mu Q_j)}\right] \tag{3.5}$$

The modulus of subgrade reaction k has been defined as a linear function of the deformation and since k is assumed to be constant, elasticity of the subgrade is implied. Attempts have previously been made to replace k by a modulus of elasticity E_s and Yang (Ref 5) reports a relationship

$$k = \text{function}\left[\frac{E_s}{(1 - \mu_s^2)}\right]$$

Vesic and Saxena (Ref 5) also suggested a modification of k by using an E_s-value. Constant correlations between k and E_s values shown by van Til et al (Ref 42) suggest that k and E_s can be used interchangeably, provided the corrected constants are introduced. This notion is reinforced by an inspection of the stress solutions with elastic solid subgrade theory and comparison with the Winkler foundation approach. Thus, the relationship between deflection, load, and subgrade support can be written with great confidence as

$$\text{Deflection } y = \text{function}\left[\frac{P(1 - \mu_s^2)}{\pi E_s r}\right]$$

for an elastic solid subgrade, according to Timoshenko (Ref 43)

r = horizontal distance from the point load P.

The equation for E/k can then be written as a function of

$$\left[\frac{y}{h^3(Q_i + \mu Q_j)}\right] \tag{3.6}$$

assuming the Poisson's ratios of concrete and the subgrade are close enough to

$$\frac{(1 - \mu^2)}{(1 - \mu_s^2)} \approx 1$$

It is now possible to use the Slab 49 finite element program (Ref 8) and derive materials properties E/k with a knowledge of deflection y and curvatures Q_i and Q_j, as measured with the Dynaflect.

CONSTRUCTION OF REGRESSION MODEL

The background and detailed development of the various theories that may have a bearing on the structural performance of CRCP have been discussed previously. It has been shown that analysis by regression is inevitable but that considerable advantage is to be gained from the inclusion of theoretical models. This section will cover the amalgamation of all relevant theoretical models into a single workable equation.

The following stochastical model is used as a basis:

$$Z = \frac{\log n - \log N}{\sqrt{s^2}} \tag{3.1}$$

Using the fatigue equation, log N was shown to be

$$\log N = \log\left[C(f_c/\sigma_c)^d\right] \tag{3.2}$$

where σ_c can be written as

$$\sigma_c = C_1 \frac{(1+\mu)P}{h^2} \log \ell/b + C_2\bar{X}\frac{P}{h^2} \tag{3.3}$$

according to Westergaard, or

$$C_3 \frac{P}{Lh^2} \sqrt[4]{\frac{E\,I}{k}} \tag{A1.9}$$

if the beam equation is used. As was pointed out in a previous section, constants C_1, C_2, and C_3 can be considered functions of load transfer, either through granular interlock or dowel action of the longitudinal steel reinforcement.

Granular interlock can be written in terms of stress on the aggregate particles, Eq A2.4, and if the fatigue equation 3.2, is used, the constants will also be related to the particle wearing strength which is related to the Los Angeles Abrasion value. Thus, load transfer through granular interlock K_2 can be written as a function of

$$C_1, C_2, C_3 = F\left(\frac{P_2\gamma_R}{WhL\gamma_c\left(\frac{\pi}{2} - \theta + \frac{1}{2}\sin 2\theta - \frac{2\Delta x}{R}\right) f_c(LA)^{d(L)}}\right)$$

where

P_2 = load transfered by aggregate interlock,

γ_R, γ_c = density of aggregate and concrete respectively,

W = percentage of aggregate with diameter $2R$,

L = length of crack, and

Δx = crack width.

$\frac{\pi}{2} - \theta + \frac{1}{2}\sin 2\theta - \frac{2\Delta x}{R}$ relates to the loaded area of the aggregate.

The angle of weathering θ is unknown and changes from

$$\cos^{-1}\frac{\Delta x}{R}$$

for new pavements to 0 for old worn sections.

Referring to Fig 3.7, θ can be calculated as

$$\theta = \frac{\pi}{2} - \tan^{-1}\frac{f}{\Delta x} - \tan^{-1}\frac{g}{2R}$$

where

$g = \sqrt{\Delta x^2 + f^2}$,

Δx = crack width, and

f = vertical movement between two butts of the slab at a crack.

The value of f can be measured in the field by physically applying a load and measuring the relative movement. However, since the accuracy of crack width measurement by utilization of a surface microscope (Ref 14) is questionable and since ease of measurement of properties is a primary objective, the accurate measurement of f was not attempted. An indirect method was employed instead. This method involves the calculation of an amplitude of waves in a pavement surface, from measurements by profilometer. A computer program ROKYRD, developed by Williamson et al (Ref 44), was used to determine the amplitude for different wavelengths, but since movement at a crack is associated with very short waves, the 10 percent worst values of amplitude for waves 0-1 ft (0-0.3 m) was used. A 10 percentile value was decided on since it was found to correlate the highest with distress on a concrete pavement (Ref 44).

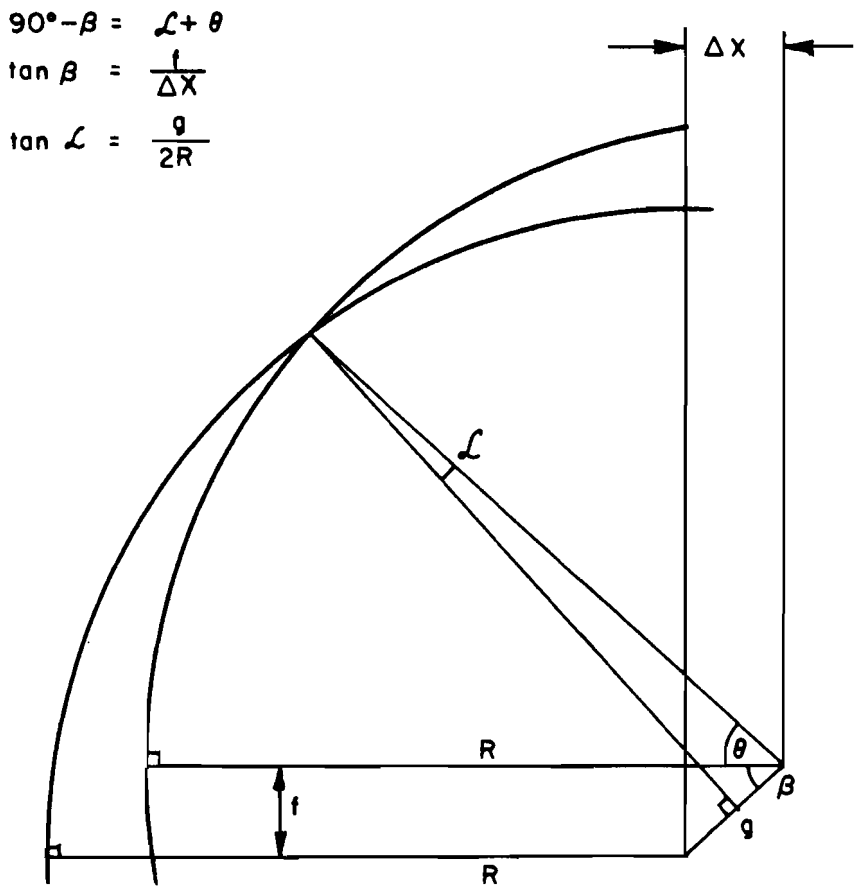

Fig 3.7. Relation between θ , crack width Δx , and movement f .

The factor for load transfer by granular interlock can therefore be written as:

$$K_2 = C_2 \left[\frac{P_2 \gamma_R \left(\frac{\Delta x}{R}\right)^{d(R)} (LA)^{d(L)} (A)^{d(A)}}{WhL\gamma_c f_c (\bar{x}\alpha\Delta T)^{d(\alpha)}} \right]^{d_2} \qquad (3.7)$$

where

LA = Los Angeles Abrasion value,

A = amplitude as measured with the Profilometer,

$\bar{x}\alpha\Delta T$ = the thermal change in crack width, and therefore the change in load transfer which is calculated by using the thermal coefficient α, temperature change ΔT and crack spacing.

The equation for bearing on the concrete was written as:

$$\text{bearing} = C \frac{P_1 S}{Ld^2} \sqrt[4]{\frac{E_c}{E_d}} \qquad (A2.8)$$

where

S = spacing of steel reinforcement,

d = diameter of steel bars,

E_d = modulus of elasticity of steel, and

E_c = modulus of elasticity of concrete.

This can also be intercorporated into the fatigue equations by writing the concrete bearing strength in terms of K_c, which, according to Grinter (Ref 45), can be considered a function of E_c the modulus of elasticity of concrete and which can be written as

$$33\gamma_c^{1.5}\sqrt{f_p} \tag{3.8}$$

according to the ACI (Ref 30). The concrete bearing strength f_p was shown to be a function of flexural strength (Ref 28), and, since seven day strengths are available on construction records, f_c will be used instead of f_p where f_c relates to seven day flexural strength. This will also be applied to Eq 3.7. Combining the last two equations, a relation for load transfer by dowel action can be written as

$$K_1 = C_1 \left(\frac{SP_1}{Ld^2 \, E_d^{0.25} \, \gamma_c^{1.125} \, f_c^{0.375}} \right)^{d_1} \tag{3.9}$$

In both Eqs 3.7 and 3.9, loads of magnitude P_2 and P_1 were used to signify the force of aggregates and steel respectively. Since the forces are dependent on each other and on the wheel load P in Eq 3.3, P_2 and P_1 can be written as

$$P_1 = C_4(P)^{d(K_1)}$$

and

$$P_2 = C_5(P)^{d(K_2)}$$

in Eqs 3.7 and 3.9 respectively.

The final form of 3.1 can be written

$$Z = \left[\log n - \log C \; K_1 K_2 \left(\frac{P}{f_c Lh^2} \sqrt[4]{\frac{EI}{k}} \right)^{d\sigma} \right] \frac{1}{S} \tag{3.10}$$

for the beam equation. A similar equation can be written using the Westergaard format, 3.3. A substitution for EI/k, using Eq 3.6, will be discussed

in the next chapter under the regression analysis since a separate regression equation is developed for this purpose.

The development of an analysis model was discussed in this chapter. Initially, basic models were discussed, but it became evident that proper simulation should include load transfer mechanisms. The final equations is in a form that can be readily applied in regression analysis although the beam theory will have to be used as a first approximation to get estimated values for $d(K_1)$ and $d(K_2)$ which can be used to find C_1 and C_2 in Eq 3.3, the better equation of the two since it is based on slab theory. The development of the strategy to be followed in the regression exercise, as well as the solution of the S^2 term, the standard deviations of log n and log N combined, by Taylor series, will be discussed in the next chapter.

CHAPTER 4. THE SELECTION OF STUDY SECTIONS AND THE REGRESSION TECHNIQUE

The evolution of a study hypothesis that requires the use of regression techniques in the analysis was discussed in previous chapters. Models which are based on theoretical considerations were derived in a format to be directly applicable in regression. The selection of study sections directly applicable to the problem of structural performance of CRCP needs to be addressed next, but a discussion of some fundamentals in the regression technique may prove to be helpful for the experimental design.

This chapter will be devoted to a discussion of the regression technique, the measures of accuracy or precision, and the significance of variables that enter the equation. The selection of a test site and the breakdown into study sections will subsequently be considered, with the statistical requirements as a background. Lastly, a paragraph will be spent on the acquirement of data and the possible inference of information in the event of a lack.

THE TECHNIQUE OF REGRESSION

Regression techniques can be defined as methods by which a mathematical relationship between two or more variables is established by the method of least squares. That is, an equation for the estimated value of Y where Y depends on one or more independent variables X is derived such that the sum of squares S of deviations of the predicted Y values from the observed Y values is minimized. The equation can be written in mathematical form (Ref 46):

$$\text{Estimated } Y = \hat{Y} = b_1 + b_2x_2 + b_3x_3 \ldots b_kx_k \qquad (4.1)$$

where the independent variables x_2, x_3, . . . x_k are shown as first order terms and are combined through constants b_1, b_2, b_3 . . . b_k to render

an estimated value of Y, called $\hat{Y}$. The independent variables can also be of higher order, which does not alter the basic theory.

The sum of squares of deviations S can be calculated:

$$S = \sum_{i=1}^{n} (Y_i - \hat{Y}_i)^2 \tag{4.2}$$

and through regression an equation for $\hat{Y}_i$ is derived such that S is a minimum.

Some basic concepts of regression are illustrated in Fig 4.1, which shows a plot of one dependent variable Y versus the independent variable X. A line which is fitted through these points intercepts the Y-axis at a value b_o, while the slope of the line is b_1. The predicted value corresponding to X_{2i} is shown to be $\hat{Y}_i$, but the observed value is Y_i. Thus, S can be calculated for different sets of Y_i values by adjusting b_o and b_1 until a minimum value of S is found.

The stepwise regression procedure is one of the techniques used in regression and involves the insertion, and possibly the deletion, of independent variables one at a time. An investigation of the contributions of each variable in improving the correlation coefficient is made at the same time by comparing the partial F criterion of each variable with a preselected F value. Any dependent variable that does not contribute significantly to the equation is removed (Ref 86). The F can be calculated:

$$F = \frac{\text{mean of } (\hat{Y}_i - \overline{Y})^2}{\text{mean of } (Y_i - \hat{Y}_i)^2} \tag{4.3}$$

where

$\overline{Y}$ = mean of all Y values in the sample universe,

$Y_i - \overline{Y}$ = the deviation of the predicted value of the ith observation from the mean, and

$Y_i - \hat{Y}_i$ = the deviation of the i-th observation from its predicted or fitted value (see Fig 4.1).

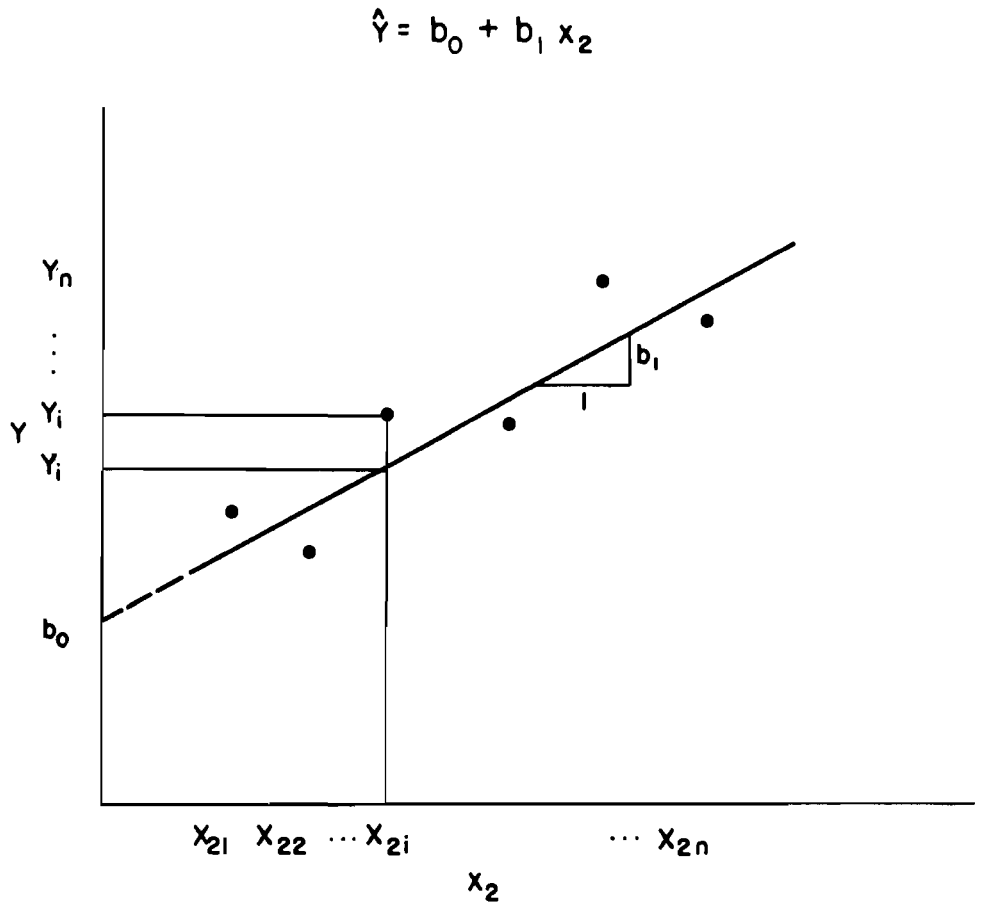

Fig 4.1. A hypothetical regression line with data points (X_{2i}, Y_i).

If F is significantly greater than 1, a relationship is judged to exist between X and Y, but if not, there is insufficient evidence that there is such a relationship. The preselected F value or critical F depends on the probability of concluding that Y and X are related when they are not. This probability is 0.25 for $F = 1.32$, 0.10 for $F = 2.71$, and 0.05 for $F = 3.84$ if a large sample is assumed.

Generally, the correlation of two random variables can be written as

$$r = \frac{\Sigma(X_i - \bar{X})(Y_i - \bar{Y})}{\sqrt{\Sigma(X_i - \bar{X})^2(Y_i - \bar{Y})^2}} \tag{4.4}$$

and is usually calculated automatically in any regression program. The value of r is zero if no correlation exists between X and Y and is equal to one for a perfect correlation. The standard error s.e. gives some indication as to the difference between the actual and predicted values, and is related to S:

$$\text{s.e.} = \left[\frac{1}{n-k}\sum_{i=1}^{n}(Y_i - \hat{Y}_i)^2\right]^{1/2} \tag{4.5}$$

where k is the number of terms, including the y-intercept in the regression model. It is the aim to minimize the s.e. in order to optimize the representation of the data points by the model. Minimizing the s.e. is the same as minimizing the sum of squares S.

The regression analysis in this study will be performed stepwise, using a computer program. The details of the analysis itself will be discussed in a following chapter. The critical F values chosen, the r achieved, and the magnitude of the s.e. will be important considerations in selecting the best equation.

SELECTION OF TEST SITE LOCATIONS

The sections to be investigated were selected with a regression analysis in mind. However, since no guarantee of success could be assumed for the regression analysis and considering the possibility of a future analysis by

way of other techniques, such as statistical comparisons between sections, the layout had to be as versatile as possible.

Several restrictive factors that influenced the site selection existed. Highway sections that incorporated as big a variety in construction materials and techniques as possible and were built over a long period of time had to be chosen. It was advantageous to select one stretch of highway through one district to limit the possibility of a big variation in traffic composition, to assure a uniform maintenance program and technique, and to facilitate the process of data gathering. Other requirements were the inclusion of a wide variety of subgrade types, a variation in climate, and a change in terrain that could be associated with drainage characteristics.

Two Interstate Highways were selected which best suited the requirements mentioned above. These were Interstate 10 through District 13 in south Texas and Interstate 45 through District 17 in east Texas, Fig 4.2. Both highways carry heavy traffic on sections that were built between 1964 and 1970. A variety of subgrade types exist in the two districts; siliceous river gravel, crushed sandstone, and crushed limestone were used for the concrete on different project in District 17. Unfortunately, neither the drier nor the colder climatic regions of west or northwest Texas are represented in the study. However, it was felt that the difference in climatic conditions could be handled by the proposed gross analysis, and it is reported on elsewhere (Ref 47).

Test Sections

Both the highways selected are comprised of projects that were built between 1964 and 1970. These projects could be considered as subpopulations in stratified sampling of the total highway length, and as such the sections could be sampled individually using techniques of simple random sampling. However, each subpopulation could be subdivided into sub-subpopulations if the geometry of the highway were considered. Stratification could consist of sections in cut, in fill, or on ground level; stratification with regard to curves left or right and straight sections; and uphill, downhill, and level sections. Since the horizontal and vertical geometry posed some problems as regards the positioning of the load (heavy trucks tend to move closer to the edge when going uphill or around curves to the right), it was decided to investigate these effects under a separate item, namely, by comparison of

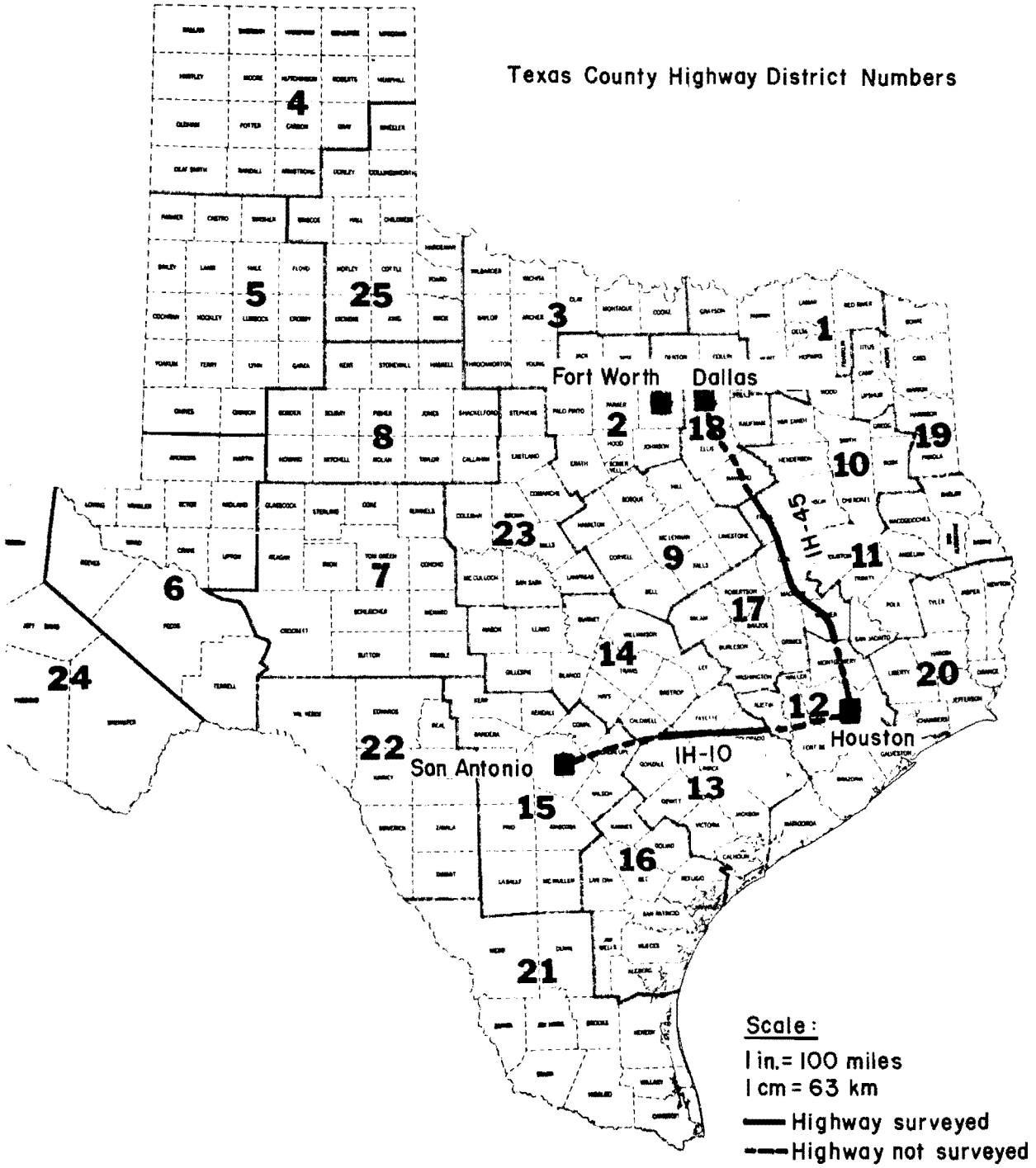

Fig 4.2. Sites of sections under investigation.

structural performance with geometry using regression techniques. These results will be discussed later on. Level straight sections were, therefore, randomly selected with stratification regarding cut, fill, and ground level. These sections were 600 ft (183 m) long, which was a restriction that originated from previous studies of CRCP performance (Ref 14). It was decided to retain this basic length since computer programs developed under this project were geared to handle sections of length 600 ft (183 m). Thirty sections were selected on each highway, which, when combined, could be considered a large sample, and when handled separately, could still be deemed satisfactory since it is desirable to have twenty or more degrees of freedom for error in a regression analysis. The number of degrees of freedom for error is the difference between the number of observations and the number of variables in a regression model. The accuracy with which the standard error, the standard deviation of the universe, and therefore, the reliability of the final regression model, is determined by the sample size. This can be shown in terms of degrees of freedom for the F-test, which involves testing whether a certain assumption is true or not, and the t-test, with which the significance of the difference between two population means can be tested. Figure 4.3 shows a plot of the critical values used for hypothesis tests or confidence interval calculations of these two distributions against the degrees of freedom for a 0.95 probability. The t-curve levels off at about 4 degrees of freedom and F-value at about 5. Thus, a sample size, n, of 6 can be considered as the minimum for maximum benefit under the usual condition of n-1 degrees of freedom in testing. In other words, the accuracy or sensitivity of the statistical analyses increases sharply as the sample size increases to 6, but the increase in sensitivity point is much slower as the sample size increases beyond 6. Therefore, 6 observations were made within each 600 ft (183 m) sections, which means an observation every 100 ft (30.48 m), which is also the frequency with which slab thickness and concrete strength was measured at the time of construction.

DATA MEASUREMENTS

The regression model is based on a difference density function which is assumed to be normally distributed, see Fig 3.1 and compare with Eq 3.1. This implies a normally distributed $\log N$ and $\log n$, unless it can be

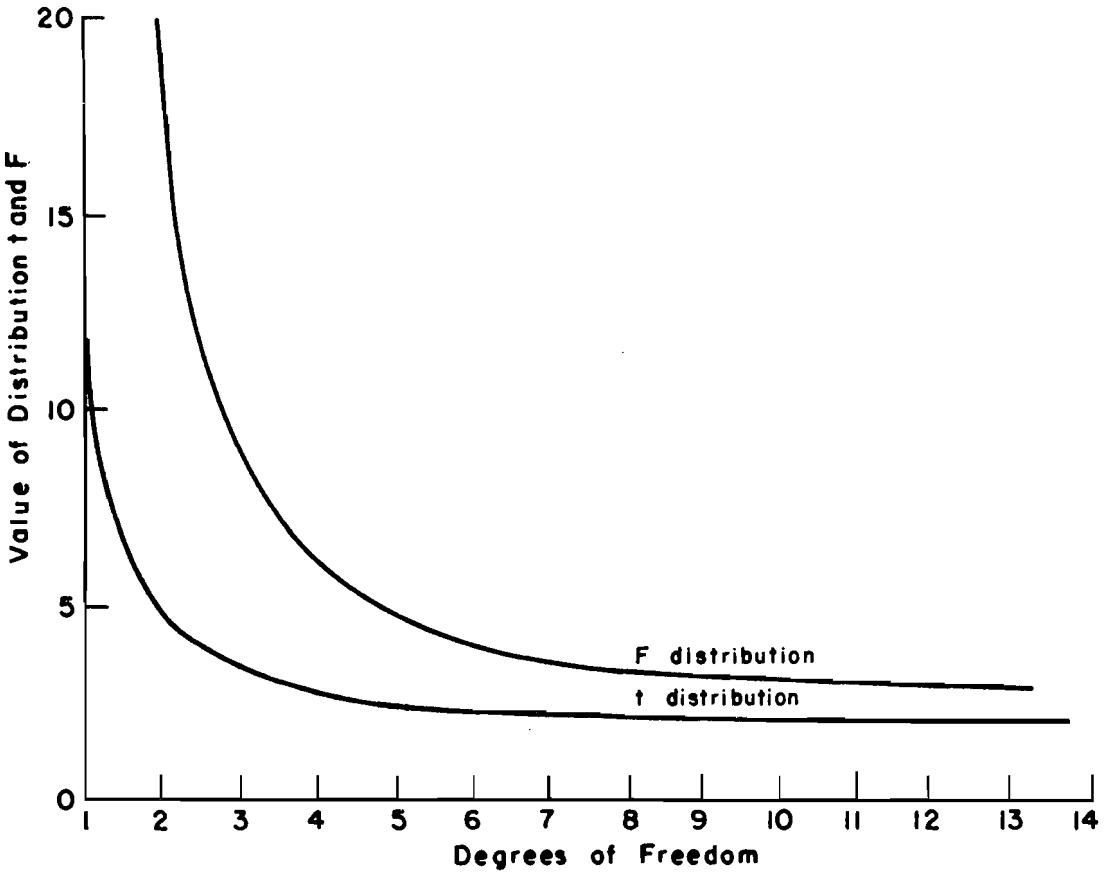

Fig 4.3: The change in value for the F and t distribution, with a change in degrees of freedom.

shown that log n - log N is normally distributed. Darter and Hudson (Ref 77), in an extensive study of Eq 3.1, show that both log n , the actual load applications on the pavement, and log N , the allowable load applications until failure, can be considered normally distributed.

The actual load applications on the highway sections were estimated by the State Department of Highways and Public Transportation using vehicle classification counts and data from loadometer stations (Ref 48). This information is used in the analysis, together with the variance of load applications. Darter and Hudson (Ref 33) calculated values of variance that range between 0.0037 and 0.0453, with a suggested average value of 0.023. Since no loadometer stations are permanently in operation on these highways, no actual variance is available and the estimated values will, therefore, be used.

An extensive source of construction control data exists in the original construction files. Information on pavement thickness, concrete aggregates, slump of fresh concrete, and entrained air content, as well as concrete temperatures, could be obtained. Data on subgrade strength, however, were insufficient, as mentioned previously, but relevant information was inferred from deflection measurements using the finite element program developed by Hudson and Matlock (Ref 11). Theoretical values for deflection and radius of curvature were calculated for different slab and subgrade stiffnesses by using the above mentioned program. A third variable, crack spacing, was also introduced and a regression model was constructed that related EI/k to deflection y , radius of curvature Δy (where Δy signifies the difference in deflection between two points, one at the load and the other 12 inches - from the load), crack spacing x , and slab thickness h . The equation, using Eq 3.6 as a basis, for stiffness ratio is

$$EI/k = 1902 \frac{x^{0.13} y^{2.05}}{\Delta y^{2.08}} \quad in^4$$

$$= 14513590 \frac{x^{0.13} y^{2.05}}{\Delta y^{2.08}} \quad mm^4 \qquad (4.6)$$

with E measured in psi or MN/m^2, k in pci or MN/m^3 and the rest in inches or mm. The equation, with a correlation coefficient r of 0.994 and standard error of 0.031, was derived for loading between transverse cracks and 18 inches (45 cm) from the pavement edge, assuming a 90 percent reduction in slab stiffness

at the transverse cracks. The pavement was assumed to be 24 ft (7.32 m) wide with a longitudinal construction joint down the center of the pavement.

The variance in the magnitude of the vertical load, due to an uneven road profile, was calculated using a computer program, DYMOL. This program utilizes mathematical simulation techniques of the interaction between vehicles and a defined road surface profile as measured with the Surface Dynamics Profilometer (Ref 49). A four axle truck with mean axle load of 18000 pounds (80 kN) and a vehicle speed of 55 miles per hour (88 km/hr) was used to calculate variance of loading. The largest variances were found for sections subjected to considerable subgrade activity in the form of swell and settlement. Variances of 1800 lbs (8 kN) were not uncommon and the average variance was found to be in the order of 1130 lbs (5 kN).

SUMMARY

The selection of study sections as well as data acquirement pertinent to the pavement characteristics was addressed primarily with a regression study in mind. The usefulness of data to other ways of analysis and the applicability to other measurement means were also kept in mind. The site location was selected such that encroachment on the gross analysis (Ref 47) could be avoided since the gross study concentrates on factors that vary throughout the state.

Some discussion was devoted to the inference of slab and subgrade stiffness from Dynaflect deflections. It was shown that although no absolute value of stiffness ratio can be calculated from measured deflections stiffness ratio is a function of curvature and deflection.

CHAPTER 5. THE REGRESSION ANALYSIS

The previous chapter was devoted to the construction of several theoretical models which could be integrated, to allow analysis through regression. The developed theoretical model will suffice, assuming a perfect fit of the variables, but variation can be anticipated. Thus, the regression process will be approached in several steps in order to explain as much of the measured distress as possible.

The analysis is divided into four parts, as shown in Fig 5.1:

(1) An analysis based on the theoretical models discussed is made. The stochastical concept will be used as a basis and the fatigue concept will be incorporated with utilization of the beam and Westergaard approach to calculate stress in the slab. The decrease in the load transfer capabilities of the slab at the cracks will also be expressed in terms of the fatigue model, as discussed in the previous chapter.

(2) The difference between the actually measured and the theoretically accounted for amounts of distress will subsequently be expressed in terms of other measurable variables which do not necessarily fit into the theoretical model. Also included in the analysis is the unaccounted for variation of S, the standard deviation of $\log N - \log n$. This is due to the fact that the calculated S is based either on laboratory and field measured values or on values provided through previous studies of similar variables, such as the variance in estimating $\log n$, the actual number of load applications applied. An important source of error in S is the actual strength of the concrete in the field and the variation experienced due to insufficient compaction or vibration. The extent of this variation cannot be determined without an elaborate field study. Therefore, it is assumed that these variations can be explained by variables such as slump of the concrete during construction, temperature at the time of construction, construction equipment, water factor, and so forth. All the above mentioned variables may also relate to distress not accounted for in the theoretical analysis.

(3) The results of 1 and 2 above may be used in new design or in the rehabilitation/maintenance process, but a combination of equations is desirable in order to be able to predict future distress. The combined equation needs to take into account the present condition of the pavement as well as the design and construction variables previously derived. A technique of predicting future distress in terms of present condition as well as the combination of all terms in one equation will be discussed.

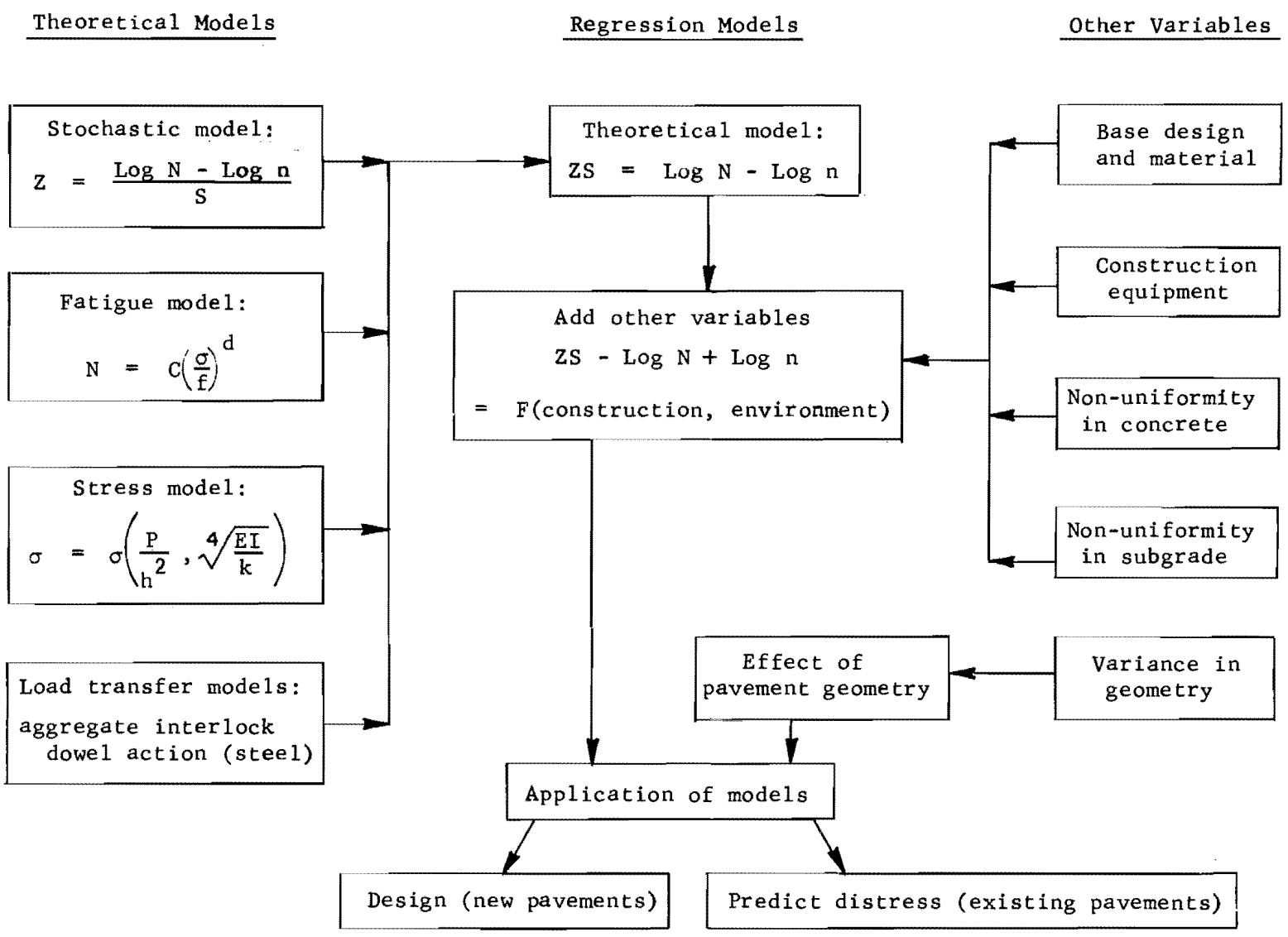

Fig 5.1. Flow diagram of Regression Program.

(4) Finally, the effect of other variables, such as highway geometry, needs to be investigated, since the test sections were selected on level, straight sections.

REGRESSION ANALYSIS OF THE THEORETICAL EQUATION

The format of the beam equation, as shown in Eq 3.10, can be used in a regression analysis whereby the values of d_o , $d(K_1)$, $d(K_2)$, and C can be derived. A regression will be much easier with the beam equation since the Westergaard format requires the derivation by regression of a power function:

$$Z = \left[\log n - \log C\, K_1 K_2 \frac{P}{f_c h^2}\left(C_1 \log \frac{\ell}{b} + C_2 \bar{x}\right)^{d_o}\right] \frac{1}{S} \qquad (5.1)$$

where C_1 , C_2 and d are coefficients that have to be derived simultaneously by one regression step. Since crack deterioration and loss of load transfer factors are obtained with the beam equation, the values of $d(K_1)$ and $d(K_2)$, the fatigue coefficients for load transfer in Eqs 3.7 and 3.9, can be assumed to be the same for the Westergaard equation and subsequently C_1 and C_2 may be derived for Westergaard if desired. It will be shown later on, however, that inclusion of the Westergaard format does not significantly improve the model. This seems to indicate that the easier format of the beam equation is also a reliable equation for stress analysis in a CRCP.

Substituting the relevant equations for K_1 and K_2 , as shown in Eqs 3.9 and 3.7 respectively into Eq 3.10, and replacing EI/k with Eq 4.6, an equation for a positive ZS can be written:

$$\begin{aligned} ZS = {} & -\log n + d_2 \log\left(\frac{P\gamma_R}{L\gamma_c f_c}\right) + d(R) \log \frac{\Delta x}{R} + d(L) \log LA \\ & + d(A) \log A + d(\alpha) \log (x\alpha\Delta T) + d_1 \log\left(\frac{SP}{Ld^2 E^{0.25}\gamma_c^{1.25} f_c^{0.375}}\right) \\ & + d_o \log\left(\frac{P}{Lh^2 f_c} \frac{x^{0.033} y^{0.51}}{\Delta y^{0.52}}\right) + \text{intercept} \end{aligned} \qquad (5.2)$$

It will be noted that Eq 3.8 is used to reduce the values of concrete bearing, compressive, flexural or tensile strength to a seven day flexural strength f_c , as measured in the field laboratory at the time of construction. The value of P is taken as 18 kip (80 kN) and L as 12 ft (3.66 mm) or one lane width. These values are based on the assumption that the construction joint, between the two traffic lanes, allows little or no load to be transferred from one lane to the other. This assumption seems valid since it was earlier shown, in Chapter 3 and Appendix 2, that load transfer depends on crack width and the amount of steel which act as dowels. In both respects of crack width and dowel steel, the longitudinal construction joint can be considered inferior if compared to load transfer conditions at transverse cracks. It was also indicated that the highest stresses occur in the middle of the beam between two cracks if proper load transfer is assumed at the cracks but crack deterioration causes a loss in load transfer which results in higher stresses in the beam if the load is placed at the crack. The occurrence of transverse cracks in a beam can therefore be traced to the above cycle: the cracking of a beam under loading at a point midway between two transverse cracks until load transfer at the deteriorating cracks is small enough to move the point of critical stress in the beam from between the cracks to close to the deteriorated cracks. However, the above mechanism does not seem to be present transversely, since no longitudinal cracking is experienced on the sections under investigation. This seems to indicate that transverse beam action can be neglected.

The term associated with the coefficient d_1 in Eq 5.2 represents the load transfer through dowel action of the longitudinal steel reinforcement. Since the reinforcement does not change in the sections under investigation the only value that changes is the strength of the concrete. However, because of this sole dependency on concrete strength, a high intercorrelation is experienced between terms d_1 and d_2 of Eq 5.2 which tends to distort the validity of the derived coefficient. The term d_1 is therefore excluded from the subsequent regression runs. Several suggestions on the use of this term are discussed later on in the report.

The form $ZS = \log N - \log n$ is used in the regression analysis instead of the regular form $Z = \frac{\log N - \log n}{S}$ for the same reason as mentioned for the exclusion of the term for dowel action; namely, a high

intercorrelation between terms. The second format contains an S term in each variable so that high intercorrelation is experienced which leads to distorted values for the coefficients as well as a wrong impression of the reliability of the equation in terms of r^2. Therefore, the term ZS will be kept throughout the rest of the report and will be treated as one entity. Separation of the two terms is necessary, however, to be able to interpret the results of the regression.

The Quantification of the Standard Deviation S

The calculation of S is discussed in Appendix 4. Using Eq A4.4, S can be written as (covariance and second derivatives are ignored):

$$S^2 = (\log e)^2 \left[\left(\frac{d_2 + d_1 + d}{P} \right)^2 S_P^2 + \left(\frac{d_2 + 1.25d}{h} \right)^2 S_h^2 + \left(\frac{.5d_2 + d}{f_c} \right)^2 S_{f_c}^2 + \left(\frac{d(R)}{\Delta x} \right)^2 S_{\Delta x}^2 + \left(\frac{d(\alpha) + .033d}{\bar{x}} \right)^2 S_{\bar{x}}^2 + \left(\frac{0.51d}{y} \right)^2 S_y^2 + \left(\frac{0.52d}{\Delta y} \right)^2 {}_{\Delta y}^2 \right] + S_{\log n}^2 \qquad (5.3)$$

where S^2 denotes variance of the terms as signified by the subscripts. The variances of several terms, which include thermal coefficient α, Los Angeles Abrasion (LA) and amplitude (A), cannot be determined from construction or other records and are therefore excluded. This means that the value of S will be too small. However, these excluded variances are assumed to be insignificantly small since the terms excluded are generally associated with material and other properties which were strictly controlled on the construction site. As will be shown later, this is a valid assumption since terms associated with Los Angeles Abrasion, amplitude, and thermal coefficient are insignificant or even disappear.

The Valuation of Distress in Terms of Z

The value of Z is determined from a normal distribution table and is a measure of the distance from the mean of the distribution of the difference density function to the line that depicts the proportion of the section that has failed, as shown in Fig 3.1. Thus, if 3 percent of the sectional area

has failed, Z will have a value of 1.88. The value of Z can be determined for each type of distress where the different types of distress can be defined as follows (Ref 4):

(1) Transverse cracking: the combined area of the section that experiences transverse cracking which occurs in clusters where the crack spacing is in the order of 2 feet (0.6 m) or less.

(2) Minor spalling: the widening of existing cracks through secondary cracking or breaking of the crack edges. This can also be defined as crack deterioration.

(3) Severe spalling: the deterioration of the surface at the crack through a loss of concrete surface, generally about 4 to 6 inches (100 to 150 mm) wide and no deeper than 0.4 inch (10 mm).

(4) Minor pumping: when vertical water movement from below the slab (at the pavement edge) creates stains of fine soil material on the shoulder.

(5) Severe pumping: a severe loss of fine soil is obvious through pumping.

(6) Minor punch-outs: closely spaced transverse cracks are linked by longitudinal cracking. (Not to be confused with longitudinal cracking that stretches for several feet (meters) and may occur irrespective of the existence of closely spaced transverse cracking.)

(7) Severe punch-outs: the blocks created by minor punch-outs start to move under traffic loading and become loose.

(8) Patches: the maintenance patches due to structural failure. This can be in asphaltic or portland cement concrete but excludes surface patching such as of small overlays or of severe spalling.

In order to compare and/or combine distress types, it is important to use a common yardstick in the measurement of each distress individually. Thus, since all quantitative distress must relate to Z , the standardized normal variable, distress is measured in terms of the percentage of sectional area that exhibits this distress. This implies that repair patches can, for instance, actually be measured in square feet (m^2) and expressed in terms of square feet patched per square feet of road area surveyed (m^2 per m^2 road area surveyed), which means patching is expressed as a percent of area surveyed. Thereby, Z can be determined from a standard normal table. The other types of distress are measured with their definitions as given above in mind. Therefore, transverse cracking and pumping are measured in terms of the percentage of road length that has this type of distress; spalling is measured as a percentage of cracks in a section length that exhibits spalling; repair patches are measured as explained above, but punch-outs, which were

actually determined in the survey (Ref 1) in terms of the length of the punch-out, have to be converted to an equivalent area repaired. Figure 5.2 contains the conversion of length of punch-out to an equivalent area repaired, which can easily be converted to a percentage in terms of the actual pavement area surveyed. These values can now be used to combine any distress types if needed and the relative values of Z are independent of units of measurement of even length of section under consideration.

Regression of the Theoretical Model

Both sides of Eq 5.2 are influenced by the coefficients to be derived. For this reason, a process of iteration is employed whereby the coefficients are guessed as a first approximation. The value of S is calculated from this assumption and the true coefficients are then found by regression. Then S is recalculated with the new values and the regression is repeated. This process is carried on until both sides balance out, which usually occurs at the lowest standard error (s.e.) and the highest correlation r^2. As expected, log n, which supposedly has a coefficient of one, has a coefficient less than one. Multiplying throughout the final equation to get a coefficient of one for $\log n$, raises the value of ZS, which implies that S is not large enough. This can be explained by the fact that the variance of concrete strength as measured in the laboratory does not accurately reflect the actual variance in the field. Other sources of error can be the variance of $\log n$, i.e., the number of loads applied to the pavement, as well as the exclusion of the variance in concrete density γ_c and thermal coefficient α. All these factors, except $\log n$, are associated with construction variables and will be discussed in the next paragraph. Table 5.1 shows the magnitude of variance for each factor in Eq 5.3 for two of the most important types of distress, severe punch-outs and repair patches. It is interesting to note from the table that the variance of crack spacing $S_{\bar{x}}$ is by far the biggest contributor to S and that road roughness contributes almost three times as much to S as the variance of $\log n$, the estimated number of load applications.

Table 5.2 contains the results of the regression analysis using Eq 5.2. The tabulated values have been adjusted in order to have the coefficient of $\log n$ equal to one. The values of the coefficient for $\log n$ varied between 0.75 and 0.96 before adjustment, which indicates that the calculated values for S were between 1.33 and 1.04 times too low. The value of S is

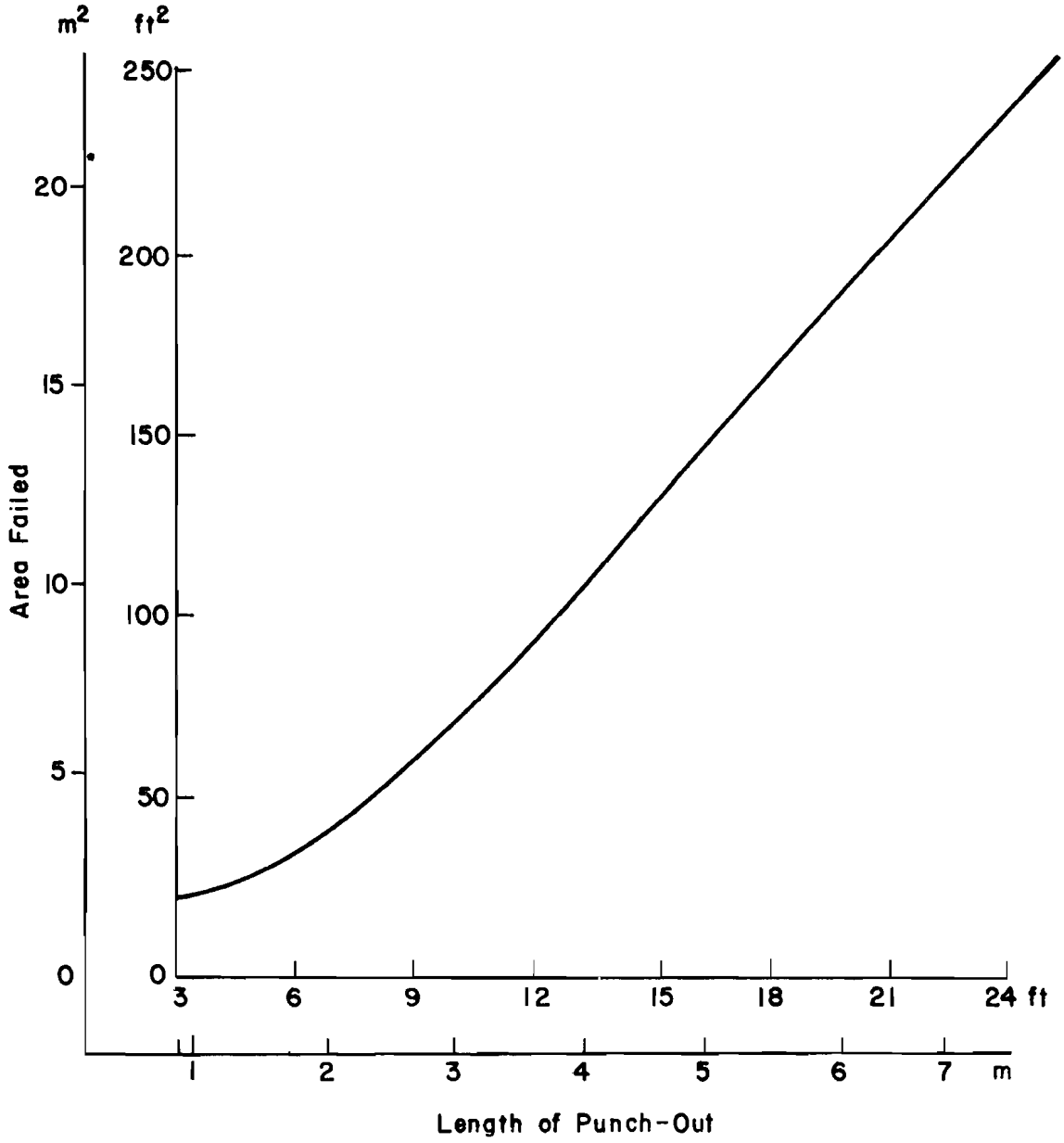

Fig 5.2. Conversion of punch-out length to equivalent area of repair patch.

TABLE 5.1. RELATIVE CONTRIBUTIONS OF THE VARIABLES TO THE MAGNITUDE OF STANDARD DEVIATION S EQ 5.3

Source	Severe Punch-outs	Repair Patches
Load P*	.093	.082
Strength f_c	.060	.069
Curvature $\triangle y$	.097	.089
Deflection y	.042	.039
Crack spacing $\bar{x}$	.147	.191
Thickness h	.039	.047
Crack width $\triangle x$	.000	.000
Loads applied log n	.036	.036
Total value of S	.514	.553

*The variance of P depends on the road roughness and is calculated by a computer program DYMOL (Ref 49).

TABLE 5.2 REGRESSION COEFFICIENTS USING EQ 5.2 FOR DIFFERENT DISTRESS TYPES

Distress type	Coefficient d_2	d(R)	$d(\alpha)$	d	Intercept*	Standard Error	r^2
Repair patches	+8.80	-0.28	-2.77	-2.20	-8.75 (10.84)	0.47	0.43
Severe punch-outs	+8.46	-0.26	-1.27	-3.02	-6.45 (8.51)	0.48	0.28
Minor punch-outs	+7.09	-0.52	-	-4.11	-5.14 (0.99)	0.63	0.25
Severe pumping	+9.01	-0.30	-2.34	-2.18	-8.64 (11.63)	0.38	0.49
Minor pumping	+15.37	-0.57	-3.30	-1.42	-13.82 (29.82)	0.67	0.49
Severe spalling	+7.80	-0.26	-1.92	-1.36	-4.11 (15.52)	0.28	0.53
Minor spalling	+8.33	-0.24	-2.55	-1.35	-7.76 (13.69)	0.30	0.58
Transverse cracks	+8.54	-0.33	-1.18	-1.57	-5.20 (15.84)	0.31	0.44

* Values in brackets are the intercept values if the variables in Eq 5.2 are measured in kN , kPa , cm, and °C. All other coefficients are unaffected by a change.

Units otherwise are in pounds, inches, and °F.

adjusted to its proper value through a regression of construction and other variables as discussed in a later paragraph.

The values of the coefficients as shown in Table 5.2 are now used to examine the importance of the Westergaard equation in predicting minor and severe punch-outs, as well as repair patches. This is done by regressing the following equation, which is an adjusted form of Eqs 5.1 and 5.2 to include the Westergaard format:

$$C \cdot 10^{ZS} \cdot n \cdot \left(\frac{1250\gamma_R}{h\gamma_c f_c^{0.5}}\right)^{d_2} \cdot \left(\frac{\Delta x}{R}\right)^{d(R)} \cdot (LA)^{d(L)} \cdot (A)^{d(A)} \cdot (12\bar{x}\alpha\Delta T)^{d(\alpha)} = \left[\frac{P}{f_c h^2}\left(C_1 \log \ell/b + C_2\bar{x}\right)\right]^{d_o} \quad (5.4)$$

where

C = antilog of the intercept derived from a regression of Eq 5.2.

As a first assumption, d_o is assumed to have the same value for Westergaard as for the beam equation. However, in each of the three cases, namely, repair patches and minor and severe punch-outs, the Westergaard format is found to add no more significant value to what is explained by the beam equation. The F-value of the coefficient C_2 is less than 0.7 and thus insignificant. The values of the coefficients, themselves, however, suggest the use of the edge loading format of the Westergaard equation (Ref 6).

The conclusion can therefore be drawn that the distress in CRCP can be explained adequately by using the beam equation. This equation will henceforth be used as the basis for the theoretical equation.

ADDITION OF OTHER VARIABLES

The first part of the regression analysis relates to a theoretical model based on the fatigue concept. The correlation between ZS , the standard deviation times a measure of failure, and log N - log n , the difference between the actual and the theoretical maximum possible number of load

applications, was shown to be low, especially for the more severe types of distress. This can be mainly attributed to an incorrect estimate of S but also to a hitherto unexplained variation in Z because of construction, environmental, and other variables. The main contributors to an incorrect S include the unaccounted for variation in the strength of concrete, variation in subgrade support variation in actually applied loads, and a loss of effective slab thickness due to poor densification of concrete at the bottom of the slab.

The standard deviation of the strength of the concrete was based on laboratory compacted and tested samples of beams, tested for flexural strength. The strength of concrete not only plays a role in the flexural strength of the slab itself but is also included in the analysis of load transfer either through granular interlock or by dowel action of the longitudinal steel reinforcement. It is shown in Appendix 2 that the latter is the most important means of load transfer but due to a lack of variability, the term which includes the prpperties of the steel reinforcement, is excluded from the first regression step. The variation in strength of the concrete that surrounds the steel is of utmost importance in this respect. This variation in strength can also be related indirectly to variables which can be measured more readily than the strength of concrete at the steel interface. These variables include workability of concrete, method of construction, densification of concrete, steel placement method, and other inherent qualities of the concrete that may affect its final strength.

One other variable that needs attention in this respect is crack spacing $\bar{x}$ and its standard deviation $S_{\bar{x}}$. It was shown by McCullough et al (Ref 14) that crack spacing can be predicted from known design variables. Assuming that these design variables, which include concrete strength, slab thickness, uniformity of subgrade support, etc., are absolutely uniform throughout the actual slab in the field, the crack spacing will be even, with no standard deviation $S_{\bar{x}}$. However, $S_{\bar{x}}$ is larger than zero and therefore can be used to indicate not only variation in slab properties but also nonuniform subgrade support.

Subgrade support and slab stiffness were incorporated in the theoretical equation as a ratio of deflection and curvature under Dynaflect loading. As such, variation in subgrade support was tied into S by a theoretically considered relationship to deflection, but, since theory assumes uniform support

of the slab, variation of subgrade support needs to be considered as insufficiently expressed by deflection alone. Many reports (Refs 1, 6, 10, 14, and 19) cover this subject and investigate the variation of subgrade properties, some of which will be incorporated in this regression. Other variables that may reflect some of the variance of subgrade support include type of base and geometry of the sections. The loss of subgrade support due to pumping of the base as well as the adaptability of the base to uneven settlement or subgrade swell influence subgrade support. The contribution of geometry of the pavement to subgrade support relates to the susceptibility of the subgrade to settlement (high embankments) and swelling clay activity (profile at ground level and in excavations where variation in moisture with changes in season is the highest). As mentioned before, a fixed ratio of curvature and deflection was considered before in the quantification of slab/subgrade stiffness and it can be assumed that deflection and curvature individually may explain some variation in S too. These are therefore also included separately in this second regression study.

An attempt to explain the manifestation of distress through a theoretical equation, based on fatigue principles as well as a stress analysis, was not fully successful. As can be expected several other variables not included in the first regression, may have a significant influence on the development of distress. These variables with some previously used variables such as deflection and flexural strength together are included in the second regression. Since the variations in S and Z are so closely related, no attempt will be made to differentiate between the two, but SZ will be treated as a unity in this respect. Therefore, interpretation of the signs of coefficients must be made in the light of this reality.

The variables that are included in the second regression are summarized in Table 5.3. The categories, which relate to the justification of their inclusion as discussed in this paragraph, are also indicated in the table. These categories may primarily be of concern to improve the measurement of a true standard deviation S, but can also be interpreted as having an effect on the manifestation of distress as reflected by Z. Thus an increase in the cement content may decrease workability whereby S will be increased

TABLE 5.3. OTHER POSSIBLE VARIABLES INCLUDED IN THE SECOND STEP OF REGRESSION ANALYSIS

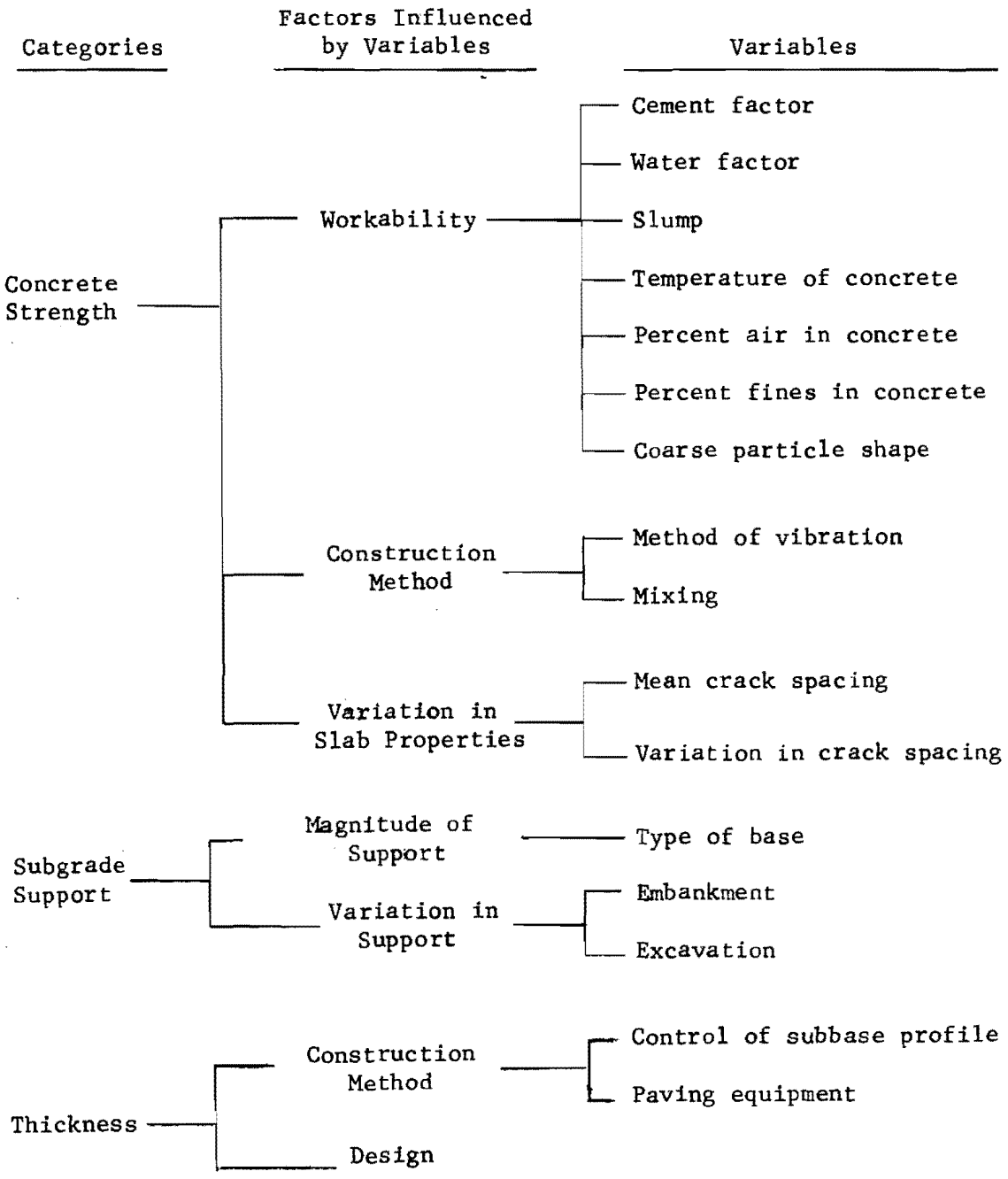

but on the other hand an increase in cement content can increase the slab strength which causes less failure i.e. increasing the value of Z .

The format that will be used in the second regression analysis is compatible with the first regression:

$$ZS - \log N + \log n = \text{independent variables as in tables 5.3 and 5.4.} \quad (5.5)$$

Table 5.4 shows the different types of distress and the independent variables used in the regression as well as some important statistical measures, to indicate the reliability and significance of the equation for each distress. It will be noticed that the individual independent variables are multiplied by a time factor, the age of each section under consideration. This is done to eliminate the time effects that these variables may have on the range of the dependent variable. This can be illustrated by Fig 5.3, which shows a plot of failure, where failure indicates the sum of repair patches and an equivalent repair area of severe punch-outs, versus time. The two lines A and A' , show intercepts with the axis at time zero and imply failure can be expected if the cement content is low at time zero, that is, before any load has been applied. On the other hand, A and A' have been multiplied by time t and the resulting lines B and B' indicate zero effect on failure at time zero. Multiplication with time, therefore, ensures the inclusion of the time effect that Z has on S in the term ZS . This implies that distress manifestation is not only a function of load applications, through a stress anlaysis and the fatigue concept, but also of construction and environmental factors through time. A discussion of the results of the regression will be presented in the next chapter.

THE COMBINATION OF EQUATIONS

The involvement of all possible variables in the structural performance of a CRCP was researched in the first part of this chapter. Equations were developed for the eight types of distress manifestations that were distinguished in a previous study (Ref 1). Design against the occurrence of these distress types is now possible. However, the alliance between the different distresses has not been discussed and, since failures, for example, were

TABLE 5.4. COEFFICIENTS OF THE SECOND REGRESSION STEP.

Distress+ Variables x age*	Transverse Cracks	Spalling		Pumping		Punch-Outs		Repair Patches
		Minor	Severe	Minor	Severe	Minor	Severe	
Standard Deviation f_c, psi								.0013
Variance $f_c \times 10^{-4}$ psi^2							.0642	
1/Variance f_c, psi^{-2}		-.9501		2.2065			-1.3339	
Slump, inches	-.0168	-.0134			-.0744			-.0369
1/slump, $inches^{-1}$					-.1312	.1843		
Concrete temperature, °F								-.0015
$1/\bar{x}$**, ft^{-1}		-.3181		-1.1750				
1/Std. dev. $\bar{x}$, ft^{-1}					.7822			
$1/\bar{x}^2$, ft^{-2}	-.5228		-1.1934		-1.1178	-2.5986	-1.7804	
Variance $\bar{x}$, ft^2	-.0032	-.0030	-.0046					
1/Variance $\bar{x}$, ft^{-2}	.1525	.4916	.5725	.9269	1.8975	.7562	-.1233	
Std. dev. deflection, inches				315.2	-961.9	02522.9		
1/Std. dev. deflection $\times 10^{-4}$, $inches^{-1}$	.0141			.0744			-.0052	
Variance deflection, in^2					2511856	7622053	-951882	
1/Variance deflection $\times 10^{-9}$, in^{-2}	-.0141		-.0061	-.0715	-.0097	-.0307		

(Continued)

TABLE 5.4. (Continued)

Distress+ Variables x age*	Transverse Cracks	Spalling		Pumping		Punch Outs		Repair Patches
		Minor	Severe	Minor	Severe	Minor	Severe	
Percent -100 sieve of aggregate		.0043	.0129					
Surface vibration (dummy)						-.0987	-.0338	.0628
Internal vibration (dummy)		.0179	.0365					
Central mixing (dummy)						-.0600		
Asphalt base (dummy)			-.0272	.0342	.0296		.0303	.1380
Cement stabilized base (dummy)						-.0813		.1395
Fill (dummy)	-.0136	-.0150	-.0297	-.0831	-.0366			
Intercept	.2216	.2371	-1.1153	.8027	.7830	2.4191	.1148	-.4000
r^2	.525	.789	.809	.769	.838	.841	.644	.554
Standard error	.226	.285	.372	.679	.418	1.003	.548	.468

\+ Distress is measured in terms of ZS - log N + log n.

* All variables are multiplied by the age of the section under investigation. Dummy implies a value of one if variable is used.

** $\bar{x}$ = mean crack spacing at the time of survey.

Conversion of coefficients to the metric system:

1 in = 25.4 mm
1 psi = 6.984 kPa
1 °F = 0.5556 °C
1 ft = 0.3048 m

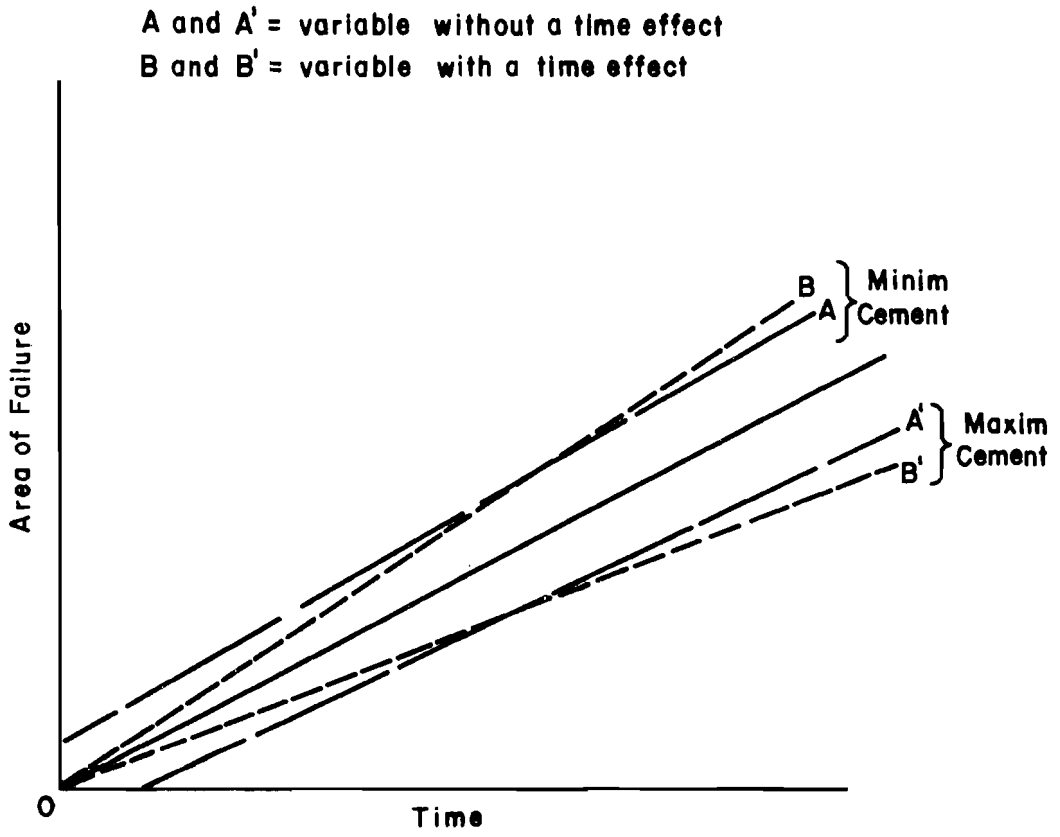

Fig 5.3. Failures as a function of time for a maximum/minimum cement content.

shown in a previous study to be dependent on the occurrence of the other types of distress (Ref 1), an equation that depicts this relationship needs to be derived.

A technique by which distress can be predicted from a one-time condition survey was developed by Williamson (Ref 47). This technique involves the quantitative back prediction of distress using equations that relate present condition to design, environmental, construction, and other variables such as age and number of load applications. The equations developed earlier in this chapter can be utilized in calculating distress at a randomly selected time in the past.

Equation 5.5 can for the present condition be written as

$$(ZS)_t - \log N + (\log n)_t = f(G,t) \tag{5.6}$$

where

$(ZS)_t$ = the standardized normal variable times standard deviation which relates to the distressed area at time t,

N = number of load applications designed for,

n_t = number of loads actually applied over the lifetime t of the pavement,

G = other variables such as construction, environmental, and design variables.

Calculation of ZS for a time increment j into the past, results in

$$X_{t-j} = (ZS)_{t-j} = \log N - (\log n)_{t-j} = g(G,t-j) \tag{5.7}$$

Equation 5.7, for the different distress types, can now be employed to generate a final equation in which failure at time t, for example, is related to the other "minor" types of distress and failures at time $t-j$:

$$X_t(\text{severe punch-outs}) = F\left[X_{t-j}(\text{severe punch-outs}), X_{t-j}(\text{minor punch-outs}), X_{t-j}(\text{pumping}), X_{t-j}(\text{spalling}), X_{t-j}(\text{transverse cracking}), X_{t-j}\ \bar{x}, t-j, \Delta \log n\right] \quad (5.8)$$

where

$\Delta \log n$ = the added amount of load applications during time $t-j$.

It will be noted that two measures of crack spacing are included. Transverse cracking, relates to the clusters of closely spaced transverse cracks as defined in the first part of this chapter and $\bar{x}$ signifies the mean crack spacing at time $t-j$. The latter is included for two reasons namely that it is possible to design a CRCP for a particular mean crack spacing (Ref 14) as well as the fact that mean crack spacing is relatively easy to measure at any time of the life of a CRCP.

The coefficients of equations for minor and severe punch outs, all based on the conceptual Eq 5.8, are summarized in Table 5.5. Two equations are shown for severe punch-outs, the first a function of severe punch-outs at time $t-j$ and the second equation without this variable.

The first set of coefficients of severe punch-outs indicate that further structural failure can be expected wherever minor pumping and severe punch-outs are present. On the other hand, the second set of coefficients for severe punch-outs relate the occurrence of structural failure more to minor spalling and minor punch-outs. This need not be seen as a controversy since high intercorrelations exist between the different types of distress. It is found for instance that correlation with severe punch-outs decreases from $r = 0.767$ for minor punch-out, through 0.732 for minor pumping, 0.697 for severe pumping, 0.723 for minor spalling to 0.540 for transverse cracking. Thus, it can be stated that severe punch-outs is a function of the minor types of distress, the exact relationship depending on the individual correlations.

TABLE 5.5. COEFFICIENTS ASSOCIATED WITH MINOR DISTRESSES WHICH PREDICT FUTURE SEVERE TYPES OF DISTRESS

	Dependent Variable ZS at Time t	
ZS at Time t-j	Minor Punch-Outs	Severe Punch-Outs*
Δ log n	3.206	2.216	0.823
$(\Delta \log n)^2$	-2.393	-2.078	-2.214
Transverse cracks	0	0	0
Minor spalling	0	0	0.808
Minor pumping	0	0.171	0
Minor punch-outs	1.161	0	0.186
Severe punch-outs	0	1.063	0
Failures	0	0	0
Crack spacing $\bar{x}$	0	0.103	0
$\bar{x}.\Delta$ log n	-0.943	-0.486	0
Intercept	-0.688	-1.203	1.142
r^2	0.808	0.749	0.671

* The first set of coefficients relate future severe punch-outs to the present amount of severe punch-outs whereas the second set excludes the present amount of severe punch-outs.

Since repair patches were made prior to the condition survey, no record exists as to the type of distress that was repaired. It is reasonable to expect that prediction of future structural failure must rather be based on the occurrence of severe punch-outs and not on repair patches since existing repair patches may represent failed areas as a result of poor construction practice, unusual failures or even preventive maintenance where minor distress has occurred.

Combination of Equations to Predict Structural Failure

Two different sets of equations are now available, the first, Eq 5.6 relating distress to design, environmental and construction variables and the second, Eq. 5.8, which indicates the correlation between other types of distress at an earlier stage and present failures. The second equation, 5.8, can be used to predict future structural failures in terms of the present structural condition but this prediction will be insensitive to the design and construction variables in Eq 5.6. In order to incorporate these variables into the equation, Eqs 5.6 and 5.8 can be combined utilizing their respective correlation coefficients, $r^2_{5.6}$ and $r^2_{5.8}$ (Ref 53).

$$X_{t+i}(\text{punch-outs}) = \frac{X_t(\text{punch-outs}) \cdot r^2_{5.8} + X_t \cdot r^2_{5.6}}{r^2_{5.8} + r^2_{5.6}} \qquad (5.9)$$

where

X_t = the value of Eq 5.6 calculated for punch-outs from theoretical considerations, and

$X_t(\text{punch-outs})$ = punch-outs as a function of other types of distress as in Eq 5.8.

Equation 5.9 can thus be employed in predicting future structural failures in terms of the present condition of the pavement and the measurable design, construction, and environmental variables as reflected in Eq 5.6.

The combination of equations in Eq 5.9 is shown to be in terms of punch-outs but, as can be expected, any distress type can be predicted for rehabilitation/maintenance purposes on this basis. The combination for structural failure in the form of severe punch-outs will be discussed in the next chapter.

The Variation of S with Time

The combination of Z , a measure of the distressed area, and S in Eqs 5.7, 5.8, and 5.9, implies a dependency of both Z and S on the independent variables. In order to interpret the significance of the different independent variables and their coefficients, a knowledge of the predictability of S in the future may be helpful.

The standard deviation S was shown to be dependent on design and environmental variables in Eq 5.3. It is possible to predict a future S by prediction of S_p^2 , Δx , $S_{\Delta x}^2$, $\bar{x}$, $S_{\bar{x}}^2$, y , S_y^2 , and $S_{\log n}^2$, where the terms are as defined previously. However, a rough estimate of a change in S with time can be made utilizing the data available on this project. It must, however, be recognized that the model is developed for climatic, subgrade, construction, and other variables prevailing at the test site under investigation. Thus, extrapolation to other conditions may be erroneous and even dangerous.

The same principles are applied here as were applied in the prediction of ZS , namely, that a future S is determined in terms of the present S and in terms of different combination of $\Delta \log n$ and Δt , the increase in load application and age, respectively. The resulting equation can be written as summarized for the different coefficients in Table 5.6:

$$S_t = S_{t-j} + b_1(\Delta \log n) + b_2(\Delta \log n)^2 + b_3(\Delta \text{ age}) + b_4(\Delta \text{ age})^2 + \text{intercept} \qquad (5.10)$$

where Δ age is measured in years and $\Delta \log n$ in number of load applications.

As can be seen from the r^2 of the equations, the reliability is not good, especially for repair patches, and care must be exercised in the application of this result.

THE INFLUENCE OF GEOMETRY

The analysis discussed thus far is based on randomly selected sections on a level, straight highway. However, the condition survey for the total length can be utilized to research the relative influence of geometry on the

TABLE 5.6 PREDICTION OF THE FUTURE S IN TERMS OF AN INCREASE IN AGE AND LOADING.

S for **	Independent variable*					
	Δ log n	(Δ log n)^2	ΔAge	(ΔAge)	I	r^2
Transverse cracks	0.42	0	0.26	-.02	-2.64	0.44
Minor spalling	1.68	0	0.76	-.05	-11.00	0.50
Severe spalling	0.91	0	0.45	-.03	-5.82	0.48
Minor pumping	1.58	0	0.78	-.05	-10.23	0.48
Severe pumping	1.09	0	0.48	-.03	-6.73	0.41
Minor punch-outs	1.34	0	0.66	-.05	-8.62	0.48
Severe punch-outs	0.35	0	0.27	-.02	-2.13	0.38
Repair patches	0	-0.04	0	.002	1.72	0.27

*Age is measured in years and log n in log number of load applications:

**Equation used: $S_t = S_{t-j} + b_1(\Delta \log n) + b_2(\Delta \log n)^2 + b_3(age) + b_4(age)^2 + intercept$

occurrence of distress. The condition survey mentioned above was done in 0.2-mile (0.32 km) sections and consisted of a quantitative estimate of the amount of distress (Ref 1). Construction plans were used to tie survey sections to geometry in the form of vertical and horizontal alignment. An association with the speed of traffic was done through engineering judgment and was done by classification into two categories: fast and slow. The distinction is necessary since sections with similar geometry but with different approach gradients may influence the positioning of vehicle loads on the pavement. For example, sections which are preceeded by a long downgrade may be influenced by the relative positioning of heavy vehicles on the road (slower vehicles tend to move closer to the outside edge).

The significant results of the regression analysis are summarized in Table 5.7 where turn left or right refers to a curve in the highway; crest and sag to the transition of the vertical alighment; and cut, fill and transition referring to the average cross-sectional profile of each section investigated. It is obvious from the r^2 achieved that the contribution of geometry to distress is insignificant except for minor pumping, which depends on geometry to a certain extent. It can therefore be concluded that geometry need not be taken into account unless minor pumping is of concern.

This chapter was devoted to a generation of regression steps; whereby, all possible variables were researched in their effect on distress manifestation. Certain variables such as climatic conditions and the effect of steel reinforcement were not included because of lack in variability and high intercorrelation between terms in the case of steel reinforcement or because the influence of climatic conditions on structural failure were researched on a statewide basis in another study (Ref 5). The influence of these factors either need to be researched further or in the event that the influence is fairly insignificant, as is the case with the influence of geometry, only be aware of the possible effects and consideration for it in the design stage.

TABLE 5.7. THE EFFECT OF GEOMETRY ON THE OCCURRENCE OF DISTRESS

	Distress				
Variable*	Pumping	Minor Spalling	Severe Spalling	Minor Punch Outs	Severe Punch Outs
Turn left	-0.8	0.0	1.7	0.0	-6.6
Turn right	0.0	0.0	-3.0	0.0	0.0
Crest	-2.7	0.0	0.0	-22.3	0.0
Slope	0.0	0.0	0.5	0.0	-1.5
Sag	-2.3	0.0	0.0	-11.8	0.0
Slow traffic	0.6	-2.3	0.0	0.0	0.0
Fast traffic	0.0	-3.5	1.6	0.0	0.0
Cut	0.6	-2.3	0.7	0.0	-8.6
Fill	-0.6	-2.6	0.0	0.0	-3.9
Transition	0.0	-1.5	0.8	16.8	0.0
r^2	0.18	0.04	.04	0.01	0.01

* All variables are dummy variables except for slope which is measured in percent. A positive value for slope signifies an uphill condition. A dummy variable is assigned the value of 1.0 if the condition exists and zero if not.

CHAPTER 6. DISCUSSION AND APPLICATION OF RESULTS

The regression analysis was accomplished by way of two basic steps. The first step was to relate distress to the previously derived theoretical models. The basic concepts that were used in this respect were the stochastical nature of distress and the fact that distress is a fatigue related phenomenon. The second part of the regression analysis was devoted to an explanation of variance not accounted for in the first model. This approach allows the application of the results on conditions other than those prevailing at the site investigated. Some of these conditions include a drastic change in pavement thickness, concrete strength or magnitude of load, and even a different subgrade support.

Care must, however, be exercised in applying the total model to other conditions found at the test site. A discrete assessment of the influence of these variables will be necessary if the model is applied elsewhere, especially if it is kept in mind that the additional variables not only describe the variance not accounted for in the theoretical model, but also the occurrence of theoretically unexplained distress.

A discussion of all the facets in the regression analysis with respect to the results will be presented in this chapter. The theoretical models will be discussed first, especially the importance of load transfer at transverse cracks either through dowel action of the longitudinal steel reinforcement or through aggregate interlock. A discussion on the relevance of the standard deviation of $\log N$ and $\log n$ will be followed by the importance of construction and other variables. Lastly some practical applications in design and construction will be highlighted with special reference to the importance and implication of coefficients in the final regression model.

THEORETICAL ANALYSIS

The theoretical model is based on the stochastical assumption that the difference between the actual number of loads applied and the theoretical

maximum number of load applications possible, follows a normal distribution. This means that area failed can be expressed in terms of the standard normal variable Z . The calculation of the maximum number of load applications is based on the fatigue concept, which requires some form of stress calculation in the slab as a result of a wheel load. Consequently, two basic equations for stress calculation were investigated; namely, the simulation of a CRCP by a beam and the Westergaard equation.

Distress Mechanism of CRCP

It has been indicated previously that the assumption of the CRCP being a continuous beam on an electric foundation rendered reasonable results and was less complicated to work with than the Westergaard equation. The Westergaard equation can be used provided the format for the edge loading condition is employed. It has been shown that the simulation of CRCP as a beam is as accurate as the Westergaard approach. Furthermore, radial cracking, a characteristic of torsional failure in a slab, is seldom seen on CRCP and seldom leads to structural failure. Torsional failure occurs so infrequently on CRCP in Texas that no accurate analysis of its effect was possible because of a lack of data. The assumption that a CRCP can be simulated by a beam, leads to a hypothesized distress mechanism: beam action occurs in a longitudinal direction on a new pavement and, as the cumulative load applications increase, transverse cracks occur first between two shrinkage cracks. As crack deterioration progresses and loss of load transfer results transvers cracks appear closer to the deteriorating cracks. Consequently, the relatively narrow transverse crack spacing (2-3 ft or 0.6-0.9 m) eventually results in transverse beams because of a total loss of load transfer at the cracks. A further increase in fatigue distress leads to so-called longitudinal cracks which show up in the narrow transverse beams. These can generally be defined as minor punch-outs. Minor punch-outs eventually may lead to severe punch-outs as a result of total crack deterioration and it may become necessary to repair the structural failure.

An important step in the analysis was the characterization of slab and subgrade stiffness. A ratio of concrete slab stiffness to subgrade stiffness was determined with the help of Dynaflect measured deflections. This method is useful in structural evaluation and can be applied for maintenance/rehabilitation purposes. However, the method of simple substitution of

$$x^{0.033}\ y^{0.51}/\Delta y^{0.52}$$

with EI/k cannot be employed in design of new pavement. The value of EI/k can be substituted into the equation for design purposes, provided the correct relationship with a Dynaflect measured y , Δy , and x has been established through actual field calibration. Simple substitution of EI/k will undoubtedly have an effect on the coefficients that were derived for the beam equation.

Dowel Action of the Longitudinal Steel Reinforcement

Although the term for dowel action of the longitudinal steel reinforcement never entered the regression model because of high intercorrelation and a lack of variation in steel reinforcement, as discussed previously, the steel nevertheless performs a very important function in load transfer. This is illustrated by calculation of the load on the concrete due to load transfer by the steel at a crack. Using Eq A2.8 and assuming half an axle load is transferred by dowel action (a void is assumed to exist under the slab at the crack), the stress on the concrete around the steel can reach a value of 700 psi (4.82 MPa). Assuming strain in the concrete due to this loading occurs over 1 inch (25.4 mm) of concrete, a deflection of 0.0002 inch (0.005 mm) will result, which is just enough to enact granular interlock for a crack width of 0.014 inch (0.35 mm) and a 1-inch (25.4-mm) diameter aggregate (Eq A2.1 and Fig A2.2). However, it is clear that the bulk of the load transfer is carried by the dowel action of the steel and, thus, the concrete surrounding the steel at the crack. The importance of the bearing capacity of the concrete, especially below the steel where the concrete is prone to honeycombing due to difficulty in vibrating or compacting it properly, is therefore an important consideration in design, construction, and maintenance procedures. The use of repair patches in maintenance requires the restoration of load transfer through dowel action, especially since restoration of aggregate interlock is almost impossible. This requirement is important, especially for small repair patches. Larger patches may be considered as a slab on their own, and load transfer may not be crucial then.

Granular Interlock and Load Transfer

The importance of load transfer by the steel reinforcement as well as the sensitivity of the concrete strength around the steel indicates that aggregate interlock will become more important when deterioration of the concrete around the steel occurs with time. While dowel action is critically dependent on concrete strength, the aggregate interlock relies more on crack width and aggregate size.

The results of the theoretical regression equation show that the ratio of crack width to radius of the largest aggregates is only critical for non-crushed aggregates. The fact that $\Delta x/R$ is not important in the case of crushed aggregates may be due to a non-spherical shape; thus the theory does not hold, or, that the flat sides of a crushed particle represent a big radius R which makes small changes in Δx insignificant. Since the range of particle sizes for crushed aggregate is small for the sections under investigation, R is relatively constant so that only crack width varies to a relatively great extent. In spite of the great range of crack widths for crushed aggregate sections, $\Delta x/R$ never entered the regression equation, which can only mean that crack widths are not as important for crushed aggregates as for non-crushed aggregate pavements. It also can be assumed that the concrete around the steel reinforcement is stressed less for crushed aggregate concrete due to the fact that granular interlock comes into play at a much earlier stage of relative deflection between the two ends of a crack than was theoretically anticipated. The possible need to specify that the largest aggregate fraction must be of crushed stone origin thus arises. This does not preclude the usage of natural deposits of finer aggregate since these may assist in the workability of the concrete and compaction around the steel will benefit from this, as will be discussed later.

THE STANDARD DEVIATION OF LOG N AND LOG n

The largest unknown in the analysis can be defined as the standard deviation S of $\log N$ and $\log n$ combined. Table 5.1 contains a summary of the contribution of the variables to the magnitude of S used in the theoretical regression analysis for structural failures. The largest contributors are the standard deviations of crack spacing, curvature and deflection of the slab, and load applied as related to pavement roughness.

The standard deviation of log n , the actual number of load applications, is about 35 percent of that of the applied load (Table 5.1). The question is whether an estimate of actual number of load applications can be made accurate enough, considering the influence of road roughness and vehicle characteristic on the dynamic loading of a pavement (Ref 49). An important point to consider in this respect is the accuracy of the determined in-motion weight of vehicles if the pavement approach to the scales is not absolutely level. It can be considered an impossibility to combine the standard deviation of load P and log n into one value, since it will involve the in-motion weighing of vehicles at points relatively close together (Dymol calculates the load every 6 inches (150 mm) in an average case (Ref 49)).

The fact that S depends so heavily on the variance of vehicle loading precipitates the question of the importance of swelling clays and nonuniform settlement of the subgrade. Since the variance of deflection is also a function of subgrade characteristics, it becomes clear that although swell, settlement, and subgrade moisture movements could not be entered in the theoretical model, they contribute significantly to the structural performance of a CRCP. The most reputable factor here is unquestionably the seasonal and other variation in subgrade moisture, as was pointed out in Chapter 2. Moisture affects subgrade movement and causes hydraulic erosion, of which pumping is the most significant. The question of pumping and permeability will, however, be addressed in a later stage; suffice to indicate at this stage its relationship to a variation in S through its effect on pavement roughness and deflection.

The importance of the variance of slab curvature under loading comes as no surprise since curvature is associated with slab stiffness, as was discussed in Chapter 3. Slab stiffness depends on the slab properties, of which the most important is the modulus of elasticity, and as such is a function of concrete density and strength of the concrete (Ref 30). The significance of construction considerations therefore cannot be overlooked in this respect. The same influence of construction variables can be applied to the variance in crack spacing where the variance in crack spacing relates to the thermal properties in the theoretical equation and, as such, stresses the importance of a variation in crack width and load transfer with a change in temperature.

The results of the first regression analysis have indicated a discrepancy in the calculated and regressed values of S . This can be attributed to a lack of information on the true standard deviation of several variables which can be traced back to construction variables. This lack in modelling S properly has led to the development of a second regression analysis which incorporates other variables.

SIGNIFICANCE OF CONSTRUCTION, ENVIRONMENTAL, AND OTHER VARIABLES

The previous paragraph was devoted to a discussion of the standard deviation S where it was shown that the calculated S is too small and needs adjustment. Since the theoretically calculated S does not explain fully the actual standard deviation, especially when it is considered that the standard deviation of variables associated with dowel action is not included in the theoretical S , other factors are included in the second step in regression to account for the hitherto unexplained difference between the theoretically calculated and the actual standard deviation.

The significant variables are summarized in Table 5.4 in terms of their coefficients. It will be noticed from this table that the signs of several coefficients tend to indicate a decrease in S , the opposite to what can be expected. This however, needs to be seen against the background of the format used in this regression ZS . Thus, variables that, contrary to good engineering judgment, may be indicative of a decrease in S must be looked upon as having an influence on Z as well. Hence, a decrease in ZS may very well be seen as a decrease in Z , which means an increase in distress. However, the equation must be evaluated on its statistical basis and with a regression analysis in mind, the implication of which is that the variables as combined in Table 5.4 show a best-fit with $ZS - \log N + \log n$. Therefore, the equation needs to be interpreted as a whole notwithstanding the different signs of the variables.

The most important variables that appear are different combinations of the standard deviations of concrete strength, crack spacing and deflection. All these variables relate to variation in the pavement system. Other variables that are of significance pertain to concrete compaction in the sense that they either contribute to improved workability of the concrete and better compaction or reduce the possibility of distress. These variables include

(1) a high slump,

(2) low concrete temperature

(3) proper vibration and mixing, and

(4) the shape of the aggregate in the concrete.

The amount of fines in the concrete is only evident in spalling and needs to be interpreted not as being instrumental in increasing standard deviation, but as a preventive measure for distress in the form of spalling. The same principles need to be applied in the interpretation of the presence of different base materials.

The evaluation of the precision of an equation was discussed in Chapter 4. Precision can be measured in terms of r^2 (Eq 4.4), where an r^2 of 0.90 is considered to be very good and 0.70 is acceptable, or the standard error (s.e.) (Eq 4.5), which gives an indication of the difference between the actual and predicted values of the dependent variable.

The values of r^2 as shown in Table 5.4 are good save for transverse cracking, repair patches, and severe punch-outs, the latter being a border case. The equation depicted by the coefficients in Table 5.4, Eq 5.5, however, excludes the correlation between ZS and log N - log n. The value of the correlation of ZS is really of interest in the combination of regression equations, and, therefore, a correlation of ZS versus all the other variables which include log N - log n, needs to be determined. This is possible by using the correlation matrix that is automatically calculated by the regression program. In this case, the correlations are

0.855 for transverse cracking,
0.942 for minor spalling,
0.918 for severe spalling,
0.928 for minor pumping,
0.945 for severe pumping,
0.934 for minor punch-outs,
0.862 for severe punch-outs, and
0.629 for repair patches.

Regarding the partial F , which is a test for significance of the regression and which was discussed in Chapter 4, a minimum value of 1.32 was used. This means that all variables in the equation have a maximum probability of 0.25 of being in the equation by chance. To test the possibility of inclusion of other terms or combinations of variables already in the regression model, a lack-of-fit and pure error test can be performed. Basically, the test amounts to a determination of pure error from repeated runs which renders a lack-of-fit if subtracted from the residuals of the regression (Ref 46). The ratio of mean square due to regression and mean square due to pure error produces an F value which must be 1.0 for perfection. A large value implies an inadequate equation, i.e., more terms are needed. The critical F between the two judgments of adequate and inadequate depends on the degrees of freedom and amounts to 2.19 in the case of the second regression. Calculation of an F ratio from data pertaining to severe punch-outs renders a value of 1.036, which means adequacy but not perfection. This however, can be considered very good for the equation under investigation.

PRACTICAL APPLICATIONS

The two sets of equations that were derived with the aid of theoretical and regression techniques can be applied directly in design or rehabilitation. However, a third equation was necessary to allow the prediction of future distress in terms of the present structural condition and the design/construction variables. Some design and rehabilitation/maintenance considerations will be discussed in terms of the practical application of the equations with special reference to the interpretation of the coefficients of the variables.

Design and Construction of New Pavements

The first set of equations, derived in terms of theoretical considerations, are suitable for the design of new pavements. Since design usually is geared towards the tolerance of a limited amount of structural failure, it is suggested that the equation for severe punch-outs be used. The motivation for this suggestion is founded on the field experience that minor punch-outs may stay minor for many years and without any cause of concern to the maintenance engineer. Design on the basis of the equation for repair patches may be fundamentally erroneous since the equation is based on the existence of repair patches that could have been required due to poor construction in a

few isolated cases, repairs of minor distress as a preventive measure, or the extraordinary occurrence of structural failure, which is not accounted for in the basic assumptions of the theoretical equations. That the latter may be true is illustrated by the fact that the repair patch equations render the lowest r^2 for the same format of equations and, thus, are questionable from a design point of view.

The above discussion does not imply the disregarding of other types of distress, such as spalling or pumping, since it was clearly illustrated by previous research (Ref 1), in Chapter 5, and in Appendix 3 that minor types of distress lead to ultimate structural failure. Thus, consideration for designing against the occurrence of pumping, spalling, minor punch-outs, and transverse cracking is recommended. Transverse cracks, as defined under the condition survey (Ref 1) and as meant under the discussion above, is not deemed to be of importance in the regression equation for the prediction of future severe punch-outs, but the irregular spacing of transverse cracks is included in the analysis as a standard devation of crack spacing.

The Fatigue Coefficients. The coefficient of the fatigue equation for stress in the CRCP, as shown in Table 5.2, has a value of -3.02 for severe punch-outs. Comparing this value with the values discussed in Chapter 3 as shown in Table 3.1, indicates that -3.02 is too low. However, if the format of Eq 3.9 is used to calculate a traffic equivalence factor by keeping all variables constant and by varying the value of P, a comparison can be made with the equivalence factors as proposed by AASHTO (Ref 50). The format of Eq 3.9 is valid in this case since the equivalence factor is defined as

> the damage per pass caused to a specific pavement system by the vehicle in question relative to the damage per pass or an arbitrarily selected standard vehicle moving on the same pavement system." (Ref 6)

The equation to calculate equivalency can then be written as

$$\text{Equivalence } e = \left(\frac{P_1}{P_2}\right)^{-d_o} \tag{6.1}$$

where

P_1 = weight of the standard axle,
P_2 = weight of the axle in question, and
d_o = fatigue coefficient for stress.

The results, as well as a few comparative values from the AASHTO recommended equivalencies (Ref 50) are shown in Table 6.1. If it is kept in mind that the serviceability index of the pavement sections investigated in this study ranges from 3.6 to 4.2 and structural failure can be premature because of construction probelms, as shown in the second step of the regression analysis, then a value of -3.02 doe not seem to be out of range. Comparison of the equivalencies for $d = -4.34$, the value suggested by Yimprasert and McCullough (Ref 34) for edge loading condition at the AASHO Road test, shows a fatigue coefficient of approximately -3.6 can be recommended if rehabilitation is considered for pavements with a serviceability index P_t of 3.0. The value of 3.0 is selected for P_t since a CRCP section which had a P_t of 3.0 was overlayed in 1975 because it was deemed as structurally failed. A plot of traffic equivalencies against serviceability index P_t using data from Table 6.1 is shown in Fig 6.1. A P_t value of 3.0 will render an equivalency of approximately 10.0 for the 34-kip (151.2 kN) axle load, which, if calculated back using Eq 6.1, generates a fatigue coefficient of -3.62.

The Fatigue Coefficient for Dowel Action. The term for dowel action of the longitudinal steel reinforcement, has not been entered in the equations because of high intercorrelation problems as discussed in Chapter 5. However, suggestions can be made as to the magnitude of the fatigue coefficient and can be utilized in the event of a change from the design actually used at the site under investigation. Coefficients discussed in Chapter 3 range from 3.2 to about 40. Conversion of the plots shown in Fig 2.3 into the format of Eq 3.2, shows a range in the fatigue coefficient d of 21.5 for cantilever testing by Clemmer (Ref 26) to 27.7 for full-cycle loading as tested by Hilsdorf and Kesler (Ref 27). Since fatiguing of the concrete around the steel is a combination of direct compression directly above and beneath the steel and tension next to the steel, as discussed in Chapter 3 and Appendix 2, the value of d can be expected to approach a theoretical value of approximately

TABLE 6.1. TRAFFIC EQUIVALENCE FACTORS FOR SEVERE PUNCH-OUTS USING REGRESSION RESULTS

Single Axle Load		Equation 6.1		AASHTO*	
kips	kN	d = -3.02	d = -4.34	P_t = 2.5	P_t = 2.0
10	44.5	0.17	0.08	.08	.08
18	80.1	1.00	1.00	1.00	1.00
26	115.7	3.04	4.93	4.42	4.77
34	151.2	6.83	15.80	12.94	14.95

*Ref 91: P_t = terminal serviceability index

d = value of the fatigue coefficient

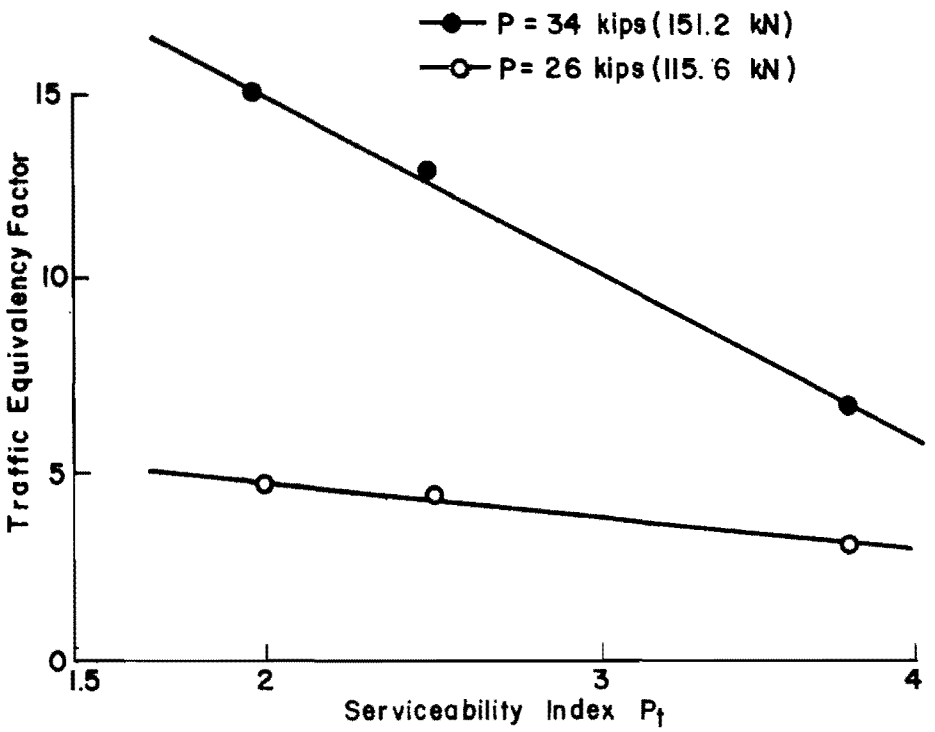

Fig 6.1. Traffic equivalence as a function of serviceability.

25. However, considering the difficulty in compacting the concrete to a high density around the steel in the slab, a much lower value of d can be expected. A regression analysis renders a fatigue coefficient for dowel action of between 1.5 and 2.0 times the coefficient d_2 for aggregate interlock if high intercorrelation between terms is not needed. This implies a d for dowel action of between 12 and 18.

The Fatigue Equation for Aggregate Interlock. The influence of granular interlock was presented in terms of three models:

(1) the influence of slab thickness h and flexural strength f_c together with the relative densities of aggregate and concrete,

(2) a ratio of crack width Δx and equivalent radius R of the 10 percent largest aggregates, and

(3) a variation in crack width with temperature change.

The coefficients of each of these models were represented by d_2, $d(R)$, and $d(\alpha)$, respectively, in Table 5.2. The interpretation of the signs associated with two of these coefficients is in line with engineering judgment: The sign of the coefficient of model 2 implies that an increase in crack width or a decrease in the equivalent aggregate radius results in more distress. In order to obtain this result a time adjustment to the value of R was necessary since smaller aggregates were used on the younger projects that were investigated. This adjustement will, however, not affect the use of the model in design or other applications. The third model also renders a sign to the coefficient that is in accordance with engineering judgment, since more distress can be expected with larger thermal movements at the cracks.

The first model associating h and f_c with ZS seems to indicate that distress, expressed in terms of Z, increases with an increase in slab thickness and flexural strength. This is contrary to engineering judgment and also contrary to the implication of the stress term, associated with coefficient d_o in Table 5.2. Again, as discussed before in the case of the significance of a term for dowel action, it can be concluded that the variation in aggregate interlock, in terms of slab thickness and concrete strength, is not sufficient to render a meaningful coefficient. This conception is strengthened by an investigation of the correlation between the d_2 term and ZS, the dependent variable. In all instances of different distress types, it is shown that the correlation between ZS and the term associated with the coefficient d_2 is less than 0.05, or r^2 is less than 0.0025.

This low correlation is not only true for ZS but also for Z and S where the maximum r^2 is 0.01 for Z and S individually.

The conclusion can therefore be made that the variation in thickness and flexural strength is too small in the sections that were investigated to produce any meaningful results for granular interlock. It is therefore suggested that this factor not be taken into account at this stage, but that it be incorporated into the final design equation for severe punch-outs as a constant.

Other Considerations. A discussion of design problems that may lead to structural failure was presented above. Some of the important elements mentioned include nonuniform settlement of the subgrade and swell, both of which are substantially influenced by moisture movement in the subgrade or base layers. Although the actual theoretical models for settlement and swell are not included in the final equation, it is possible to design with these problems in mind.

An important aspect of moisture movement is the hydraulic erosion of layers and, more specifically, the problem of pumping. Tests of the base and shoulder material on the test sections have revealed a maximum permeability of 5×10^{-4} cm/second or 1.42 feet/day. Compare this value with the recommended minimum of 20×10^{-4} cm/second or 5.67 feet/day for non-pumping unbound layers, as discussed in Appendix 3.

The question of pumping affects the structural performance of the CRCP, but settlement and swell may affect the road roughness, also, and, thereby, the variance of traffic loading S_p^2. Since S_p^2 has a considerable influence on the standard deviation S of log N and log n combined (see Table 5.1), an anticipated magnitude of S_p^2 for design purposes needs to be established. The range of values that can be expected for the other variables is probably not well known either and for the convenience of the designer, Table 6.2, which contains the mean and standard deviations of the variables measured in this project, is included.

It is important to realize that the values in Table 6.2 represent the order of magnitude but that the true values need to be determined for each individual case before application. The S value of severe punch-outs as calculated in this study is included for convenience, since design against this type of structural failure is recommended.

TABLE 6.2 THE VALUES OF VARIABLES AND STANDARD DEVIATIONS AS MEASURED ON THE TEST SECTIONS.

Variable	Mean	Standard Deviation
Thickness h in.(mm)	8.207 (208.5)	0.160 (4.06)
7-day flexural strength f_c psi (kPa)	660.1 (4551)	73.9 (510)
Slump in (mm)	1.79 (45.5)	0.44 (11.2)
Concrete temperature °F(°C)	103.2 (39.6)	10.6 (5.9)
Mean crack spacing $\bar{x}$ ft (m)	4.49 (1.36)	2.85 (0.87)
Age - years	8.63	2.82
Crack width Δx in.(mm)	.021 (0.53)	.006 (0.15)
% fines smaller than No. 100 sieve (150 μ)	2.45	1.05
Axle load P Kip (kN)	18 (80.1)	0.92
Deflection y in.(mm)	.00045 (.0114)	.00014 (.0036)
curvature Δy in.(mm)	.000041 (.0010)	.000022 (.0006)
Coarse aggregate in.(mm) size (diam. 2R)	1.03 (26.2)	0.23 (5.8)
Aggregate abrasion LA	26.0	3.2
Thermal coefficient	5.1×10^{-6}	0.7×10^{-6}
Temperature range °F(°C)	22.8 (12.7)	0.6 (0.3)
Diameter steel in.(mm)	0.625 (15.88)	0
Standard deviation S for severe punch-outs	0.694	0.196

Construction Variables. Some important construction considerations need to be discussed before maintenance/rehabilitation is considered. It is clear from the second step in the regression analysis that construction variables have an important role. The most prominent observation is the influence of the workability of the concrete mix and the variables that influence compaction. Hence slump, the shape of the aggregate, and concrete temperature are important considerations in workability, which in collaboration with vibration constitutes an important influence on the density of the concrete, especially around the steel reinforcement and at the bottom of the concrete layer, where it is needed. Some interesting speculations may stem from these observations; namely, the possibility of using temperature control on the mix or a slow hardening cement to enable proper compaction before setting of the mix. Another possibility is the use of well-rounded fine particles in the mix for an increase in workability and a crushed coarse aggregate for proper load transfer.

The method of steel placement may also be mentioned in this respect, although it was not investigated in this study. It is easy to contemplate an increase in structural performance due to an improved bedding of the steel reinforcement in the concrete, if the steel is placed during the placement of the concrete. This technique should be considered against the technique of placing the steel beforehand, which leads to the possibility of poor compaction under the steel, specially in the vicinity of the chairs on which the reinforcement rests.

Recommended Design Equation. The recommended model for design of new pavements is the equation for severe punch-outs. The basis for this recommendation is the need to design against structural failure where minor punch-outs, although eligible to be defined as structural failure, have not always progressed to a severe punch-out. It was shown that a fatigue coefficient d_o can be selected from Fig 6.2 on the basis of a serviceability, P_t i.e., a serviceability index at which the pavement is regarded as having structurally failed. It is recommended that a value for d_o of -3.62, which coincides with a serviceability of 3.0, be accepted for design of new pavements since it was found that frequent repair work becomes necessary on a CRCP when the serviceability index gets as low as 3.0.

The recommended equation for the design of new CRCP is

$$ZS = -1.044 - 0.26 \log \frac{\Delta x}{R} - 1.27 \log (\bar{x}\alpha\Delta T) - 3.62 \log\left(\frac{P}{Lh^2 f_c} \quad \frac{x^{0.033} y^{0.51}}{\Delta_y 0.52}\right) - \log n + 6.42 \times 10^{-6} (\text{variance } f_c) - \frac{1.33}{\text{variance } f_c} - \frac{256}{\bar{x}^2} + \frac{0.76}{\text{variance } \bar{x}} - 9.52 \times 10^{5} (\text{variance y}) - 0.034(\text{surface vibration}) + 0.030(\text{asphalt base}) \quad (6.2a)$$

where all variables are measured in pounds, inches, or ^{0}F, or

$$ZS = -16.58 - 0.26 \log \frac{\Delta x}{R} - 1.27 \log (\bar{x}\alpha\Delta T) - 3.62 \log\left(\frac{P}{Lh^2 f_c} \quad \frac{x^{0.033} y^{0.51}}{\Delta y^{0.52}}\right) - \log n + 1.35 \times 10^{-7} (\text{variance } f_c) - \frac{63.23}{\text{variance } f_c} - \frac{1652}{\bar{x}^2} + \frac{4.90}{\text{variance } \bar{x}} - 1.475 \times 10^{5} (\text{variance y}) - 0.034(\text{surface vibration}) + 0.030(\text{asphalt base}) \quad (6.2b)$$

where P is measured in kN and the rest in terms of kPa , cm , or ^{0}C.

The value of S , the combined standard deviation of log N and log n , is of great importance:

$$S^2 = \left(5.25 \frac{S_p}{p}\right)^2 + \left(6.82 \frac{S_h}{h}\right)^2 + \left(3.41 \frac{S_{fc}}{fc}\right)^2 + \left(0.11 \frac{S_{\Delta x}}{\Delta x}\right)^2 + \left(0.60 \frac{S_{\bar{x}}}{\bar{x}}\right)^2 + \left(0.80 \frac{S_y}{y}\right)^2 + \left(0.82 \frac{S_{\Delta y}}{\Delta y}\right)^2 + \left(S_{\log n}\right)^2 \quad (6.3)$$

where the correct sign of the coefficient is used and the value of d_2 is included.

Maintenance and Rehabilitation of CRCP

The previous paragraphs on the design and construction implications have touched on many aspects that are as applicable to maintenance/rehabilitation operations as to design and construction of new pavements. Important considerations in this respect include the prevention of a loss of load transfer properties at cracks whereby the continuous beam action is reduced to create small transverse beams susceptible to the occurrence of punch-outs. Part of the load transfer problem relates to a loss of subgrade support at the vicinity of the crack. This can be caused by pumping or subgrade movement as a result of swell and settlement. The installation of subsurface drains, sealing of side joints, or the timely overlaying of CRCP with a thin asphaltic concrete overlay may prevent the accumulation or entrance of surface water and in the case of an overlay keep foreign material such as dust, from entering the cracks whereby an agent is introduced which enhances the loss of interlock. The voids created under the slab as a result of subgrade movement can be mended by the introduction of a filler such as a lime/cement/sand mixture, known as mudjacking but more research is necessary in this respect since mudjacking can lead to secondary stresses in the slab as a result of too much filler.

The repairing of areas that have failed structurally, poses several questions in the light of the discussion so far. One of the worthy aspects to consider is the cause of failure. This also needs to be seen in the light of preventive maintenance since it is reasonable to expect that existing problem areas is indicative of future distress, as was implied by the two sets of coefficients for severe punch-outs in Table 5.5. Since one of the roots of structural failure was shown to be the loss of load transfer, the question of restoration of load transfer in the event of a repair patch being made needs to be considered. The transfer of load by way of dowel action of the steel increases in significance for a repair patch since the reinstatement of aggregate becomes a virtual impossibility. The re-establishment of sound concrete around the steel bars in the existing concrete, at the edges of the repair patch, needs to be considered. Furthermore, the introduction of

additional dowel bars may be advantageous as well as the roughening up of the concrete face in an effort to enhance the simulation of aggregate interlock.

The size and shape of the repair patch may be used to advantage since small repair patches are more reliant on load transfer than bigger repair patches which might be considered as a slab on its own.

Prediction of Distress. Distress prediction has been entertained as a combination of area and standard deviation of $\log N$ and $\log n$. However, the form ZS impairs the interpretation of the significance of the individual independent variables. A further impediment is the prediction of S into the future, since Z is actually of interest. An equation, 5.10, provides some means to predict a future S in terms of a present S and some time factors. Assuming a relationship between time and load applications as was derived in Eq 5.10, and as shown in Fig 6.2(a), a plot of conceptual values for S and ZS with time may resemble Fig 6.2(b). The solid line for ZS indicates the increase in distress (decrease of Z), if no preventive maintenance techniques is employed, and the dotted line if certain minor types of distress is maintained whereby future structural failures are inhibited. The values of ZS are based on predictions of severe punch-outs and the value of Z obviously depends on the magnitude of S. Hence, the Z can be increased (distress is decreased) by a reduction in S.

The prediction of S is of considerable importance and depends on time and the number of load applications. The crude model developed in Chapter 5 to predict S, should be employed with caution. It is advised that greater confidence be put in a prediction of S from basic principles such as a prediction of deflection, curvature, road roughness and mean crack spacing instead of on time and $\Delta \log n$ only. Minor types of distress may influence a future change in S since transverse cracking, pumping and spalling causes a reduction in slab stiffness, increase curvature under loading, contributes to higher deflections and causes road roughness. Again, as was mentioned before in Chapter 6, moisture movement in the subgrade may be conducive to the same results in deflection and road roughness as mentioned above whereby S is increased.

The recommended equation to use in the prediction of future punch-outs can be written in terms of the design/construction variables and the present structural condition:

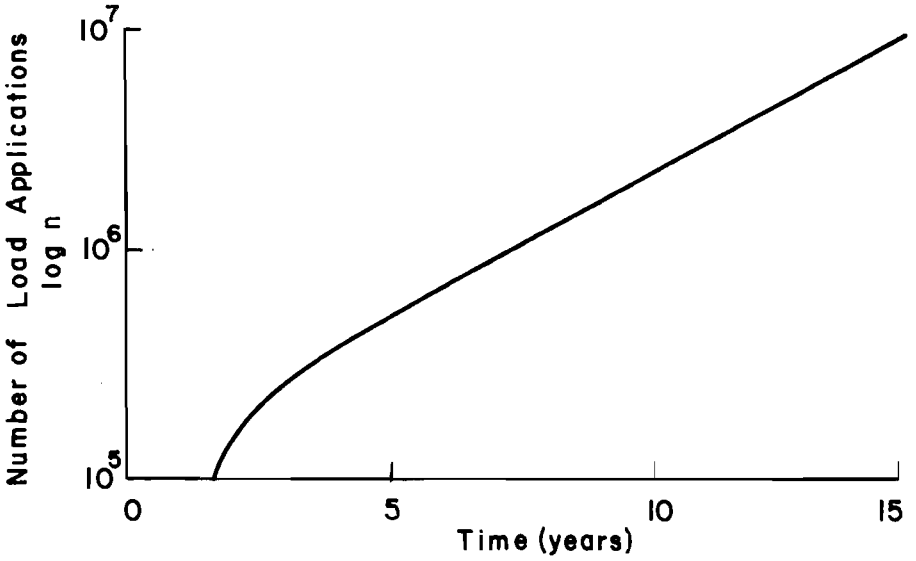

(a) Number of load applications with time.

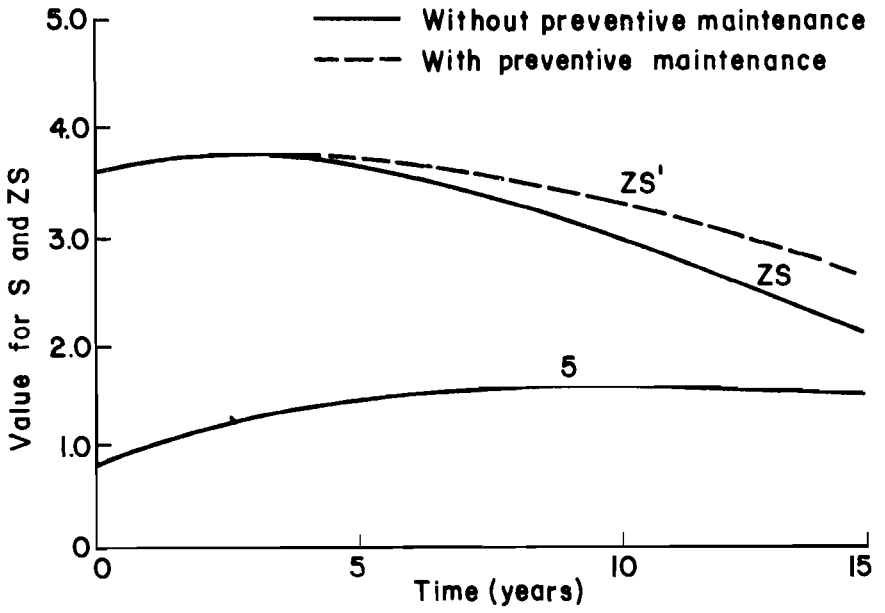

(b) Change in S and SZ with time.

Fig 6.2. Conceptual prediction of distress Z and standard deviation S with time.

$$ZS_t = \Big[-0.56 - 0.13 \log\left(\frac{\Delta x}{R}\right) - 0.63 \log (x\alpha\Delta T) - 1.50 \log\left(\frac{P}{Lh^2 f_c} \frac{x^{0.033} y^{0.51}}{\Delta y^{0.52}}\right) - 0.50 \log n + 3.20 \times 10^{-6}(\text{variance } f_c) - \frac{0.664}{\text{variance } f_c} - \frac{125}{x^2} + \frac{0.38}{\text{variance } \bar{x}} - 4.74 \times 10^5(\text{variance } y) - 0.017(\text{surface vibration}) + 0.015(\text{asphalt base}) + 1.112(\Delta \log n) - 1.043(\Delta \log n)^2 + 0.086\, ZS\ (\text{minor pumping}) + 0.536\, ZS\ (\text{severe punch-outs}) - 0.020\, \bar{x}\,(\Delta \log n) + 0.004\, \bar{x}\Big]_{t-j} \qquad (6.4a)$$

where units are in terms of pounds, inches, or °F , or

$$ZS_t = \Big[-6.91 - 0.13 \log\left(\frac{\Delta x}{R}\right) - 0.63 \log (x\alpha\Delta T) - 1.50 \log\left(\frac{P}{Lh^2 f_c} \frac{x^{0.033} y^{0.51}}{\Delta y^{0.52}}\right) - 0.50 \log n + 3.20 \times 10^{-6}(\text{variance } f_c) - \frac{0.664}{\text{variance } f_c} - \frac{125}{x^2} + \frac{0.38}{\text{variance } \bar{x}} - 4.74 \times 10^5(\text{variance } y) - 0.17(\text{surface vibration}) + 0.015(\text{asphalt base}) + 1.112(\Delta \log n) - 1.043(\Delta \log n)^2 + 0.086\, ZS\ (\text{minor pumping}) + 0.536\, ZS\ (\text{severe punch-outs}) - 0.020\, \bar{x}(\Delta \log n) + 0.004\, \bar{x}\Big]_{t-j} \qquad (6.4b)$$

where load is in kN and the other units are kPa , cm , or °C .

The value of S , the standard deviation of the maximum number of load applications until failure, and the number of load applications actually applied combined is of great importance. The value of S to be used in Eq 6.4 is reproduced here for convenience:

$$S^2 = \left(4.99 \frac{S_p}{P}\right)^2 + \left(6.30 \frac{S_h}{h}\right)^2 + \left(0.53 \frac{S_{f_c}}{f_c}\right)^2 + \left(0.11 \frac{S_{\Delta x}}{\Delta x}\right)^2$$
$$\left(0.59 \frac{S_{\bar{x}}}{\bar{x}}\right)^2 + \left(0.67 \frac{S_y}{y}\right)^2 + \left(0.68 \frac{S_{\Delta y}}{\Delta y}\right)^2 + \left(S_{\log n}\right)^2 \quad (6.5)$$

where the correct sign of the coefficient is used and the d_2 term is included.

The most significant factor was shown to be the value of S with time. Since $\log N$, the anticipated maximum number of load applications, is purely a function of design parameters and since $\log N - \log n$, where $\log n$ is the actual number of loads applied to date, depends only on design and construction variables, the value of SZ will be constant at a specific point in time. The implication of this is that Z can be increased by a reduction in S which should also be seen in the light of preventive maintenance.

Two sets of equations, one for the design of new CRCP and the second to be used in the prediciton of future punch-outs on existing pavements, were summarized. Both equations are written in terms of S, the standard deviation of $\log N$ and $\log n$ combined, which can be measured and/or calculated, and Z, the standard normal variable, which can be determined if the ratio of area failed to area surveyed is known. By changing the different design variables such as slab thickness h, concrete flexural strength f_c or uncrushed coarse aggregate radius R, the relative influence on SZ can be determined from which Z and thus area failed can be calculated if S is known. The implications of these equations together with other conclusions of the study will be discussed in the final chapter.

CHAPTER 7. SUMMARY, CONCLUSIONS AND RECOMMENDATIONS

The implementation of the pavement management system has recognized within its framework a need for pavement network monitoring to evaluate the structural performance of pavements. A condition survey of CRCP in the rural districts of Texas provides the data base for this study which attempts to explain structural performance in terms of design, construction and environmental variables.

The research is founded on theory to allow for extrapolation to conditions other than those prevailing at the site investigated but also to enhance understanding of the reasons for distress so that improved measures and appropriate repair techniques can be employed. However all the distress could not be explained by the theoretical models only and certain construction and environmental variables had to be included. The calculation of stress forms the basis of the analysis. A fatigue model relates number of load applications to stress in the pavement and a stochastic model bridges the gap between number of load applications and the area of distress as measured by a condition survey.

The stress in the pavement is calculated by using an equation based on the assumption that a CRCP can be simulated by a beam on an elastic foundation This solution is compared with results obtained from a calculation of stress using the Westergaard equations and it is found that for the purpose of this anlaysis, no significant difference exist. Since the fatigue coefficients need to be derived both for the stress equation as well as for the load transfer models, regression analysis has to be employed which makes the use of the beam simulation model more attractive.

An important consideration in the calculation of stress in a pavement is the evaluation of load transfer at the transverse cracks. Two load transfer models, an aggregate interlock and a dowel action model for the longitudinal steel reinforcement, are considered in the evaluation and it is found that a considerable amount of distress is related to the load transfer characteristics of the pavement.

Some of the most important conclusions regarding the structural performance of a CRCP can be summarized as follows:

(1) The simulation of CRCP as a beam on an elastic subgrade renders accurate enough results, if it is compared to the results of the Westergaard equations. The mechanism of distress in CRCP can then be described

   (a) transverse cracking occurs midway between shrinkage cracks in the CRCP due to wheel loads and as a result of longitudinal beam action of the pavement,

   (b) because of a decrease in load transfer at the cracks with time, the CRCP begins to act as an end-loaded beam with subsequent closely spaced transversed cracking, 2 to 3 ft (0.6 to 0.9 m), and

   (c) a total loss of load transfer at the cracks eventually leads to narrow transverse beams which break up to form punch-outs.

(2) Load transfer at the transverse cracks, either through aggregate interlock or through dowel action of the steel reinforcement, plays a significant role. Factors that have an affect on improved load transfer are as follows:

   (a) the use of crushed aggregates as the largest sized particles in the concrete mix, which enhances load transfer through aggregate interlock,

   (b) proper design and mixing of concrete for increased uniformity and workability, which improves compaction and thus the strength of the concrete around the steel,

   (c) the use of concrete mixes with small thermal movements to decrease variation of crack width and thus variation in load transfer, and

   (d) the use of proper construction methods and equipment to improve the densification of concrete especially around the steel reinforcement.

(3) The significance of the effect of load transfer on structural performance emphasizes the importance of sound maintenance techniques. This specifically has a bearing on the size and the construction of repair patches. Additional analysis is necessary to determine the optimum size of a repair patch by which the effect of load transfer is minimized since the restoration of load transfer from the patch to the existing concrete can be achieved only by great effort.

(4) The most important distress manifestations to be considered at the design stage include the mean crack spacing since a big crack spacing is synonymous with a wide crack and thus a loss in load transfer. A small crack spacing on the other hand negatively affects the slab stiffness as well as road roughness. Therefore, an initial optimum crack spacing needs to be determined for design purposes. Other important distress types that warrant prevention at a design or maintenance stage are spalling, which has a possible

influence on permeability and load transfer, pumping and the resulting loss of subgrade support, and minor punch-outs, which eventually may be the forerunner of structural failure in the form of a severe punch-out.

(5) Variation in concrete properties could not be measured accurately and can be blamed for a low correlation coefficient for repair patches. The same can be said for the correlation coefficients for punch-outs.

Several recommendations stem from the conclusions:

(1) Distress needs to be analyzed on stochastical principles.

(2) Distress is a dynamic phenomenon and needs to be associated with the fatigue concept, in which stress under one load application, strength and total number of load applications play a role.

(3) The standard deviations of design variables are important considerations. Some important recommendations are to:

   (a) keep road roughness to a minimum since the standard deviation of load P is an important contributor to the magnitude of S , the standard deviation of the number of load applications,

   (b) avoid subgrade movements in the form of settlement and swell, which increase the variance of subgrade support,

   (c) prevent pumping/erosion of the base material by proper base and shoulder design with emphasis on permeability and grading,

   (d) avoid great seasonal changes in subgrade moisture by sealing the side joints and cracks or by the control of percolation of surface water into the subgrade through adjacent side drains, and

   (e) consider the timely overlaying of CRCP with a layer of asphaltic concrete. An overlay has the benefits of restoring the riding quality (reduction of variance in loading) and of sealing the surface against the penetration of moisture or foreign material which affects subgrade support and crack deterioration.

(4) The importance of the standard deviation of the number of load applications S generates a need to predict S accurately, especially for maintenance/rehabilitation purposes. The model proposed in Chapter 6 is not reliable and more research is recommended in this area.

(5) The measurement of the ratio of slab to subgrade stiffness was accomplished by using the Dynaflect. However, the relative influence of swell, settlement, erosion, climate and age were not researched. It is recommended that a model to predict a change in stiffness ratio be considered since it is of prime importance in structural performance.

The results of the analysis provide a means of designing new continuously reinforced concrete pavements as well as predicting future distress on existing pavements of the same type. The recommended model for design is the equation for severe punch-outs. The basis of this recommendation is the need to design against structural failures that severely impair the performance of the pavement from a user's point of view. The equation for repair patches, although eligible to be categorized under the same definition, does not always represent the repair of a severe punch-out and is therefore not used from a design point of view. The same principle is applicable in the case of predicting future structural failure since severe punch-outs need to be repaired whereas the other forms of distress manifestations such as transverse cracking, spalling and pumping only need to be attended to as an exercise in preventive maintenance. It is therefore recommended that severe punch-outs be considered important from a design and maintenance point of view but that the minor types of distress be maintained as a preventive measure to prolong the structural life of the pavement.

REFERENCES

1. McCullough, B. F., and P. J. Strauss, "A Performance Survey of Continuously Reinforced Concrete Pavements in Texas," Research Report 21-1f, Center for Highway Research, The University of Texas at Austin, November 1974.

2. Westergaard, H. M., "Theory of Elasticity and Plasticity," Harvard University Press, Cambridge, Massachusetts, 1952.

3. Timoshenko, Stephen P., "Uber die Biegung der allzeitig unterstutzten rechteckigen Platte unter Wirkung in Einzellast," The Collected Papers of Stephen Timoshenko, McGraw-Hill, New York, 1953. The paper was first published in Der Bauingenieur No. 2, 1922.

4. Westergaard, H. M., "Computation of Stresses in Concrete Roads," Proceedings, Vol 5, Part I, Highway Research Board; also in Public Roads, Vol 7, No. 2, April 1926.

5. Yang, Nai C., "Design of Functional Pavements," McGraw-Hill Co., New York, 1972.

6. Yoder, E. J., and M. W. Witczak, "Principles of Pavement Design," 2nd Edition, John Wiley and Sons, 1975.

7. Zuk, William, "Analysis of Special Problems in Continuously Reinforced Concrete Pavements," Bulletin 214, Highway Research Board, 1959.

8. Hudson, W. R., and Hudson Matlock, "Discontinuous Orthotropic Plates and Pavement Slabs," Research Report 56-6, Center for Highway Research, The University of Texas at Austin, May 1966.

9. Timoshenko, S., and S. Woinowshy-Grieger, "Theory of Plates and Shells," 2nd Edition, McGraw-Hill, New York, 1959.

10. Huang, Y. H., and S. T. Wang, "Finite-Element Analysis of Concrete Slabs and its Implications for Rigid Pavement Design," Highway Research Record Number 466, Highway Research Board, 1973.

11. Holl, D. L., "Thin Plates on Elastic Foundations," Proceedings, Fifth International Conference on Applied Mechanics, Cambridge, Massachusetts, 1938.

12. Fung, Y. C., "Foundation of Solid Mechanics," Prentice Hall Inc., New Jersey, 1965.

13. Cedergren, H. R., J. A. Arman, and K. H. O'Brien, "Development of Guidelines for the Design of Subsurface Drainage Systems for Highway Pavement Structural Sections," Report FHWA-RD-73-14, Federal Highway Administration, Washington, D. C., February 1973.

14. McCullough, B. F., A. Abou-Ayyash, W. R. Hudson, and J. P. Randall, "Design of Continuously Reinforced Concrete Pavements for Highways," Research Report 1-15, National Cooperative Highway Research Program, Center for Highway Research, The University of Texas at Austin, August 1975.

15. Croney, D., J. D. Coleman, and W. P. M. Black, "Movement and Distribution of Water in Soil in Relation to Highway Design and Performance," Special Report 40, Highway Research Board, 1958.

16. Russam, K., and J. D. Coleman, "The Effect of Climatic Factors on Subgrade Moisture Conditions," Geotechnique, Vol XI, March 1961.

17. Baver, L. D., "Soil Physics," John Wiley and Sons, New York, 1956.

18. Thom, H. C. S., "Quantitative Evaluation of Climatic Factors in Relation to Soil Moisture Regime," Highway Research Record No. 301, Highway Research Board, 1970.

19. Poehl, R., and Frank H. Scrivner, "Seasonal Variations of Pavement Deflections in Texas," Research Report 136-1, Texas Transportation Institute, Texas A&M University, January 1971.

20. Cumberledge, G., G. L. Hoffman, A. C. Bhajandas, and R. J. Cominsky, "Moisture Variation in Highway Subgrades and the Associated Change in Surface Deflections," Transportation Research Board No. 497, Transportation Research Board, 1974.

21. Stowe, W. W., R. L. Hardy, and J. P. Fero, "Model Evaluation of Soil Factors Affecting Rigid Pavement Pumpings," Highway Research Record No. 111, Highway Research Board, 1966.

22. Allen, Harold, "Maintenance of Concrete Pavement as Related to the Pumping Action of Slabs, Final Report of a committee, Proceedings, Vol 28, Highway Research Board, 1948.

23. The AASHO Road Test, Report 5, Pavement Research, Special Report 61E, Highway Research Board, 1962.

24. Nowlen, W. J., "Influence of Aggregate Properties on Effectiveness of Interlock Joints in Concrete Pavements," Bulletin D139, Vol 10, No. 2, Portland Cement Association, May 1968.

25. Mitchell, James K., "Temperature Effects on the Engineering Properties and Behavior of Soils," Special Report 103, Proceedings of a Symposium, Highway Research Board, 1969.

26. Murdock, J. W., and C. E. Kesler, "Effect of Range of Stress on Fatigue Strength of Plain Concrete Beams," Journal of the American Concrete Institute Proceedings, Vol 55, 1958.

27. Hilsdorf, H., and C. E. Kesler, "The Behavior of Concrete in Flexure and Varying Repeated Loads," Urbana, University of Illinois, T and A. M. Report No. 172, 1960.

28. Orchard, D. F., "Concrete Technology," Vol II, John Wiley and Sons, New York, 1973.

29. Road Research Laboratory, "Concrete Roads," Department of Scientific and Industrial Research, Harmondsworth, England, 1955.

30. Building Code Requirements for Reinforced Concrete (ACI 318-71), American Concrete Institute, Detroit, Michigan, 1972.

31. Troxell, G. E., H. E. Davis, and J. W. Kelly, "Composition and Properties of Concrete," McGraw-Hill Book Company, New York, 1968.

32. Shelby, M. D., and B. F. McCullough, "Determining and Evaluating the Stresses of an In-Service Continuously Reinforced Concrete Pavement," Departmental Research Report No. 62-1, Texas Highway Department, 1962.

33. Darter, M. I., and W. R. Hudson, "Probabilistic Design Concepts Applied to Flexible Pavement System Design," Research Report 123-18, Center for Highway Research, The University of Texas at Austin, May 1973.

34. Yimprasert, P., and B. F. McCullough, "Fatigue and Stress Analysis Concepts for Modifying the Rigid Pavement Design System," Research Report 123-16, Center for Highway Research, The University of Texas at Austin, January 1973.

35. Packard, R. G., "Design of Concrete Airport Pavements," Portland Cement Association, 1973.

36. Vesic, A. S., and S. K. Saxena, "Analysis of Structural Behavior of Road Test Rigid Pavements," Research Report 1-4(1), National Cooperative Highway Research Program, Washington, D. C., 1968.

37. Treybig, H. J., B. F. McCullough, W. R. Hudson, F. N. Finn, Robert Phil Smith, John P Zaniewski, Harold von Quintus and Robert F. Carmichael, "Flexible and Rigid Overlays of Rigid Pavements," Vol I, Development of New Criteria, Austin Research Engineers Inc., April 1976.

38. Wang, Mian-Chang, and James K. Mitchell, "Stress-deformation Prediction in Cement-treated Soil Pavements," Highway Research Record No. 351, Highway Research Board, 1971.

39. Heukelom, W., and C. R. Foster, "Dynamic Testing of Pavements," Proceedings, Vol 86, No. SM1, American Society of Civil Engineers, February 1960.

40. Scrivner, F. H., C. H. Machalak, and W. M. Moore, "Calculation of the Elastic Moduli of a Two-Layer Pavement System from Measured Surface Delfections," Highway Research Record No. 431, Highway Research Board, 1973.

41. Moore, W. M., J. W. Hall Jr., and D. I. Hanson, "State-of-the-Art on Nondestructive Structural Evaluation of Pavements," Paper presented at the 55th Annual meeting of the Transportation Research Board, January 1976.

42. Van Til, C. J., B. F. McCullough, B. A. Vallerga, and H. G. Hicks, "Evaluation of AASHO Interim Guides for Design of Pavement Structures," Report 128, National Cooperative Highway Research Program, Highway Research Board, 1972.

43. Timoshenko S., "Theory of Elasticity," McGraw-Hill Book Company, New York, 1934.

44. Williamson, H. J., W. R. Hudson, and C. D. Zinn, "A Study of the Relationships Between Various Classes of Road-Surface Roughness and Human Ratings of Riding Quality," Research Report 156-5F, Center for Highway Research, The University of Texas at Austin, August 1975.

45. Grinter, L. E., Discussion on "Dowel Bars Across Pavement Joints," Transactions, Vol 103 of the American Society of Civil Engineers, 1938, p 1157.

46. Draper, N. R., and H. Smith, "Applied Regression Analysis," John Wiley and Sons, New York, 1966.

47. Machado, J., and Hugh J. Williamson, "Prediction of Future Distress in Rural Texas CRCP," Research Report No. 177-8, (being prepared for publication), Center for Highway Research, The University of Texas at Austin, 1976.

48. Buffington, J. L., D. L. Schafer, and W. G. Adkins, "Procedures for Estimating the Total Load Experience of a Highway as Contributed by Cargo Vehicles," Research Report 131-2F, Texas Transportation Institute, Texas A&M University, 1970.

49. Machemehl, Randy, Clyde E. Lee, "Dynamic Traffic Loading of Pavements," Research Report 160-1F, Center for Highway Research, The University of Texas at Austin, December 1974.

50. "AASHTO Interim Guide for Design of Pavement Structures 1972," published by the American Association of State Highway and Transportation Officials, Washington, D. C., 1974.

51. Orchard, D. F., "Concrete Technology Volume 1," John Wiley and Sons, New York, 1973.

52. Reese, Lymon C., "Interaction of Soils and Structures," CE 394.1 class-notes, The University of Texas at Austin, Fall 1974.

53. Treybig, H. J., "Performance of Continuously Reinforced Concrete Pavement in Texas," Highway Research Record No. 29, Highway Research Board, 1969.

54. Colley, B. E., and W. J. Nowlen, "Performance of Subbase for Concrete Pavement Under Repetitive Loading," Bulletin 202, Highway Research Board, 1958.

55. Lindsay, J. D., "A Ten Year Report on the Illinois Continuously Reinforced Pavement," Bulletin 21L, Highway Research Board, 1959.

56. Childs, L. D., and F. E. Behn, "Concrete Pavement Subbase Study in Ohio," Bulletin 202, Highway Research Board, 1958.

57. Chamberlin, W. P., and E. J. Yoder, "Effect of Base Course Gradation on Results of Laboratory Pumping Test," Bulletin 202, Highway Research Board, 1958.

58. Faiz, Asif, and E. J. Yoder, "Factors Influencing the Performance of Continuously Reinforced Concrete Pavements," Transportation Research Record 485, Transportation Research Board, 1974.

59. Leopold, L. B., M. G. Wolman, and J. P. Miller, "Fluvial Processes in Geomorphology," W. H. Freeman and Company, San Francisco, 1964.

60. Akky, M. R., and C. K. Shen, "Erodibility of Cement Stabilized Sandy Soil, Special Report 135, Highway Research Board, 1973.

61. Seed, H. B., and C. R. Chan, "Structure and Strength of Compacted Clays," Journal Soil Mechanics and Foundations Division, Vol 85, American Society of Civil Engineers, 1959.

62. Graf, W. H., "Hydraulics of Sediment Transport," McGraw-Hill, New York, 1970.

63. Moynahan, T. J., and Y. M. Sternberg, "Effects of a Highway Subdrainage of Gradation and Direction of Flow Within a Densely Graded Base Course Material," Transportation Research Record No. 497, Transportation Research Board, 1974.

64. Strohm, W. E., E. H. Nettles and C. C. Calhoun, "Study of Drainage Characteristics of Base Course Materials," Highway Research Record No. 203, Highway Research Board, 1967.

65. Sokolnikoff, I. S., and E. S. Sokolnikoff, "Higher Mathematics for Engineers and Physicists," McGraw-Hill Book Company, 1941.

APPENDIX 1

SIMULATION OF CRCP BY A BEAM ON ELASTIC FOUNDATION

APPENDIX 1. SIMULATION OF CRCP BY A BEAM ON ELASTIC FOUNDATION

Stresses in a concrete slab on an elastic foundation are best calculated by using some discrete element method or the Westergaard approach. However, a continuously reinforced pavement can, under certain conditions, be assumed to be closely simulated by a continuous beam on an elastic foundation. This will be true in the early life of the pavement when the transverse crack width is narrow enough not to have a significant influence on the slab stiffness. The loading is assured to be a strip load on the beam, that is, the pavement dimension in a transverse direction, as well as the vehicular dimensions are small in comparison with the length of the pavement.

Other assumptions are

(1) Deflections are small in comparison with the beam (slab) thickness.

(2) There is no deformation in the middle plane of the beam.

(3) Plane sections initially perpendicular to the axis of the beam remain plane in the bent beam.

(4) Hooke's law is valid (i.e., E = constant).

(5) The applied load lies in the plane of symmetry.

(6) A Winkler type foundation is assumed.

The basic relationship for determining the characteristics of a deflection curve can be written as follows (Ref 7):

$$\frac{d^2y}{dx^2} = \frac{d\theta}{dx} = \frac{1}{\rho} = \frac{M}{EI}$$

where

y = deflection at any point

θ = slope of deflection curve, at x,

M = bending moment, as a function of external loads,

E = modulus of elasticity of the material,

I = moment of inertia of the entire cross-sectional area, and

ρ = radius of curvature.

The singularity functions can be utilized to determine the slope, deflection, and distributed load of the beam with characteristic deflection curve as discussed above:

$$\frac{d^2M}{dx^2} = \frac{dV}{dx} = -\omega(x)$$

where

V = shear at a point, distance x from the origin, and

$\omega(x)$ = the continuous subgrade support as a function of x.

Therefore, if EI is assumed to be constant,

$$\frac{d^4y}{dx^4} = -\frac{\omega}{EI}$$

of which

$\omega = Ky$, where K is the subgrade modulus of support, and

$$B^4 = \frac{K}{4EI}$$

so that the differential equation can be written as

$$\frac{d^4y}{dx^4} + 4B^4y = 0$$

or

$$(D^4 + 4B^4)y = 0,$$

With characteristic equation

$$m^4 + 4B^4 = 0$$

This can be solved as a linear differential equation with roots (Ref 72):

$$m_1 = -m_3 = B(1 + i)$$

$$m_2 = -m_4 = B(-1 + i)$$

The solution of y then is

$$y = e^{Bx}(C_1 \cos Bx + C_2 \sin Bx) + e^{0Bx}(C_3 \cos Bx + C_4 \sin Bx) \quad \text{(A1.1)}$$

Differentiate y to get the slope

$$\frac{dy}{dx} = Be^{Bx}(C_1 \cos Bx + C_2 \sin Bx - C_1 \sin Bx + C_2 \cos Bx) + Be^{-Bx}(-C_3 \cos Bx - C_4 \sin Bx - C_3 \sin Bx + C_4 \cos Bx) \quad \text{(A1.2)}$$

$$\frac{d^2y}{dx^2} = 2B^2e^{Bx}(C_2 \cos Bx - C_1 \sin Bx) + 2B^2e^{-Bx}(C_3 \sin Bx - C_4 \cos Bx) \quad \text{(A1.3)}$$

$$\frac{d^3y}{dx^3} = 2B^3e^{Bx}(C_2 \cos Bx - C_1 \sin Bx - C_2 \sin Bx - C_1 \cos Bx) + 2B^3e^{-Bx}(-C_3 \sin Bx + C_4 \cos Bx + C_3 \cos Bx + C_4 \sin Bx) \quad \text{(A1.4)}$$

$$\frac{d^4y}{dx^4} = 4B^4e^{Bx}(-C_2 \sin Bx - C_1 \cos Bx) + 4B^4e^{-Bx}(-C_3 \cos Bx - C_4 \sin Bx) \quad \text{(A1.5)}$$

Since the length of the beam is infinite, y can be regarded as zero where x equals infinity. That is

$$C_1 = C_2 = 0$$

from the first Eq A1.1. Selecting the origin at the point of loading as shown in Fig A1.1, it can be said that

$$\frac{dy}{dx} = 0 \quad \text{at} \quad x = 0 \text{ , and}$$

therefore

$$-C_3 + C_4 = 0 \quad \text{or} \quad C_3 = C_4$$

from the second equation (A1.2), and since B is not zero. The shear in the beam will be a maximum at the point of loading, and from Eq A1.4

$$\frac{d^3y}{dx^3} = -2B^3 (C_4 + C_3) = \frac{V}{EI} = \frac{P}{2EI}$$

or

$$C_4 = C_3 = -\frac{P}{8B^3} \times \frac{1}{EI}$$

Substitute back in A1.3 for the maximum moment, which occurs at the point of loading:

$$\frac{d^2y}{dx^2} = \frac{M}{EI} = 2B^2 \times \frac{P}{8B^3} \times \frac{1}{EI} = \frac{P}{4BEI}$$

where

$$M = \frac{P}{4B}$$

but

$$B = \sqrt[4]{\frac{K}{4EI}}$$

Thus,

$$M = \frac{P}{4}\sqrt[4]{\frac{4EI}{K}} \qquad \text{(A1.6)}$$

However, stress at the extreme fibers can be written (Ref 9)

$$\text{stress} = \frac{MZ}{I}$$

where

Z = distance from neutral axis to extreme fibres = h/2 ;

I = moment of inertia as defined previously

= $1/12\ h^3$ for a unit width of slab (beam), and

h = thickness of the beam or slab.

Thus,

$$\text{maximum stress} = \frac{12Ph}{8\ h^3}\sqrt[4]{\frac{4EI}{K}}$$

$$= 2.1213\ \frac{P}{h^2}\sqrt[4]{\frac{EI}{K}} \qquad \text{(A1.7)}$$

for "mid-loading" condition. A similar approach can be followed for <u>loading at the end of an infinite beam</u>:

$y = 0$ when x approaches infinity (i.e., $C_1 = C_2$ in Eqs A.1 to A.4

Select the origin of axis at the point of loading, that is, at the end, as in Fig A1.2.

Then,

$$\text{moment} = 0 \text{ at } x = 0$$

or

$$\frac{d^2y}{dx^2} = 0 = -C_4$$

from equation A1.3 and since B cannot be zero. Also at

$$x = 0 , V = P$$

and

$$\frac{d^3y}{dx^3} = \frac{P}{EI} = 2B^3C_3$$

or

$$C_3 = \frac{P}{2B^3EI}$$

Substituting back into Eq A1.4

$$V = Pe^{-Bx}(\cos Bx - \sin Bx)$$

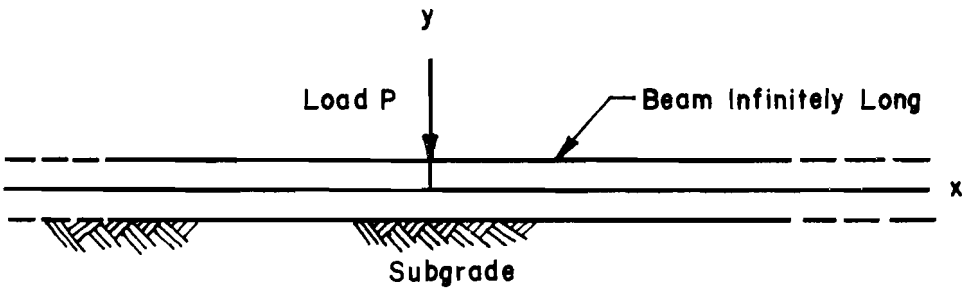

Fig A1.1. Infinite beam on an elastic Winkler foundation loaded in the center.

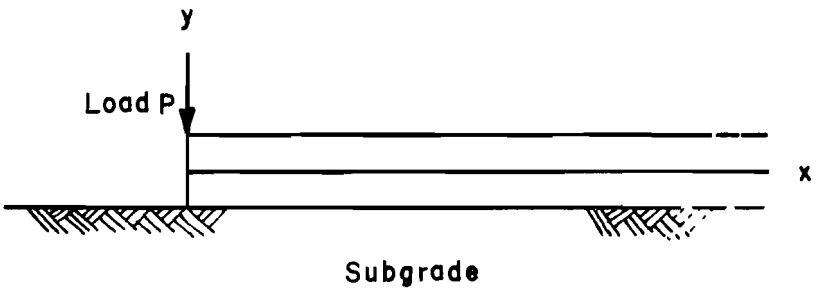

Fig A1.2. Infinite beam on an elastic foundation loaded at the end.

but

$$\frac{d^2y}{dx^2} = \text{a maximum where } \frac{d^3y}{dx^3} = 0$$

Therefore,

$$\cos Bx = \sin Bx \text{ at maximum moment}$$

or

$$Bx = \pi/4$$

and

$$M_{max} = \left(2B^2 e^{-\pi/4}\right)\left(\frac{P}{2B^3} \sin \pi/4\right) \qquad \text{(A1.3)}$$

$$= 0.3224 \frac{P}{B}$$

where

$$\frac{1}{B} = \sqrt[4]{\frac{4EI}{K}}$$

Using

$$\text{stress} = \frac{MZ}{I}$$

as before,

$$\text{maximum stress} = \frac{12Mh}{h^3 2} = 2.7357 \frac{P}{h^2}\sqrt[4]{\frac{EI}{K}} \qquad \text{(A1.8)}$$

for end loading. So, the stress equation has the same form for both end and mid-point loading with only a difference in the magnitude of the coefficient. In both cases, the width of the beam was assumed to be unity. With beam width equal L, Eq A1.7 and A1.8 take the form

$$\text{maximum stress} = C \frac{P}{Lh^2} \sqrt[4]{\frac{EI}{K}} \tag{A1.9}$$

where

C = 2.1213 for interior loading, or
2.7357 for end loading.

APPENDIX 2

LOAD TRANSFER AT A CRACK

APPENDIX 2. LOAD TRANSFER AT A CRACK

Load transfer at a crack is possible through moment transfer, granular interlock, and dowel action of the steel reinforcement. The contact of the ends of two slab segments, A and B Fig A2.1 , formed by a crack in a slab is essential for moment transfer since the steel reinforcement itself contributes very little in this respect (moment transfer through the stiffness of the steel bars). The purpose of this appendix is to show that the probability of moment transfer at a crack is small whereby load transfer, through granular interlock and dowel action of the steel reinforcement, increases in importance.

MOMENT TRANSFER

Calculation of the narrowing of the crack due to deflection of the slab and comparison with the measured crack width will indicate the probability of moment transfer. Deflection of a slab at a crack will cause two ends of two slab segments to get closer (Fig A2.1). Moment will be transferred as soon as A and B touch. The reduction in crack width due to a deflection-curvature Δy can be calculated:

$$\frac{\Delta x'}{h} \approx \frac{\Delta y}{L}$$

where

$\Delta x'$ = reduction of the crack width at surface due to loading

h = thickness of the slab,

Δy = difference in deflection of points B and C due to a load at B , and

L = horizontal distance between B and C .

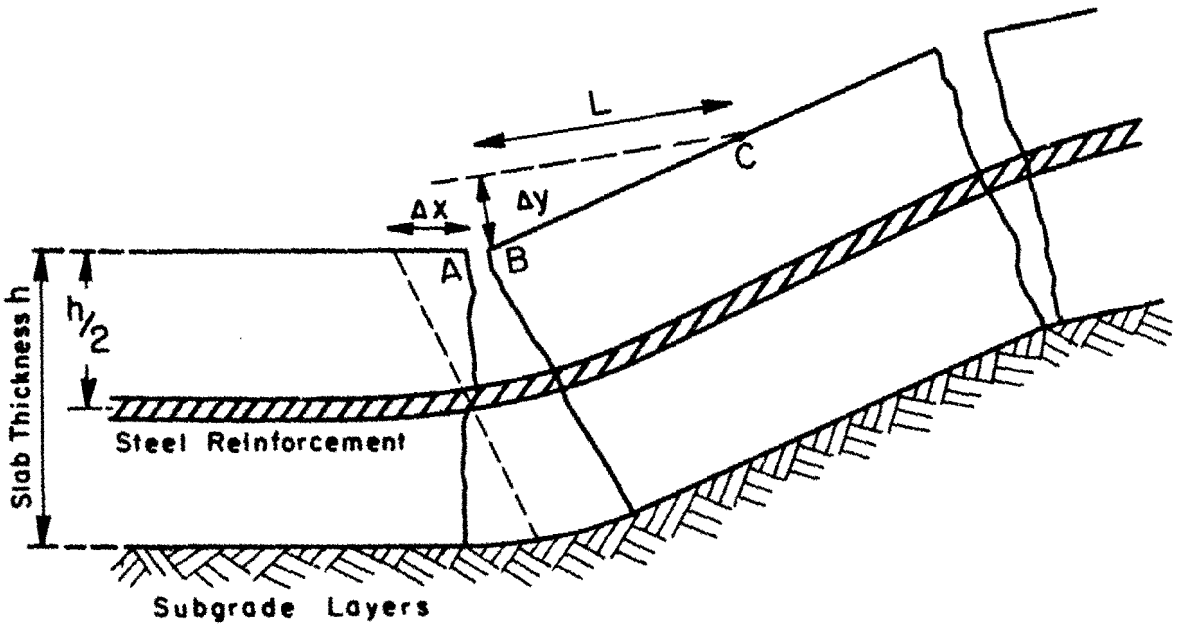

Fig A2.1. Decrease in crack width with deflection.

The value Δy may be represented as the surface curvature index measured by the Dynaflect (Ref 41). Assuming that both ends, A and B, move the same amount, then

$$\Delta x' = \frac{\Delta y h}{L}$$

will give the narrowing of the crack by deflection, assuming the steel reinforcement acts as a hinge at half the slab thickness. Typical average deflection differences Δy measured by the Dynaflect, vary from 0.02×10^{-3} inch (0.0005 mm) to 0.09×10^{-3} inch (0.0023 mm), with an average of $.03 \times 10^{-3}$ inch (0.0008 mm). Using a computer program (Ref 8), it can be shown that deflections are nine times higher for a 9000 pound load (40 KN) than for a 1000 pound load (4.4 KN), the Dynaflect load. Assuming the same order of magnitude for curvature, the corresponding figures for Δy will then be 0.18×10^{-3} inch (0.0045 mm), 0.81×10^{-3} inch (0.021 mm), and 0.27×10^{-3} inch (0.0069 mm). This results in crack narrowing of 0.12×10^{-3} inch (0.0030 mm), 0.56×10^{-3} inch (0.0142 mm), and 0.20×10^{-3} inch (0.005 mm), respectively, if an 8-inch (200-mm) pavement thickness is assumed and L = 12 inches (300 mm). Compare this to an actual crack width measurement of 25.6×10^{-3} inch (0.650 mm) as the high, 9.0×10^{-3} inch (0.229 mm) as the low and 14.7×10^{-3} inch (0.373 mm) as the average. Thus, it seems highly improbable that moment transfer will occur through the contact of concrete since crack widths are much wider than the narrowing through deflection. The accuracy of crack width measurements can be questioned and a calculation of possible crack width seems appropriate at this stage.

Assume that the yearly average pavement temperature is 75° F (24° C), and that the concrete temperature at the time of pavement construction was 95° F (35° C). The latter value is obtained from construction records. The thermal coefficient of 4.6×10^{-6}/°F (8.28×10^{-6}/°C) was measured and is in line with the literature (Ref 51). The shrinkage coefficient can vary between 0.025×10^{-2} and 0.080×10^{-2} (Ref 51) for the type of concrete used in the construction of the pavements under investigation. These shrinkage coefficients were measured for an age of 18 months for the concrete, and, since the pavements under investigation are older than 3 years, a figure of 4×10^{-4} does not seem to be out of line as a conservative value. Assuming

a 4-foot (1.2-m) crack spacing, which also is conservative, a crack width can be calculated as

$$\Delta x = 4\left[(95 - 75)(4.6 \times 10^{-6}) + (0.04 \times 10^{-2})\right] \times 12 \text{ inches}$$

$$= 24.7 \times 10^{-3} \text{ inches } (0.635 \text{ mm}) \text{ (of which } 9.2 \times 10^{-3} \text{ inches } (0.0234 \text{ mm}) \text{ is contributed by a thermal change).}$$

Thus, crack widths can be 24.7×10^{-3} inches (0.627 mm), at least, excluding the effect of the steel stress as well as friction to withstand shrinkage.

Stresses in the longitudinal steel reinforcement were measured in an inservice pavement (Ref 54) and stresses varied between 10,000 psi (68.9 MPa) and 40,000 psi (275.8 MPa), depending on the temperature. Assuming an average low of 15,000 psi (103.4 MPa) and a linear change in stress due to bond over 15 inches (0.38 m), as specified in the ACI Code (Ref 67), for each side of the crack, the change in length of the reinforcement amounts to

$$\Delta x = \frac{\text{stress} \times \text{length}}{\text{modulus of elasticity of steel}}$$

$$= \frac{1}{2} \frac{15{,}000 \times 15 \times 2}{30 \times 10^{6}}$$

$$= 7.5 \times 10^{-3} \text{ inch } (0.191) \text{ mm)}$$

and with a stress of 30,000 psi (206.8 MPa), the elongation is 15×10^{-3} inch (0.381 mm). Considering a certain amount of debonding of the steel close to the crack, a 10×10^{-3} inch (0.254-mm) crack width seems to be a reasonable low figure. Compare this to the low measured value of 9.0×10^{-3} inch (0.228 mm) and the required 1.68×10^{-3} inch (0.043 mm) to get moment transfer. It can, therefore, be concluded that moment transfer is highly questionable and that the measured crack width is probably close to the actual crack width. This will be used in subsequent calculations of granular interlock and load transfer.

Granular Interlock

The basic assumption is made that the aggregate can be simulated by a circular particle, Fig A2.2. This enables the calculation of vertical movement

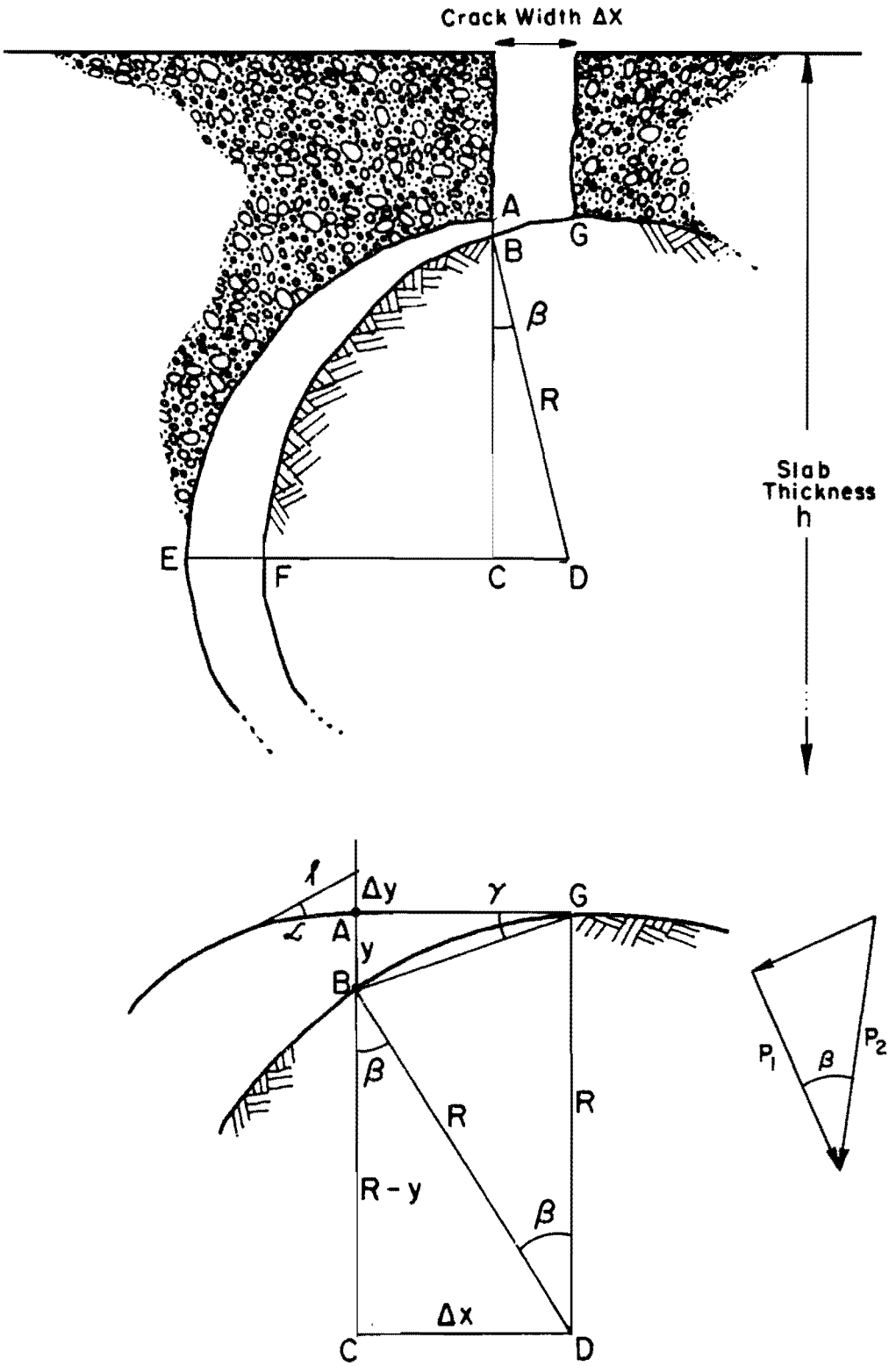

Fig A2.2. Simulation of crack in slab with aggregate (diameter 2R) protruding.

to get contact or granular interlock. The vertical movement y (AB in Fig A2.2) is calculated using the crack width Δx (EF, CD and AG in Fig A2.2.) and the diameter, 2R, of the simulated aggregate:

$$AB = y = AG \tan \gamma$$

where

$$AG = \Delta x$$

The first means of load transfer that will be investigated is shear transfer through granular interlock, but since AG is tangent to circle BG with center D,

$$\gamma = \frac{1}{2} \beta$$

and

$$\tan \frac{1}{2} \beta = \frac{\frac{1}{2} \Delta x}{R-y}$$

Then

$$y = \frac{\Delta x^2}{2(R - y)}$$

or

$$-2y^2 + 2Ry = \Delta x^2$$

Since y is a small value compared to Δx and R, y^2 can be dropped. Thus,

$$y \doteq \frac{\Delta x^2}{2R} \qquad \text{(A2.1)}$$

which will increase slightly if y^2 is included.

Therefore, a relative vertical movement of magnitude $\Delta x^2/2R$ between ends A and B, Fig A2.1, is necessary to enact load transfer through granular interlock.

Assuming that aggregate interlock exists, abrasion of the two elements, aggregate and concrete, will cause a loss of load transfer. This abrasion is a function of the friction between the concrete at A and the aggregate surface at B (Fig A2.2). Abrasion is a function of the load and the loaded area, the load being P_2 acting on a plane perpendicular to the direction of P_1. Assume that aggregate particle FBG, which has a stronger resistance to abrasion, wears out the softer concrete of surface AE, as shown in Fig A2.3(a), to a new position F'G'G'. The load on the concrete at point H is much smaller than at B' since stress can be written as a function of

P_2/horizontal projection of HB'

where

horizontal projection = R cos θ - AG

where

AG = crack width Δx

The magnitude of cos θ changes from $\Delta x/R$ when no abrasion has occurred to one when F' has progressed to fall on the surface of EHA. Thus, cos θ is a function of abrasion.

The horizontal projection of HB' constitutes the width of the loaded area on the x axis whereas the length of the area depends on the particle size and the length HB', as shown in Fig A2.3(b). This figure, Fig A2.3(b), shows a plan view of half the total bearing area (HH'B"B'). The bearing area can be written as

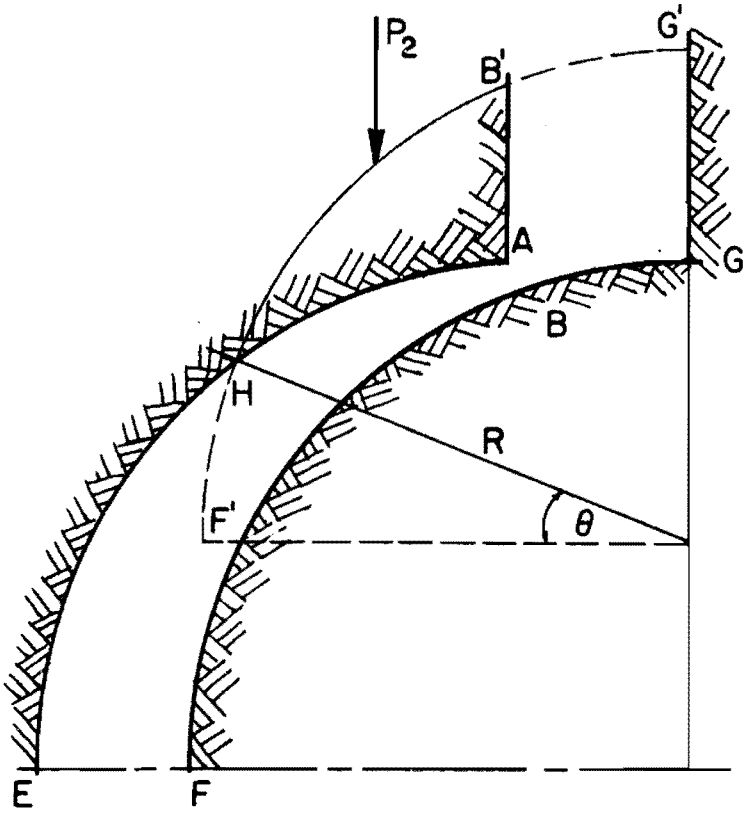

(a) Section view.

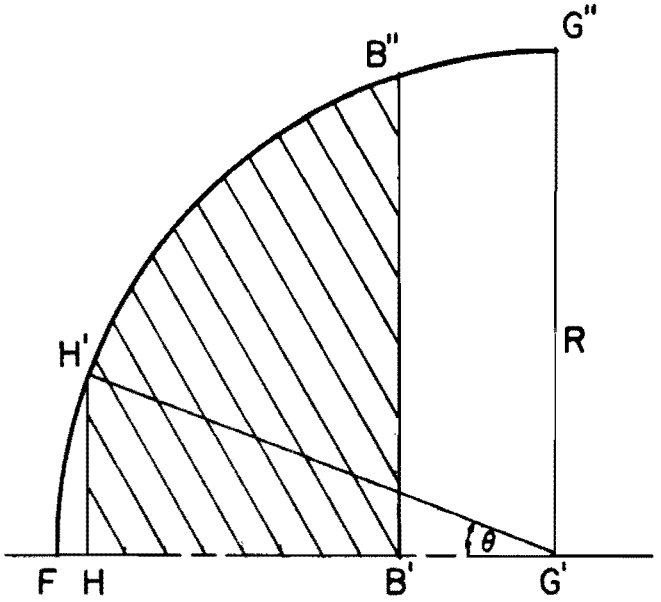

(b) Plan view of half loaded area.

Fig A2.3. The area of aggregate particle loaded when load transfer occurs.

$$2\ (\text{Area of } FG''G' - \text{Area } FH'H - \text{Area } B'B''G''G')$$

$$= \frac{\pi}{2} R^2 - (\frac{1}{2} R^2\theta - R^2 \cos\theta \sin\theta) - 2\Delta x R$$

$$= \frac{\pi}{2} R^2 - R^2(\theta - \frac{1}{2} \sin 2\theta) - 2\Delta x R$$

$$= R^2(\frac{\pi}{2} - \theta + \frac{1}{2} \sin 2\theta) - 2\Delta x R$$

$$= R^2(\frac{\pi}{2} - \theta + \frac{1}{2} \sin 2\theta - \frac{2\Delta x}{R})$$

Thus, aggregate bearing for one particle of diameter $2R$ is a function of

$$P_2/R^2\left(\frac{\pi}{2} - \theta + \frac{1}{2} \sin 2\theta - \frac{2\Delta x}{R}\right) \tag{A2.2}$$

However, this assumes that all the load P_2 transferred by aggregate is done through a single aggregate particle of diameter $2R$. The number of particles of diameter $2R$ can be calculated from a sieve analysis. This can be considered as exposed at the crack face and if all particles contribute to load transfer, the number of bearing points equals

$$\sum_{R=0}^{R=\max} \frac{WhL\gamma_c}{4/3\ \pi R^2 \gamma_R} \tag{A2.3}$$

where

W = percent of total, by weight, which has diameter $2R$,
h = slab thickness,
L = length of crack considered (length of load transfer),

γ_c = density of concrete,

γ_R = density of aggregate with diameter $2R$.

However, based on the assumption of spherical particles, only the maximum sized will contribute to load transfer. Then, aggregate bearing as a result of load transfer P_2 by aggregate interlock can be written as

$$S_2 = \frac{4.19\ P_2\ \gamma_R}{WhL\gamma_c\left(\frac{\pi}{2} - \theta + \frac{1}{2}\sin 2\theta - \frac{2\Delta x}{R}\right)} \qquad (A2.4)$$

and

W = percentage maximum sized aggregate with diameter $2R$.

Load Transfer by Dowel Action

The preceding conclusion leads to the result that the longitudinal steel reinforcement will have to carry a big portion of the shear load associated with a deflection y , Eq A2.1. This implies a load bearing on the concrete immediately above or under the reinforcement, depending on the position of the load, Fig A2.4. This load can be calculated by using pile theory (Ref 6 and 52). The equation for deflection is:

$$y = \frac{PC_1}{2E_dIB^3} + \frac{MC_2}{2E_dIB^2} \qquad (A2.5)$$

where

P = load on the steel reinforcement (dowel),
M = moment on the steel reinforcement,
K_c = modulus of concrete support,
E_d = modulus of elasticity of steel,
I = moment of inertia of steel,

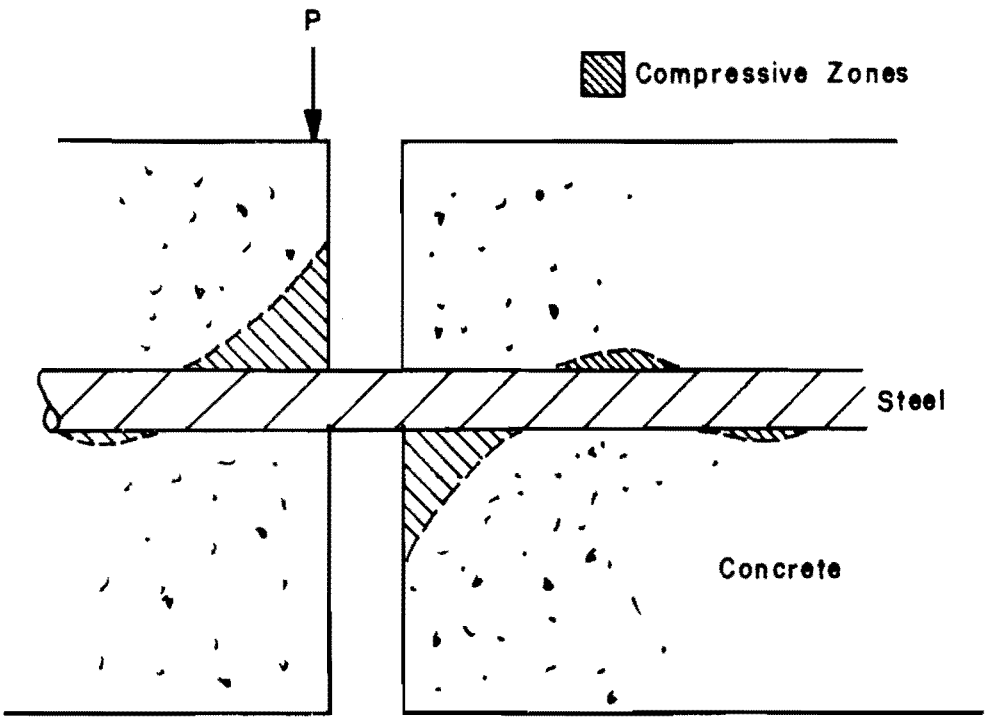

Fig A2.4. Bearing on the concrete underneath and above the steel reinforcement due to a load P .

C_1 and C_2 = constants that depend on the position of the loading and the point at which deflection is calculated,

$$B^4 = \frac{K_c}{4EI}$$

Assuming that the force of load transfer is applied vertically on the steel, then the moment in the steel reinforcement M can be written

$$M = P \frac{\Delta x}{2}$$

Hence, deflection of the steel at the edge of the crack is

$$y = \frac{P}{2EIB^3}\left[1 + \frac{B\Delta x}{2}\right] \qquad \text{(A2.6)}$$

The stress on the concrete due to a load P on the steel can be written

$$S_1 = yK_c = \frac{PK_c}{2EIB^3}\left[1 + \frac{B\Delta x}{2}\right] \qquad \text{(A2.7)}$$

With B in the order of 0.20 for concrete used in a pavement eight inches thick, $B\Delta x/2$ becomes of insignificant magnitude compared to 1 and can be be neglected:

$$S_1 \simeq \frac{PK_c}{2E_dIB^3}$$

Grinter (Ref 45), in a discussion on load transfer by dowel bars, suggested that K_c can be written in terms of E_c, the modulus of elasticity of concrete, if the steel is fully bound by the concrete, which is the case for CRCP. Thus,

$$K_c = f(E_c)$$

and

$$S_1 = C \frac{P_1}{d^2} \sqrt[4]{\frac{E_c}{E_d}}$$

for one bar, if the bar diameter is d instead of unity and

$$I = \frac{\pi d^4}{64}$$

for a rounded bar. For a lane width L and bar spacing S,

$$S_1 = C \frac{P_1 S}{Ld^2} \sqrt[4]{\frac{E_c}{E_d}} \qquad \text{(A2.8)}$$

This is, of course, at the edge of the crack, Fig A2.4. The stress decreases to 0.8S at 1/4-inch (6.35mm) from the crack edge and 0.6S at 1/2-inch from the crack edge.

SUMMARY

The probability of moment transfer at a crack appears to be very small unless crack widths are very narrow, as in the case of new pavements. The burden of the load transfer has to be carried by aggregate interlock and dowel action of the longitudinal steel reinforcement. The latter comes into play whenever any load ia applied, and the magnitude of load transfer in the case of dowel action is not dependent on crack width but only on the amount of load carried by aggregate interlock. Aggregate interlock is activated only after a certain amount of relative vertical movement between the two ends of adjoining slab segments has occurred. The value of this relative vertical movement can be calculated from Eq A2.1, which is a function of crack width. The importance of aggregate interlock can only increase with a decrease in the load bearing capacity of the concrete around the steel that acts as dowels.

APPENDIX 3

HYDRAULIC EROSION

APPENDIX 3. HYDRAULIC EROSION

The base material under a pavement slab can be eroded by water in two ways:

(1) build-up in water pressure due to the instantaneous loading on top of the slab by vehicle wheels, which causes the ejection of water and material through joints and cracks, and

(2) scouring which is caused by the high velocity flow of water over the base material.

The first occurs at any point where high deflection of the slab and a high water content exist and is defined as pumping. The latter can only result if openings, such as open joints or large voids under the slab, exist with a large enough slope to produce a relatively high velocity flow of water. Pumping will be discussed with special attention to pumping as a cause of distress. Subsequently, scouring and the effect of water movement on erosion of road bases will be treated as another form of hydraulic erosion.

PUMPING

Pumping may be defined as the ejection of material and water from beneath a pavement due to the deflection of the slab at a joint, edge, or crack (Ref 14). Heavy traffic loads which are required to deflect a pavement slab sufficiently to promote pumping cause hydrostatic pressures in the subbase/base materials, which results in the ejection of the material along with the water. Another phenomenon of pumping, also known as blowing, is the ejection of granular material under moving loads and is associated with sand. Pumping is used to define blowing of mud or other material.

Early investigations into the causes of pumping have concentrated on field surveys (Ref 22), but laboratory experiments have been conducted recently (Ref 18) to establish the relative importance of gradation of the base/subbase materials, temperature, density, and soil cohesion.

Pumping as a Cause of Pavement Failures

Pumping has been recognized as a major cause of concrete pavement failure since the 1940's (Ref 18) and contributed significantly to the structural failure of rigid pavements at the AASHO Road Test in the early 1960's (Ref 23). Pumping and the loss of subgrade support due to pumping had become such a widespread and serious problem that in 19742, a committee was appointed by the Highway Research Board to study pumping. The report of this committee was published in 1948 (Ref 22). This committee defined the visual indications of incipient pumping and of the progressive stages of actual pumping as follows:

(1) pavement spalling along the centerline near a transverse joint or crack,

(2) ejection of water through joints, cracks and/or along the edge of the pavement,

(3) discoloration of either the pavement surface or shoulder, or both, by subgrade soil near the joints and cracks,

(4) "plastered" hole or "mudboil" in the shoulder at edge of pavement.

(5) faulting of joints or cracks, and

(6) resh corner break or transverse crack a short distance ahead of a pumping joint or transverse crack.

"Such indications serve as a warning that serious pavement distress will develop unless corrective maintenance is started immediately." (Ref 22) Serious pavement distress as mentioned here develops because of a loss in subgrade support, mainly due to pumping.

The relative importance of early signs of pumping can be illustrated by a study conducted in Texas (Ref 4). This study was performed on a section of IH-35 in Falls-McLennan Counties. An experimental section was built in 1959 and was closely monitored for stresses in steel and distress manifestations. Reporting was in the form of photographs, which indicated idscoloration of the pavement shoulder as early as 1962. The first failures of the pavement occurred in 1964, with a constant increase in the number of repair patches until the last report in 1974. No special effort was made during that time to find and remedy the cause of pumping. Unknowingly at the time, repairs were generally made where evidence of pumping could have been detected in previous investigations. Therefore, preventive maintenance in the form of reduction in pumping could have stopped further maintenance. The conclusion

made in this (Ref 4) study that failures; on this particular section could be associated with pumping. An interesting outflow of this experiment was that the geometry of the highway also had some influence on the occurrence of pumping. More pumping was experienced on sections going uphill than on downhill sections. This was probably because heavy trucks tend to use the outer lane when going uphill and also tend to travel closer to the edge of the pavement.

Discoloration is often mistaken as an early sign of pumping that occurs as a result of loading on the pavement slab. This may not always be the case, especially when an asphalt stabilized base was used where discoloration cannot be taken as a sign of pumping. This phenomena was investigated in a study performed on rigid pavements in Texas (Ref 53). It was found that material between the shoulder, which was a flexible pavement, and the pavement slab was washed out because of an open side-joint and/or the geometry of the pavement (Fig A3.1). On slopes, surface water from the pavement started draining down this side joint and first washed out the fines in the joint itself and later started to erode the adjoining subbase. The fines were deposited on the shoulder where the water flowed out at level sections in the road. Therefore, discoloration on the level sections of the road could have been mistaken for pumping. Three conclusions can be drawn from this observation: first, that discoloration can occur at places where there is no problem, and, second, that a loss of subgrade support can occur without signs of pumping or subsidence but simply because of erosion. A third possibility is, of course, that discoloration of a nonpumpable subbase such as an asphalt subbase is not a sign of pumping.

The second phenomenon mentioned above was also recognized at the AASHO Road Test (Ref 23). The concrete from a few sections that have failed was removed and it was observed that subbase material had eroded, probably due to the action of water moving across the top of the subbase. The remaining subbase material was relatively undisturbed. Pumping itself, however, was a true indicator of future failures at the Road Test.

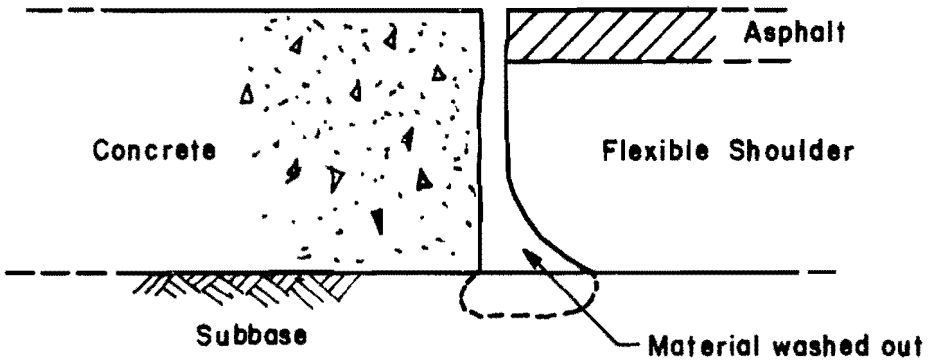

Fig A3.1. Erosion due to open side-joint.

Research

Several studies on the performance of pavements contain references to pumping as a distress manifestation (Refs 22, 54, 55, 56, 57, and 58). Field surveys and an investigation by a committee of the Highway Research (Ref 22) cited the following causes of pumping:

(1) frequent heavy axle loads,

(2) subgrade soils of such a nature that they may pump through open joints or cracks or at pavement edges,

(3) free water under the pavement, and,

(4) joints or cracks in the pavement.

Further research was concentrated on the second reason for pumping, namely, the material properties of the subgrade, since very little could be done about the other causes unless a different design approach on the pavement slab itself was possible. (The use of continuously reinforced concrete pavement, with a narrow crack width, and a pavement shoulder with permeable base layers are some alternate design possibilities that have been put to use).

With regard to material properties of layers that pump, the committee (Ref 22) suggested that pumping occurs in pavements placed on subgrade soils

(1) that contain less than 55 percent retained on the No. 270 sieve,

(2) that the shear strength of the material is not necessarily related to the pumping potential,

(3) that higher densities of compacted soil may only delay pumping, but do not prevent it,

(4) that neither cross section nor thickness have any effect on pumping, pumping,

(5) that granular subbases over fine grained subgrades may prevent pumping, and

(6) that pumping usually develops at expansion and contraction joints.

In contrast to the above, a greater possibility of pumping was found at the AASHO Road Test (Ref 23) where pavement thickness was reduced. This seems to contradict the findings of the HRB committee; however, it should be recognized that pumping is dependent on the amount of deflection of a pavement. Deflection on the otherhand is a function of subgrade support and pavement stiffness, etc., as well as the loading characteristics. The HRB committee recognized the lack of data and established a relationship between deflections

due to loads and the characteristics of the subgrade soils, which probably explains their conclusions regarding pavement thickness.

A more theoretical approach to the problem of pumping has become the next wave of interest; therefore, the following paragraphs concentrate on laboratory studies and specifically on material properties associated with pumping.

Material Research

Stowe (Ref 21) simulated pumping of an 8-inch (20-mm) unreinforced rigid pavement under a 9000-pound (40-kN) wheel load travelling at 14 miles per hour (22.4 km/h) in the laboratory. Soil erosion was found to be a key factor and a theoretical analysis indicated soil cohesion as the most important materials property. Where the rate of drainage was less than the supply of water, it was found that rate of pumping is inversely related to the soil cohesion, as measured by the indirect shear test. The effect of density, soil temperature, and stabilization on pumping could be explained by relating it to cohesion.

The research of Childs and Behn (Ref 56) indicated that potential pumping was not so much a function of cohesion but rather of permeability of the subbase layers. Open-textured subbases were performing better as far as pumping is concerned. Joint and edge pumping, as well as densification under traffic, were reduced significantly with the use of more open mixes rather than dense graded subbases. Cement treated subbases were found to be susceptible to erosion with a result of loss in subgrade support. This was especially true for clay soil-cement subbases.

Colley and Nowlen cautioned against the use of open-graded subbases in a laboratory study (Ref 54) in which the designer is encouraged to design against infiltration of subgrade material into the subbase. However, their findings were along the same lines as those of Childs and Behn (Ref 56), regarding the relative performance of continuous graded materials. Basically Colley and Nowlen tested eight different gradings of materials as shown in Fig A3.2. The respective permeabilities at different densities are shown in Fig A3.3. Materials were tested using three cycles;

(1) 150×10^3 load applications at placement moisture content (optimum AASHO),

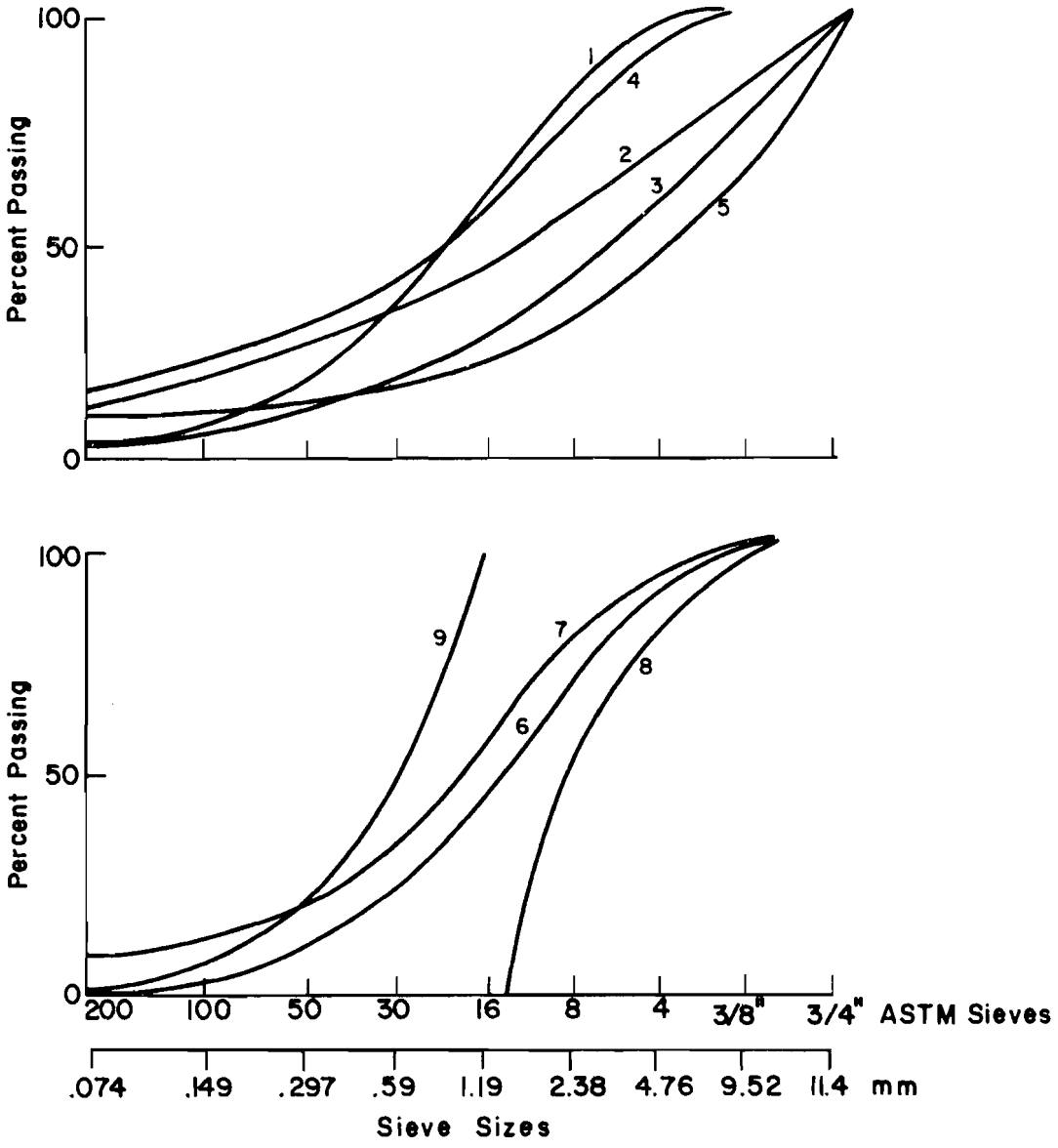

Fig A3.2. Grading of the soils tested for permeability (after Ref 54). Numbers indicate different soil types referred to in Fig A3.3 also.

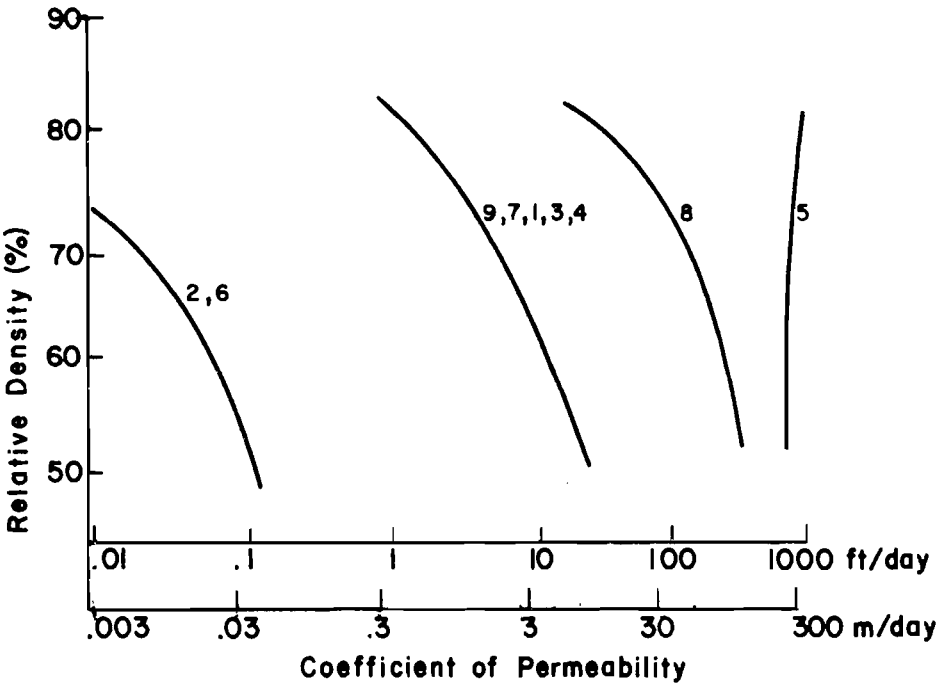

Fig A3.3. The influence of grading and density of soils on permeability (after Ref 54). Numbers indicate soil types with grading as shown in Fig A3.2.

(2) 150×10^3 load applications in a wet stage (water was added until the material was saturated at the end of the test period), and

(3) a 150×10^3 cycles at saturation.

As expected, pumping occurred at the latter stage, but only at materials No. 2 and 4. Reference to Figs A3.2 to A3.4 confirms the findings that pumping in materials with less than 10 percent fines, that is, minus No. 200 sieve (0.075 mm) material, did not occur. Permeability of greater than 3 feet (1 meter) per day also characterized non-pumping subbases, whereas the subbases that had pumping, also experienced more densification than the other materials. It is important to note that Material 2, Figs A3.2, A3.3 and A3.4 showed more pumping than Material No. 4, and very slight pumping was also experienced with Material 7, with 5 feet (1 1/2 meter) per day permeability and 12 percent fines. Granular soil-cement subbases were among the most successful constructions when densification under traffic, structural strength, and anti-pumping characteristics were considered.

Essentially, the same conclusions were made by Chamberlin and Yoder (Ref 58) regarding the design of subbases against intrusion from subgrade material. Some additional conclusions that significantly affect design principles are that high deflection contributes significantly to the intrusion of fine material as well as to the pumping of a pavement. In this respect, it is suggested that sand be given consideration as a subbase material instead of coarse gravel.

SCOURING OF THE BASE

An important phenomenon that was briefly discussed in the previous sections but needs mentioning here is the possible erosion or scouring of base layers. Cement and lime-stabilized base layers in particular, are susceptible to erosion. In Texas, erosion of lime-stabilized base has occurred to such an extent that this particular type of construction has become unpopular and is not recommended directly beneath a CRCP.

Considerable research effort has been devoted to the study of erosion, but not by pavement designers. This is probably because erosion is considered to be a problem associated with exposed surfaces. However, as indicated by Texas (Ref 53), scouring occurs in the side joint, between the concrete and the flexible shoulder. This was confirmed by a study to research

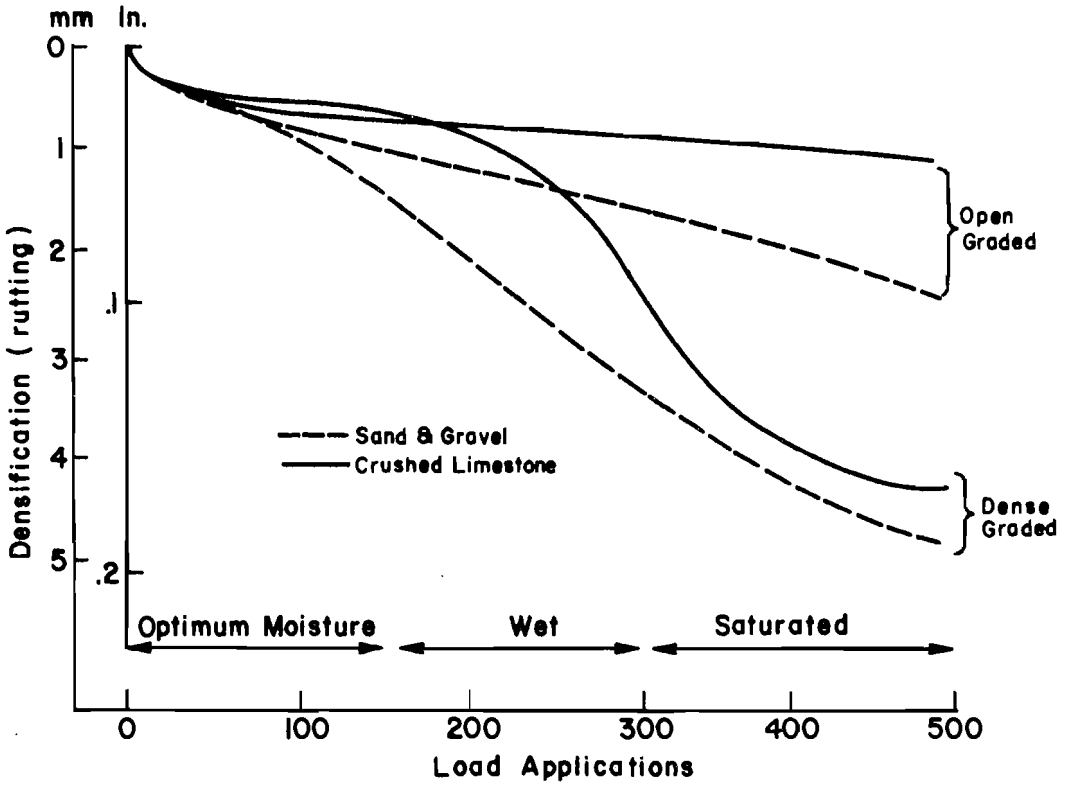

Fig A3.4. The effect of type of material and grading on densification under load applications (after Ref 54).

the relative effect of subsurface drains at the edge of the pavement, as discussed in Appendix 4.

Scouring depends on the velocity of the fluid, and Stowe (Ref 21) related the critical velocity to start erosion as

$$V^2 \geq C\,[c + d(\gamma_s - \gamma_w)\tan\theta]$$

where

V = velocity of fluid to cause scour,

C = coefficient of erosion = $\frac{g}{K\gamma_w}$

c = cohesion of the soil,

d = particle diameter,

γ_s = density of the particle,

γ_w = density of the fluid,

$\tan\theta$ = coefficient of sliding friction,

K = a drag coefficient, and

g = acceleration of gravity.

A similar equation was derived by Akky and Shen (Ref 60), who calculated the cohesion coefficient of the material by measuring a critical shear stress in an erosion test for cement-stabilized sandy soils. Critical shear stress is defined as a stress on the particle caused by the flow of a fluid which initiates the movement of the particle. Akky's approach, however, is generally followed to calculate erosion of clayey materials. Hjulstrom (Ref 61) found that fine sands were more susceptible to erosion than both finer and coarser sizes. Leopold et al (Ref 59) came to the same conclusion as Hjulstran for granular, cohesionless materials and actually measured the critical shear stresses for different sizes of particles in laboratory and field experiments. These results show a wide scatter in critical shear stresses up to 0.04-inch (1-mm) sized particles and a linear increase in critical shear stresses with an increase in particle size above 0.04 inch (1 mm). The upper and lower bounds of the measured values are shown in Fig A3.5.

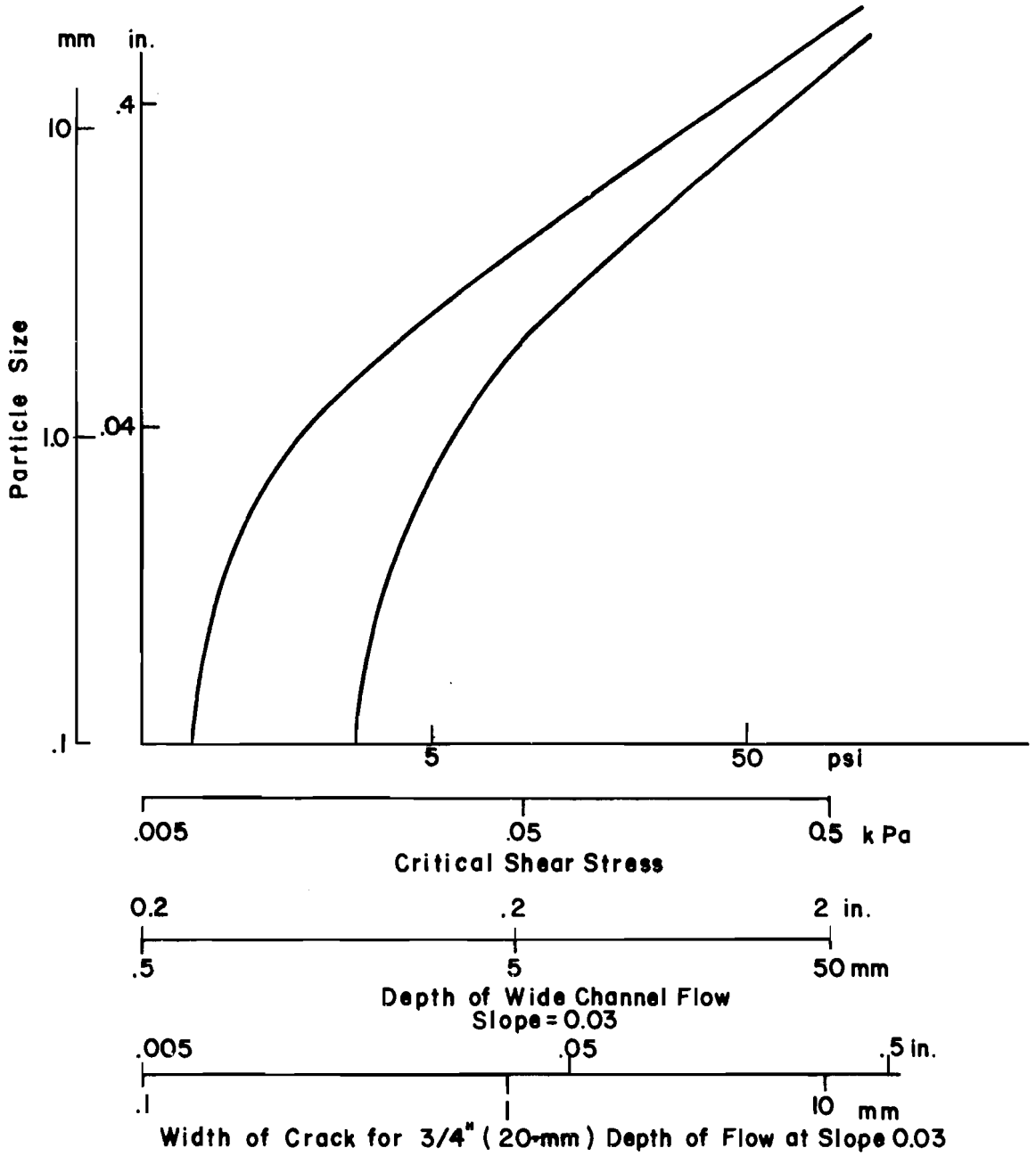

Fig A3.5. Relation between particle size and shear force to cause movement (after Ref 59).

Equivalent shear forces developed by the flow of water can be calculated by using an equation used by Graf (Ref 62);

$$T_o = f\gamma DS$$

where

f = a coefficient depending on the ratio of channel width to depth of flow (always ≤ 1),

γ = density of the fluid,

D = depth of flow,

S = slope of the water surface.

Some investigations (Ref 60) substitute the hydraulic radius for fD, which gives relatively accurate results. Thus, critical shear stresses can be calculated and compared with the measured shear stress necessary to get the particle moving. The above approach assumes no cohesion between particles. If cohesion is present, the Stowe et al (Ref 21) or Akky and Shen (Ref 60) approach needs to be followed. In this case, cohesion has to be measured before critical shear stresses can be calculated to compare with shear stresses caused by the flow of a fluid around the particle.

APPLICATIONS

Designing against the influx of surface water throughout the life of the pavement is considered impossible. Thus, the selection of materials with good drainage characteristics is becoming increasingly important. Moynahan (Ref 63) has studied the effect of gradation on permeability and concluded that the permeability of a densely-graded course base material is inversely related to fines content; even the most permeable samples of densely graded bases did not satisfy the standards for acceptable drainabe as suggested by Strohm (Ref 64). Strohm suggested a formula to calculate drainage time t, in days to obtain a 50 percent reduction in moisture

$$t = \frac{N \cdot D^2}{A \cdot K \cdot H}$$

where

N = effective porosity,
D = horizontal drainage distance in feet (m),
K = permeability of the base in feet/day (m/day),
H = hydrostatic head in feet (m),
A = constant, which can be taken as 2 .

It is suggested that t should be less than 10 days for highway pavements.

A study was performed in Texas to determine the effectiveness of a permeable base under severe raining conditions. An open graded sandstone base was utilized to construct a rigid pavement in 1959. Heavy rains resulting from the hurricane Carla provided an opportunity to study the effectiveness of opengraded base. Holes were drilled approximately 36, 84, and 240 hours after rain ceased. Since a continuously reinforced pavement was used as riding surface and a flexible pavement as shoulder, an open joint resulted between the two types of pavement. As was expected, water entered through this joint and saturation of the base; resulted however, moisture conditions were normal after about 84 hours. The lime-stabilized subbase experienced an increase of about 2 to 5 percent in moisture content and retained this moisture over an unknown period of time. This particular section, although constructed in 1959 and now being overlayed for the first time, has shown no sign of pumping. (Failures on the section are attributed mainly to poor quality concrete).

PUMPING SURVEY

A nationwide survey confirmed the general findings that were reported in previous sections. In a study of data accumulated for project NCHRP 1-15 (Ref 14), 71 sections of CRCP were surveyed for pumping. Base material for these sections included cement, lime and asphalt-stabilization, crushed stone, and sandy gravel. No section of lime or cement-stabilized bases experienced any pumping; however, two of the nine asphaltic base sections (22 percent)

and seven of thirty sandy gravel (23 percent) bases showed pumping. This seems to indicate that crushed-stone bases performed better than asphalt bases, with sandy gravel bases just as good.

Using the same sections, no relationship between age of pavement and pumping could be found, and thicker pavements experienced less pumping. Unfortunately, no reliable information on the traffic load and, hence, its relationship to pumping could be obtained.

It would be a gross underestimation of the ability of asphalt bases to conclude that they truly are subjected to pumping as indicated above. Texas experience has been excellent with this type of base, and, since it is difficult to distinguish between different qualities of asphalt bases, more research is required in this field.

CONCLUSIONS

Pumping has been recognized as a very instrumental distress mechanism which can lead to structural failure in a very short time. This is mainly due to the fact that pumping directly causes a loss of subgrade support, a consequential increase in deflections, overstressing of the top layers and fatigue cracking or structural failure. Some pertinent conclusions from the study are:

(1) Pumping and high moisture content are synonymous in pavement distress.

(2) A high fines content in the base material decreases permeability, increases the period of high moisture and thereby creates potential areas of pumping.

(3) Since pumping is the loss of fines by the expulsion of water from beneath the pavement, a high-fine-content base material is also susceptible to pumping.

(4) Loss of subgrade support is also possible because of the penetration of fines from sublayers into open graded base layers, also it is a form of pumping.

Erosion, pumping, or loss of subgrade support can be prevented by using a cohesive base or subbase layer, such as stabilizing with cement, lime, or asphalt.

Although most of the research on pumping pertains to rigid pavements, the phenomena is equally applicable to flexible pavement; however, pumping is less spectacular in flexible pavements. This probably is because the flexible

top layers adjusts to a loss in subgrade support in the form of rutting or "settling" where crocodile cracking occurs. Therefore pumping was not considered much of a problem in flexible pavements and research is still lacking in this area.

APPENDIX 4

THE CALCULATION OF STANDARD DEVIATION BY THE TAYLOR'S SERIES EXPANSION

APPENDIX 4. THE CALCULATION OF STANDARD DEVIATION BY THE TAYLOR'S SERIES EXPANSION

The value of S, the standard deviation in the equation

$$Z = \frac{\log n - \log N}{\sqrt{S^2}} \tag{3.1}$$

where

$$S^2 = S^2_{\log n} + S^2_{\log N}$$

can be calculated directly. The standard deviation of $\log N$ is affected by the standard deviations of many other variables which are used in the calculation of $\log N$; see equations 3.7, 3.8 and 3.9. Although direct computation of standard deviations of the log values is possible, an easier approach is offered by using Taylor's Theorem:

> Any function $f(x)$ that possesses a continuous derivative $f^{(n)}(x)$ in the interval (a,b) can be expanded in a form for all values of x in (a,b).

This form can be written (Ref 65) as

$$f(x) = f(a) + (x-a)f'(a) + \frac{(x-a)^2}{2!} f''(a) + - - - - -$$

$$+ \frac{(x-a)^{n-1}}{(n-1)!} f^{(n-1)}(a) + \frac{(x-a)^n}{n!} f^{(n)}(a)$$

Define

x = value of a variable, and

a = mean of the same variable.

The estimated value of $f(x)$ can then be written as

$$E\{f(x)\} \cong f(a) + f''(a)\frac{S^2}{2} + \ldots$$

where

f'' implies the second derivative of the function, and

S^2 = the variance.

For two variables x and y the equation can be written as

$$f(x,y) \cong f + f_x(x - \bar{x}) + f_y(y - \bar{y}) + f_{xy}(x - \bar{x})(y - \bar{y})$$
$$f_{xx}\frac{(x - \bar{x})^2}{2} + f_{yy}\frac{(y - \bar{y})^2}{2}$$

where

$\bar{x},\bar{y}$ = means of variables x and y,

f_x, f_y = first derivatives of the function,

f_{xx}, f_{yy} = the second derivatives of the same function for x and y.

The estimated expected value of $f(x,y)$ becomes

$$E\{f(x,y)\} \cong f + f_{xy}S_{xy} + f_{xx}\frac{S_x^2}{2} + f_{yy}\frac{S_y^2}{2} \qquad \text{(A4.1)}$$

where

S_x^2 and S_y^2 signify variance, with S_{xy} being the covariance.

Similarly,

$$E\{f(x,y)^2\} \cong E\Big[f^2 + 2ff_x(x - \bar{x}) + 2ff_y(y - \bar{y}) + 2ff_{xy}(x - \bar{x})(y - \bar{y}) + 2ff_{xx}\frac{(x - \bar{x})^2}{2} + 2ff_{yy}\frac{(y - \bar{y})^2}{2} + 2f_xf_y(x - \bar{x})(y - \bar{y}) + f_x^2(x - \bar{x})^2 + f_y^2(y - \bar{y})^2\Big]$$

$$\cong f^2 + 2\left(f_xf_y + ff_{xy}\right) S_{xy} + \left(ff_{xx} + f_x^2\right) S_x^2 + \left(ff_{yy} + f_y^2\right) S_y^2 \qquad \text{(A4.2)}$$

The variance of the function is

$$\begin{aligned} \text{Var}\ \{f(x,y)\} &= E[f(x,y) - E\{f(x,y)\}]^2 \\ &= E\{f(x,y)^2\} - 2E\ f(x,y)\ E\{f(x,y)\} + [E\{f(x,y)\}]^2 \\ &= E\{f(x,y)^2\} - [E\{f(x,y)\}]^2 \end{aligned} \qquad \text{(A4.3)}$$

Substituting (A4.1) and (A4.2) into (A4.3) gives

$$\begin{aligned} \text{Var}\ \{f(x,y)\} &= f^2 + 2\left(f_xf_y + ff_{xy}\right) S_{xy} + \left(ff_{xx} + f_x^2\right) S_x^2 \\ &\quad + \left(ff_{yy} + f_y^2\right) S_y^2 - f^2 - 2ff_{xy} S_{xy} - 2ff_{xx}\frac{S_x^2}{2} \\ &\quad - 2ff_{yy}\frac{S_y^2}{2} - \left(f_{xy} S_{xy} + f_{xx}\frac{S_x^2}{2} + f_{yy}\frac{S_y^2}{2}\right)^2 \\ &\cong 2f_xf_y S_{xy} + f_x^2 S_x^2 + f_y^2 S_y^2 - \left(f_{xy} S_{xy} + f_{xx}\frac{S_x^2}{2} \right. \\ &\quad \left. + f_{yy}\frac{S_y^2}{2}\right)^2 \end{aligned} \qquad \text{(A4.4)}$$

Thus, the standard deviation, the square root of variance, can be calculated by differentiation of the equation and combination with the variance of the individual variables involved.

THE AUTHORS

Pieter J. Strauss received his B.Sc. in Civil Engineering at the University of Pretoria, South Africa, in 1966. He has had several years experience as a consulting engineer in South Africa, during which time he supervised the construction of several highway and airport projects. He was also closely associated with the evaluation and design of rehabilitation work on the major airports in South Africa. He joined the Center for Highway Research, The University of Texas at Austin, as a research assistant in 1973. Having completed his M. S. degree at The University of Texas in Austin in 1975, he is presently pursuing a Ph.D. degree with research in the field of the structural performance of continuously reinforced concrete pavements. He is a member of several professional societies.

B. Frank McCullough is a Professor of Civil Engineering at The University of Texas at Austin. He has strong interests in pavements and pavement design and has developed design methods for continuously reinforced concrete pavements currently used by the State Department of Highways and Public Transportation, U. S. Steel Corporation, and others. He has also developed overlay design methods now being used by the FAA, U. S. Air Force, and the FHWA. During the nine years with the State Department of Highways and Public Transportation, he was active in a variety of research and design activities. He has authored over 100 publications which have appeared in national journals.

W. Ronald Hudson is a Professor of Civil Engineering at The Univeristy of Texas at Austin. He has had a wide variety of experience as a research engineer with the State Department of Highways and Public Transportation and the Center for Highway Research at The University of Texas at Austin and was Assistant Chief of the Rigid Pavement Research Branch of the AASHO Road Test. He is the author of

numerous publications and was the recipient of the 1967 ASCE J. James R. Croes Medal. He is presenlty concerned with research in the areas of (1) analysis and design of pavement management systems, (2) measurement of pavement roughness performance, (3) slab analysis and design, and (4) tensile strength of stabilized subbase materials.